Canadian Technical Report of
Fisheries and Aquatic Sciences 3103

2014

BIVALVE AQUACULTURE AND EELGRASS (*ZOSTERA MARINA*) COVERAGE ON A BAY-WIDE SCALE UTILIZING BATHYMETRIC LIDAR AND AERIAL PHOTOGRAPHY

by

M. Niles, A. Locke, T. Landry, T. Webster[1], K. Collins[1], G. Robichaud, A. Hanson[2], M. Mahoney[2], H. Vandermeulen[3], S. Doiron[4] and M.-J. Maillet[5]

Fisheries and Oceans Canada
Science Branch, Gulf Region
Moncton, NB
E1C 9B6

[1] Applied Geomatics Research Group, Centre of Geographic Science, Nova Scotia Community College, Middleton, NS B0S 1M0
[2] Environment Canada, Canadian Wildlife Service (EC-CWS), Sackville, NB E4L 1G6
[3] Fisheries and Oceans Canada, Science Branch, Maritimes Region, St Andrews, NB E5B 1W8
[4] Fisheries, Agriculture and Aquaculture, Shippagan, NB E8S 1H9
[5] Fisheries, Agriculture and Aquaculture, Bouctouche, NB E4S 2T2

© Her Majesty the Queen in Right of Canada, 2014.
Cat. No. Fs 97-6/3103E-PDF ISBN 978-1-100-24901-8 ISSN 1488-5375 (online version)

Correct citation for this publication:

Niles, M., Locke, A., Landry, T., Webster, T., Collins, K., Robichaud, G., Hanson, A., Mahoney, M., Vandermeulen, H., Doiron, S. and Maillet, M.-J. 2014. Bivalve aquaculture and eelgrass coverage on a bay-wide scale utilizing bathymetric lidar and aerial photography. Can. Tech. Rep. Fish. Aquat. Sci. 3103:xiv + 82.p.

TABLE OF CONTENTS

LIST OF FIGURES vi

LIST OF TABLES x

ABSTRACT xii

RÉSUMÉ xiii

1. INTRODUCTION 1

1.1 EELGRASS 1

1.2 AQUACULTURE 1

1.3 RELATIONSHIPS BETWEEN EELGRASS AND AQUACULTURE 2

1.4 STUDY OBJECTIVES 2

2. METHODS 3

2.1 AREA OVERVIEW 3

2.2 BATHYMETRY 3

2.2.1 Bathymetric Lidar 3

2.2.2 DEM Processing and Analysis 7

2.2.3 Supplementary Bathymetry 8

2.2.4 DEM Depth Validation 9

2.2.5 Orthophoto Mosaics 9

2.3 EELGRASS 10

2.3.1 FPI Eelgrass From Orthophoto Frames 10

2.3.2 Environment Canada and DFO 10

2.3.3 Eelgrass Coverage Per Bay 11

2.3.4 Eelgrass Coverage at 1 m Depth Intervals 11

2.4 AQUACULTURE 11

2.4.1 Aquaculture: Biomass Calculations – Boat Surveys 12

2.4.2 Aquaculture: Biomass and Depth Calculations – Orthophoto Mosaics 13

2.4.2.1 Oyster Collector Lines 13

2.4.2.2 Floating Oyster Bags (Single and Double) 14

2.4.2.3 Sub-Surface Oyster Cages 16

2.4.2.4 Oyster String Cages 16

2.4.2.5 Oystergro Cages 18

2.4.2.6 Dark Sea Oyster Cages 19

2.4.2.7 Mussel Longlines 20

3. RESULTS 22

3.1 BATHYMETRY 23

3.1.1 Surface Area of DEM Depth Intervals 23

3.1.2 Total Area Comparisons 23

3.1.3 Bathymetric Intervals, DEMs and CSRs 25

3.1.4 DEM Comparison/Validation 34

3.2 EELGRASS 34

3.2.1 Total Eelgrass Area 38

3.2.2 Overlaps with No Data 38

3.3.3 Eelgrass Coverage per Bay 39

3.3 AQUACULTURE GEAR AND BIOMASS – BOAT-BASED SURVEYS 48

3.3.1 Aquaculture Gear and Biomass – Orthophoto Mosaics 50

3.3.2 Biomass – Comparison Between Boat-based Surveys and Orthophoto Mosaics 53

4. DISCUSSION 68

4.1 BATHYMETRY 68

4.2 EELGRASS 69

4.3 AQUACULTURE 69

5. CONCLUSIONS 70

5.1 BATHYMETRY 70

5.2 EELGRASS 70

5.3 AQUACULTURE 71

5.4 RECOMMENDATIONS 71

6. ACKNOWLEDGEMENTS 72

7. REFERENCES 72

APPENDIX A: EELGRASS METHODOLOGY 76

1. DFO- EELGRASS FIELD SURVEY CRITERIA 76

2. DFO - EELGRASS TOWFISH SURVEY METHODOLOGY (H. VANDERMEULEN) 76

3. ENVIRONMENT CANADA- CANADIAN WILDLIFE SERVICE (EC-CWS) (MATT MAHONEY) CLASSIFICATION 77

3.1 EC METADATA 77

APPENDIX B: ADDITIONAL INFORMATION ON LIDAR TECHNOLOGY 81

APPENDIX C: LIST OF ABBREVIATIONS 82

LIST OF FIGURES

Figure 1: Study area on the Eastern shore of New Brunswick and Eastern tip of Prince Edward Island. Background map is a shaded relief terrain model with red polygons denoting bays where bathymetric lidar and orthophotos were acquired. Green polygons denote bays for which a bathymetric lidar survey was planned but not completed. 5

Figure 2: Airborne bathymetric lidar uses green and N1R laser. The green laser penetrates the water column to two Secchi depths and measures the timing and intensity of the returned laser pulse. Source: http://optech.ca/pdf/Brochures/SHOALS2007.pdf. 6

Figure 3: Orthophoto mosaic in St Mary's Bay, Prince Edward Island showing poor aerial photo quality. The southern edges of the individual orthophotos are affected by glint; dark patches near the center of the image are likely cloud shadow. 10

Figure 4: Collector lines in Bouctouche Bay, New Brunswick. 14

Figure 5: Collector lines in Bouctouche Bay, NB seen in the orthophoto mosaic from September, 2011. 14

Figure 6: Orange lines are interpreted and digitized collector lines in Bouctouche Bay, NB. 14

Figure 7: Floating oyster bags with white buoys; more are seen in the distance. 15

Figure 8: A double-wide line of floating oyster bags. 15

Figure 9: Single-wide floating bags in Tracadie Bay, NB in the FPI orthophoto mosaic from Sept., 2011. 15

Figure 10: Double-wide floating bags in Richibucto Bay, NB in the FPI orthophoto mosaic from Sept., 2011. 15

Figure 11: Dark lines are sub-surface oyster cages in the Tracadie Bay, NB orthophoto mosaic from Sept., 2011. 16

Figure 12: Orange lines are interpreted and digitized sub-surface oyster cages in the Tracadie Bay, NB orthophoto mosaic from Sept., 2011. 16

Figure 13: Oyster string cages. 17

Figure 14: The white end buoys of the oyster string cages are barely visible in the left orthophoto; the lines digitized between the buoys in the image on the right represent the oyster string cages in the Caraquet Bay, NB orthophoto mosaic from Sept., 2011. 17

Figure 15: Oystergro cages in Bouctouche Bay, NB. 18

Figure 16: Upside-down Oystergro cages. 18

Figure 17: Oystergro cages in Tracadie Bay, NB with 10-12 cages per line spaced 3 m apart; average line length is 43 m. Image is FPI orthophoto mosaic from Sept., 2011. 18

Figure 18: Oystergro cages in Caraquet Bay, NB with 6 cages visible per line spaced 6 m apart; average line length is 30 m. 19

Figure 19: Digitized Oystergro cages seen in the Caraquet Bay, NB orthophoto mosaic from Sept., 2011. 19

Figure 20: Dark sea oyster cages. 19

Figure 21: Typical design of a Prince Edward Island longline mussel farming setup from Drapeau et al. 2006. 20

Figure 22: Mussel longlines in St Mary's Bay, PEI. The red box shows submerged lines with white end buoys visible; the yellow box shows floating longlines. 21

Figure 23: Left: Mussel longline buoys in St Mary's Bay, PEI, seen in orthophotos from FPI, Sept. 2011. Right: Digitized mussel longlines. 21

Figure 24: The extent of the Digital Elevation Model (DEM) shows the region, referred to as Richibucto that was collected by FPI. For biomass and eelgrass calculations, Richibucto has been divided into three smaller regions: Aldouane, Bedec, and Richibucto. The polygonal outlines were used to actually subdivide Richibucto, as the FPI coastline outlines are smaller than the DEM. 22

Figure 25: Caraquet DEM and lidar-derived 1 m depth intervals. All depths are CGVD28. 26

Figure 26: Caraquet 1 m depth intervals on elevation colour-shaded relief (CSR) image. 26

Figure 27: Miscou DEM and lidar-derived 1 m depth intervals. All depths are CGVD28. 27

Figure 28: Miscou 1 m depth intervals on elevation colour-shaded relief (CSR) image. 27

Figure 29: Tracadie DEM and lidar-derived 1 m depth intervals. All depths are CGVD28. 28

Figure 30: Tracadie 1 m depth intervals on elevation colour-shaded relief (CSR) image. 28

Figure 31: Richibucto DEM and lidar-derived 1 m depth intervals. All depths are CGVD28. 29

Figure 32: Richibucto 1 m depth intervals on elevation colour-shaded relief (CSR) image. 29

Figure 33: Aldouane DEM and lidar-derived 1 m depth intervals. All depths are CGVD28. 30

Figure 34: Aldouane 1 m depth intervals on elevation colour-shaded relief (CSR) image. 30

Figure 35: Bedec DEM and lidar-derived 1 m depth intervals. All depths are CGVD28. 31

Figure 36: Bedec 1 m depth intervals on elevation colour-shaded relief (CSR) image. 31

Figure 37: Bouctouche DEM and lidar-derived 1 m depth intervals. All depths are CGVD28. 32

Figure 38: Bouctouche 1 m depth intervals on elevation colour-shaded relief (CSR) image. 32

Figure 39: St Mary's DEM and lidar-derived 1 m depth intervals. All depths are CGVD28. 33

Figure 40: St Mary's Bay 1 m depth intervals on elevation colour-shaded relief (CSR) image. 33

Figure 41. Caraquet FPI lidar bottom reflectance and eelgrass boundary. Arrows point to areas in the DEM with No Data, areas where the eelgrass polygon overlaps the DEM, and where the eelgrass polygon overlaps an area of No Data in the DEM. 39

Figure 42: Map showing the division of Shippagan Bay and Tracadie Bay, New Brunswick into smaller regions (tributaries). 40

Figure 43: Miscou FPI eelgrass boundary and EC/DFO eelgrass polygons. Background image is elevation colour-shaded relief (CSR). 42

Figure 44: Miscou FPI lidar bottom reflectance and eelgrass boundary. 42

Figure 45: Tracadie FPI lidar bottom reflectance and eelgrass boundary. 43

Figure 46: Tracadie FPI eelgrass boundary and EC/DFO eelgrass polygons. Background image is elevation colour-shaded relief (CSR). 43

Figure 47: Richibucto FPI lidar bottom reflectance and eelgrass boundary. 44

Figure 48: Richibucto FPI eelgrass boundary and EC/DFO eelgrass polygons. Background image is elevation colour-shaded relief (CSR). 44

Figure 49: Bouctouche FPI lidar bottom reflectance and eelgrass boundary 45

Figure 50: Bouctouche FPI eelgrass boundary and EC/DFO eelgrass polygons. Background image is elevation colour-shaded relief (CSR). 45

Figure 51: St Mary's Bay FPI lidar bottom reflectance and eelgrass boundary. 46

Figure 52: Shippagan Bay EC/DFO eelgrass polygons. 46

Figure 53: Neguac Bay EC/DFO eelgrass polygons. 47

Figure 54: Cocagne Harbour EC/DFO eelgrass polygons. 47

Figure 55: Tabusintac Bay EC/DFO eelgrass polygons. 48

Figure 56: Biomass of oysters (or mussels for Prince Edward Island) per bay area (tons per hectare) for 2007-2009 (left) and 2011 (right). 50

Figure 57: Number of oyster bags (or mussel socks for Prince Edward Island) per lease area (number per hectare) for 2007-2009 (left) and 2011 (right). 50

Figure 58: Caraquet orthophoto mosaic (FPI, Sept. 2011), aquaculture leases and interpreted aquaculture..... 54

Figure 59: Tracadie orthophoto mosaic (FPI, Sept. 2011), aquaculture leases and interpreted aquaculture. 55

Figure 60: Richibucto, Aldouane, and Bedec orthophoto mosaic (FPI, Sept. 2011), aquaculture leases and interpreted aquaculture. 56

Figure 61: Bouctouche orthophoto mosaic (FPI, Sept. 2011), aquaculture leases and interpreted aquaculture. 57

Figure 62: St Mary's Bay, PEI orthophoto mosaic (FPI, Sept. 2011) and interpreted aquaculture. 58

Figure 63: Shippagan Bay, NB aquaculture lease areas and EC-interpreted aquaculture polygons. 59

Figure 64: Caraquet Harbour DEM, FPI eelgrass and interpreted aquaculture. 61

Figure 65: Tracadie Bay DEM, FPI and EC/DFO eelgrass, and interpreted aquaculture. 62

Figure 66: Richibucto DEM, FPI and EC/DFO eelgrass, and interpreted aquaculture. 63

Figure 67: Aldouane DEM, FPI and EC/DFO eelgrass, and interpreted aquaculture. 64

Figure 68: Bedec DEM, FPI and EC/DFO eelgrass, and interpreted aquaculture. 65

Figure 69: Bouctouche DEM, FPI and EC/DFO eelgrass, and interpreted aquaculture. 66

Figure 70: St Mary's Bay DEM, FPI eelgrass, and interpreted aquaculture. 67

Figure 71: The turquoise image is the orthophoto mosaic; the greyscale image is the Digital Elevation Model (DEM) (m, CGVD28). Orange symbols are depth values from Canadian Hydrographic Service (CHS) chart 402401 adjusted from Chart Datum to CGVD28 as outlined in Table 3 and Section 2.1.4. Aquaculture is shown as yellow lines. Arrows indicate No Data values in the DEM. 68

LIST OF TABLES

Table 1. Depth interval definitions. 8

Table 2: Existing bathymetry data (X) for each bay and each data type. X* indicates there is a digitized chart but insurmountable issues prevented the charts from being imported into ArcGIS software. 8

Table 3: Vertical Datum corrections used to convert to CGVD28. Details on GRS80- HT2 can be obtained here: http://www.nrcan.gc.ca/earth-sciences/products-services/land-geodetic-survey/geodetic-tools/5199. 9

Table 4: Summary of Environment Canada (EC) and Department of Fisheries and Oceans (DFO) eelgrass data collection methods and years. 11

Table 5. Approximate dimension, surface area and oyster bag equivalence of each aquaculture gear type. For oyster gear, dimension is length × width × height. For mussel socks, dimension is length × radius. 13

Table 6: Surface area of DEM depth intervals (ha). *Sum Depth Area* is the sum of the area in each depth interval, except 0-1 m interval. 23

Table 7: Area of Bays shown in Figure 1, known as *Whole Area.* Although not all the bays in Figure 1 were surveyed, the area of the polygon provided by FPI was calculated to be used for various calculations in the Results section. 24

Table 8: *Difference1* represents the area of the bay that was not detected by the lidar. *%Difference1* shows the difference relative to *Whole Area*, the closest approximation available for the correct area of each bay. 25

Table 9: Sources of data for DEM depth comparison. Negative values indicate that $z_{comparison}$ was deeper than z_{DEM}. 34

Table 10: Eelgrass surface area (ha) per 1 m depth interval. See Appendix A for eelgrass quality definitions. 36

Table 11: Comparisons of different calculations of eelgrass polygons. Total Polygon Area=sum of eelgrass area per depth interval; Whole Area=areas in Table 7, Figure 1; Summed Total = Sum Eelgrass Area; Difference2 = difference between Total Polygon Area and Summed Total; No Data = % of eelgrass polygon that is No Data= Difference2/Total Polygon Area. 37

Table 12: Total eelgrass area in hectares and percent eelgrass coverage for each bay from FPI (%eelgrass = % of bay that has eelgrass = Total Polygon Area in Table 11/Whole Area in Table 6) and/or EC/DFO data. 41

Table 13: Aquaculture lease area, lease area percentage of bay, aquaculture gear area (two dimensional), bivalve biomass (BM), bivalve biomass per bay area and bags per lease area for each bay for year corresponding to eelgrass surveys (2007-2009). All oyster aquaculture. 49

Table 14: Aquaculture lease area, lease area percentage of bay, aquaculture gear area (two dimensional), bivalve biomass (BM), bivalve biomass per bay area and bags per lease area for each bay for year

corresponding to FPI (lidar) eelgrass surveys (2011). All the New Brunswick calculations are based on oyster aquaculture and St. Mary's Bay PEI is based on mussel aquaculture. 49

Table 15. Aquaculture gear spacing and line length and percentage of total for each gear type in each bay calculated from orthophoto mosaics. 52

Table 16: Orthophoto mosaics total biomass per bay, boat-based survey total biomass. Difference2= orthophoto total biomass – boat-based survey total biomass, and Difference2=100*Difference2/boat-based survey total biomass. 53

Table 17. Mean depth (m), depth ranges, and number of points used (n) of aquaculture leases (gear) for each bay. 60

Table 18: DFO Habitat field survey criteria. 77

ABSTRACT

Eelgrass (*Zostera marina*) is well established in many bays of the Southern Gulf of St Lawrence, but it is experiencing some declines here and elsewhere in Atlantic Canada. Eelgrass plays an important biophysical role in the health of ecosystems and therefore is recognized as an ecologically significant species. Current methods to map eelgrass involve a combination of field samples and traditional remote sensing consisting of aerial photographs and satellite imagery, which can be inaccurate, costly, and laborious. The main goal of this study was to use aerial photography and a remote sensing method called bathymetric lidar to map eelgrass distribution, determine water depth, and estimate bivalve aquaculture biomass for six bays in the southern Gulf of St Lawrence. Lidar-detected depths ranged from 0 to 9 m. The lidar-derived depths agreed to within ~1 m with other sources of bathymetry data such as Canadian Hydrographic Service (CHS) charts and echo sounder data. The lidar was unable to collect data for between 7% and 46% of the bay area where the water was either too deep (e.g., in channels) or too turbid for the lasers to penetrate to the bottom. Since the areal distribution of different depth ranges is important to determine the capacity of a bay to support eelgrass, the lidar dataset was coupled to a Geographic Information System (GIS) dataset. Results indicated that the seabed area for layers of 1 m depth intervals was inversely proportional to depth.

Aerial photographs were obtained during the lidar survey flights and used to map eelgrass coverage in the six surveyed bays. Additional eelgrass classifications were obtained from interpretations by Environment Canada (EC) from a variety of sources and field observations by DFO. Eelgrass coverage per bay was calculated in a GIS and the results from the different methods compared. Lidar survey and EC/DFO estimates of eelgrass coverage tended to agree. In absolute terms eelgrass coverage ranged from 374 ha (St Mary's Bay) to 4500 ha (Caraquet Bay). In relative terms eelgrass coverage ranged from 26% (St Mary's Bay) to 94% (Bedec Bay) of the total bay area. Eelgrass coverage per 1 m depth interval decreased with depth and was negligible at depths greater than 4 m as was expected given reduced light penetration with depth.

Aerial photo (orthomosaic) quality was influenced by cloud shadow, light glint, and surface roughness. Overall however, aerial photos were useful for identifying aquaculture buoys and gear type. The digitized aquaculture lines were used to estimate bivalve biomass based on buoy spacing and biomass per buoy for each aquaculture gear type. In five out of six bays compared, the values for total biomass estimated from aerial photos were within 10% of boat-based survey estimates. In relative terms, oyster lease area ranged from 0.25% (Tracadie South) to 8.73% (Bedec) of the total bay area. In PEI, mussel leases in St. Mary's Bay occupied 22.67% of the total bay area.

Bathymetric maps, eelgrass maps and aquaculture maps for several oyster bays in New Brunswick and a mussel bay in Prince Edward Island were constructed. They allowed the calculation of depth areas, eelgrass coverage and aquaculture biomass. These results will feed a concurrent study to assess the statistical relationship between bivalve aquaculture and eelgrass density on a bay-wide scale.

RÉSUMÉ

La zostère (*Zostera marina*) est répandue dans plusieurs baies du sud du golfe du St Laurent mais connait certains déclins dans ces baies et ailleurs dans les provinces Atlantiques. Surtout connu pour son rôle biophysique important dans la santé des écosystèmes, elle correspond aux critères d'une espèce d'importance écologique EIE . Les méthodes utilisées pour cartographier la zostère consistent d'une combinaison d'échantillonnage sur le terrain et de méthodes par télédétection telles les photos aériennes et images satellites qui peuvent être coûteuses et laborieuses. Un des buts de cette étude est de cartographier l'étendu spatiale de la zostère dans six baies du sud du golfe du St Laurent à l'aide de photos aériennes et d'une méthode par télédétection appelé lidar bathymétrique. Les photos aériennes ont aussi été utilisées pour estimer l'infrastructure de l'aquaculture des bivalves à partir de laquelle la biomasse a été estimée. Les profondeurs détectées par le lidar variaient entre 0 et 9 m. Les profondeurs dérivées du lidar concordaient à 1 m près aux profondeurs provenant d'autres sources telles les cartes du Service Canadien Hydrographique (SCH) et les sondes acoustiques. Une grande partie des baies a été évaluée pour la profondeur à l'exception de certaines données manquantes dans 7 à 46% de la surface des baies. Ces manques s'expliquent par des cas où l'eau était soit trop profonde (chenal) ou soit trop trouble pour que le lidar pénètre jusqu'au fond marin. La répartition spatiale des différentes profondeurs est importante pour étudier la capacité de support d'une baie par rapport à la zostère, d'où l'importance de l'information bathymétrique de cette étude. En général, la surface occupée par intervalle de profondeur de 1 m a diminuée avec la profondeur.

Lors des relevés lidar, des photos aériennes ont été obtenues simultanément et utilisées pour cartographier la zostère dans les six baies évaluées. Des cartes de répartition de la zostère ont aussi été obtenues par les interprétations d'Environnement Canada (EC) provenant d'une variété de sources et de données de terrain du Ministère des Pêches et des Océans (MPO). La superficie de la zostère a été calculée dans un système d'information géographique (SIG) pour chaque baie. Les résultats de chaque méthode ont été comparés. En général, les estimations de superficies de la zostère des relevés lidar et d'EC/MPO concordaient. En termes absolus, la surface occupée par la zostère variait de 374 ha (St Mary's Bay) à 4500 ha (Baie de Caraquet). En termes relatifs, la surface de zostère variait entre 26% (St Mary's Bay) et 94% (Bedec) de la surface totale de la baie. La surface occupée par la zostère fut calculée pour chaque intervalle de profondeur. Cette surface diminuait avec la profondeur et était négligeable à des profondeurs de plus de 4 m, ce à quoi on pouvait s'attendre vu la diminution de la pénétration de la lumière avec la profondeur.

La qualité des photos aériennes (orthomosaics) capturées lors du relevé lidar était influencée par l'ombrage des nuages, le brillant de lumière et par la rugosité de la surface. En général, les photos aériennes étaient efficaces dans l'identification des bouées et des engins de culture. Les filières d'aquaculture ont été utilisées pour estimer la biomasse des bivalves en se basant sur des informations de la distance entre les bouées et de la biomasse par bouée pour chaque type d'engin. Dans cinq des six baies, les valeurs de biomasse totale par baie estimé à partir des photos aériennes concordaient à moins de 10% de différence aux estimations par relevé en bateau. En termes relatifs, la surface occupée par les baux d'huitre variait entre 0.25% (Tracadie Sud) et 8.73% (Bedec) de la surface totale de la baie. À l'Île-du-Prince-Edward, les baux de moules dans la baie St. Mary's occupait 22.67% de la surface totale de la baie.

Des cartes de bathymétrie, de zostère et d'aquaculture de bivalve ont été construites pour plusieurs baies du Nouveau-Brunswick et une de L'Île-du-Prince-Édouard. Ceci a permis le calcul de surface de profondeur, de zostère et de biomasse de bivalves cultivés. Ces résultats serviront dans une étude connexe à évaluer la relation entre l'aquaculture des bivalves et la superficie occupée par les herbiers de zostère à l'échelle de la baie.

1. INTRODUCTION

1.1 EELGRASS

Eelgrass is established in beds on the sandy intertidal and subtidal flats in many of the bays and protected harbours of the southern Gulf of St Lawrence. Eelgrass is an important primary producer and serves several essential biophysical functions within the ecosystem, including providing shelter and protection to many organisms (seaweed, invertebrates, fish), and acting as a source of food to others, such as migratory aquatic birds (DFO, 2005). Eelgrass filters the water column, stabilizes sediments in the nearshore marine environment, and acts as a shoreline buffer (DFO, 2009).

Growth of eelgrass depends on light penetration into the water column, thus its depth distribution is limited by water clarity. It is intolerant of anoxic (low oxygen) and eutrophic (excess nutrient) conditions. Nutrient loading of 30 kg of nitrogen per hectare per year has been associated with losses of 80% to 96% of eelgrass bed area (DFO, 2009). The excess nutrients in the water fuel phytoplankton growth and reduce water clarity. Because of the link between ecosystem health and eelgrass abundance, eelgrass can be considered a measure of ecosystem health, where healthy ecosystems have an abundance of eelgrass, and stressed ecosystems have less, or declining eelgrass (Lee et al., 2004; McKenzie, 2008; Kennish and Fertig, 2011; Washington State DNR, 2011).

1.2 AQUACULTURE

Blue Mussels (*Mytilus edulis*) and Eastern Oysters (*Crassostrea virginica*) make up the majority of the bivalve aquaculture industry in New Brunswick and Prince Edward Island. In 2006 mussels and oysters ranked behind salmon as the second and third most dominant aquaculture category in Canada, and Canada ranked 12th globally in the production of both mussels and oysters (Canadian Aquaculture Industry Alliance, 2011). In 2010, PEI produced 21×10^3 tonnes of bivalve aquaculture worth $30 million, more than any other province in Canada; New Brunswick produced 976 tonnes of bivalve aquaculture worth $5.6 million (Statistics Canada, 2010).

Mussels are farmed using the longline system, wherein mussel seeds are collected and placed in mesh sleeves or socks which are then suspended in the water column until the mussels reach market size. In PEI, this cycle takes between 18 and 24 months.

There is more variation in oyster aquaculture systems and infrastructure than mussel systems. After seed collection, oysters can be suspended in the water column in a number of different styles of cages or bags (Doiron, 2008).

1.3 RELATIONSHIPS BETWEEN EELGRASS AND AQUACULTURE

Eelgrass and bivalve aquaculture are both present in bays in the southern Gulf of St Lawrence. Aquaculture can have both positive and negative effects on eelgrass health, density, and growth (Tallis et al., 2009). Both oysters and mussels are filter feeders, and the main positive impact of aquaculture on eelgrass is the improved water transparency caused by increased filtration, which allows greater light penetration (Tallis et al, 2009).

Eelgrass may also be negatively affected by shading from aquaculture, and scour damage from boats and anchors (Skinner et al. 2013).

1.4 STUDY OBJECTIVES

The status of eelgrass as an Ecologically Significant Species (ESS) (DFO 2009) emphasizes the importance of eelgrass conservation to the health of estuarine ecosystems. For effective conservation of this resource, an efficient means of mapping is required, keeping time and financial considerations in mind. One method of mapping eelgrass is through boat-based surveys equipped with video cameras, sidescan sonar and echo sounders. DFO has used this technique successfully for years (Vandermeulen, 2011). However, piecing together these data is laborious and costly, and distribution and abundance of eelgrass based on these surveys is considered to be underestimated and, in some cases, several decades old since these surveys are not done on a regular schedule (DFO, 2009). Interpretation of remote sensing methods such as aerial photos and satellite images has the potential to improve eelgrass distribution mapping, although tide state, water clarity, season and sea surface conditions can affect the detectability of eelgrass by remote sensing techniques. An Environment Canada report (2011) used a combination of a variety of remote sensing techniques and several different field samples to classify eelgrass; ground-truthing indicated the authors classified eelgrass correctly between 77.2% and 96.7% of the time. This integrated technique shows promise, but a single effective mapping technique still remains to be proven.

There is evidence to suggest that eelgrass beds in many locations, including the southern Gulf of St Lawrence, are declining (Hanson, 2004; Locke, 2005; AMEC, 2007; DFO, 2009). According to a 2009 report by DFO, declines of 30% to 95% were reported in some locations of the Maritime Provinces on inter-annual scales ranging from 2 to 20 years. The authors suggest possible reasons for these declines in eelgrass distribution include eutrophication, disturbance (uprooting and grazing) by invasive green crab, human activities, and environmental changes. In Prince Edward Island, eutrophication and nutrient enrichment of bays and estuaries is contributing to reductions in eelgrass distribution and threatening its persistence (Schmidt et al 2012).

The goals of this study, funded by the Program for Aquaculture Regulatory Research (PARR), are to use aerial photography and a remote sensing method called bathymetric lidar to obtain bivalve aquaculture biomass estimates and to map eelgrass distribution with depth for nine bays

in the southern Gulf of St Lawrence. The aerial photos and bathymetric lidar was analysed in a Geographic Information System (GIS) in order to answer questions such as: How much aquaculture biomass is present in each bay? How much eelgrass is present in each bay? How deep does the eelgrass grow? What depth has the most eelgrass?

Data from 2007 to 2009 was compiled from previous work in order to present all available data for a concurrent study on the relationship between eelgrass distribution and bivalve aquaculture biomass.

2. METHODS

2.1 AREA OVERVIEW

This study was conducted in St Mary's Bay, Prince Edward Island and several bays on the eastern coast of New Brunswick, in the southern Gulf of St Lawrence. The bays in the southern Gulf are characterized by shallow depths and a mixed geological environment of sandstone, mud and rock (AMEC, 2007). Barrier islands, sand bars, and low coastal plains are common morphological features (DFO, 2005), and tidal range is between 2.0 m and 2.5 m (CHS, 2012).

2.2 BATHYMETRY

2.2.1 Bathymetric Lidar

The primary source for depth and elevation data was bathymetric lidar, collected in September 2011 by Fugro Pelagos Inc. (FPI). Five major bays in New Brunswick and one bay in PEI were surveyed (Fig 1). Airborne bathymetric lidar is a remote sensing technology that is used to acquire elevation information about the Earth's surface. A lidar system is comprised of three technologies: GPS (Global Positioning System); an IMU (Inertial Measurement Unit); and a laser ranging system (Flood and Gutelius, 1997; Liu, 2008).

The GPS was used to determine the geographic position of the aircraft in three dimensions. The IMU was used to measure the altitude of the aircraft (roll, pitch and heading) (Liu, 2008). The roll, pitch, and heading were accurately measured to allow for the correction of the motion of the aircraft by computer software (Flood and Gutelius, 1997). The laser ranging system transmits a laser pulse towards the Earth's surface, and records the time delay between the transmission of the laser pulse and its return. In terrestrial mapping lidar systems each emitted laser pulse can have up to four returns encoded with the GPS, IMU and range data (Liu, 2008). The laser pulses are directed across a swath with an oscillating mirror. Researchers such as Flood and Gutelius (1997) and Wehr and Lohr (1999) provide a general description and overview concerning

airborne lidar technology and the principles behind it. Terrestrial airborne lidar uses NIR Laser, with a wavelength typically at 1064 nm.

Bathymetric lidar follows the same theory as traditional lidar, but includes an additional laser to penetrate the water column and return information on the ocean floor (Figure 2). FPI employs the SHOALS-1000T acquisition system. The SHOALS system is discussed in detail in Guenther et al. (2000), along with extensive background theory on bathymetric lidar. The remainder of this section on general bathymetric lidar principles has been extracted from FPI's survey report (2011).

The laser output is infrared (1064 nm) with a frequency doubled green wavelength (532 nm) in a single beam. The infrared wavelength is used to detect the water surface and does not penetrate the air/water interface. The green wavelength penetrates through the water and detects the seafloor. The green wavelength also generates red energy (645 nm) in the water column. This by-product is known as Raman scattering and is another method used to detect the sea surface. Distances from the surface and seafloor are calculated using the speed of light, index of refraction in water, and the times of the laser pulse returns recorded by the receivers.

FPI collected bathymetric lidar between September 11 and 20, 2011. The SHOALS-1000T was operated to achieve an IHO Order 1b category of survey coverage and accuracy. This was achieved by combining a 5 m x 5 m spot spacing (flying at 400 m altitude and speed-over-ground of approximately 160 knots) with a 100% coverage plan. Planned line spacing provided 30 m of sidelap. The survey was flown with sufficient options made available to the airborne operator to devise a best plan of the day for climatic and water quality considerations, such that successful data collection was possible in both shallow and deep regions of the area or in areas with known turbidity issues at various states of the tide and or wind direction and strength. A laser pulse of 1 kHz was used for all topography and bathymetry data collection. Data received by the airborne system were continually monitored for data quality during acquisition operations. Display windows show coverage and information about the system status. In addition, center waveforms at 5 Hz rate are shown in the display. All of this information allowed the airborne operator to assess the quality of data being collected.

FPI produced a continuous water to land Digital Elevation Model (DEM) for each bay surveyed using a combination of auto-processing algorithms and manual data inspection and editing. The auto-processing algorithms obtained inputs from the raw data and calculated a height, position and confidence for each laser pulse. This process, using the default environmental parameters, also performed an automated first cleaning of the data, rejecting poor land and seafloor detections. Other SHOALS specific tools, such as swapping a sounding that was falsely recognized as land to water, were used inside Fledermaus by experienced data analysts. In the shallower nearshore margins, the Shallow Water Algorithm (SWA) for bottom detection was used to recover the bathymetry values and to allow, where valid returns permitted, a seamless

join with the topographic data obtained on the specific missions for which these data were collected.

Bottom reflectance data were also recorded by the lidar system. In addition to recording the two way travel time of the green laser pulse through the water column, the intensity or amplitude of the reflected laser pulse off the seabed is also recorded. The intensity of this pulse will vary depending on bottom type, thus having the potential to assist in mapping the seabed cover type, i.e. sand vs. eelgrass. The reflectance data is represented as a grey scale image, similar to an air photo. However, it represents the reflected energy from the green laser and not the sunlight. The reflectance data were not part of the original Canadian Hydrographic Service (CHS) contract deliverable, but were a specific request for the purpose of evaluating the potential of bathymetric lidar for bottom type mapping.

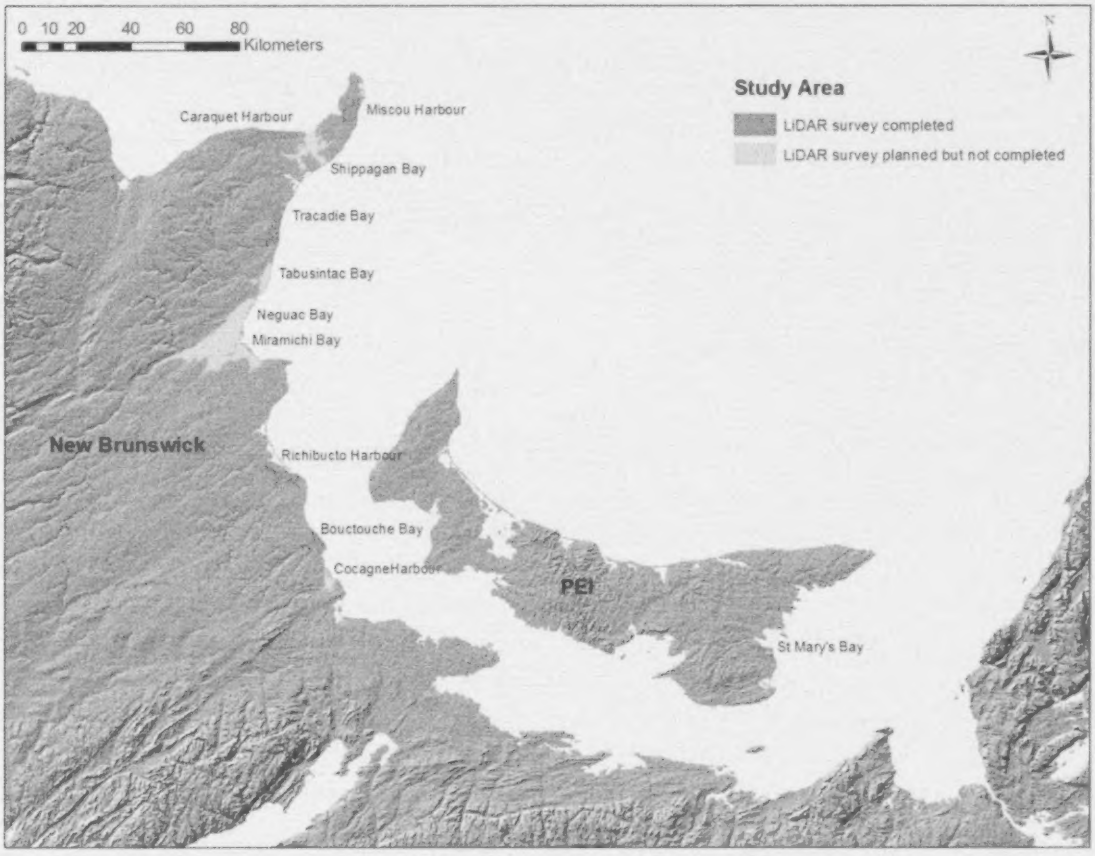

Figure 1: Study area on the Eastern shore of New Brunswick and Eastern tip of Prince Edward Island. Background map is a shaded relief terrain model with red polygons denoting bays where bathymetric lidar and orthophotos were acquired. Green polygons denote bays for which a bathymetric lidar survey was planned but not completed.

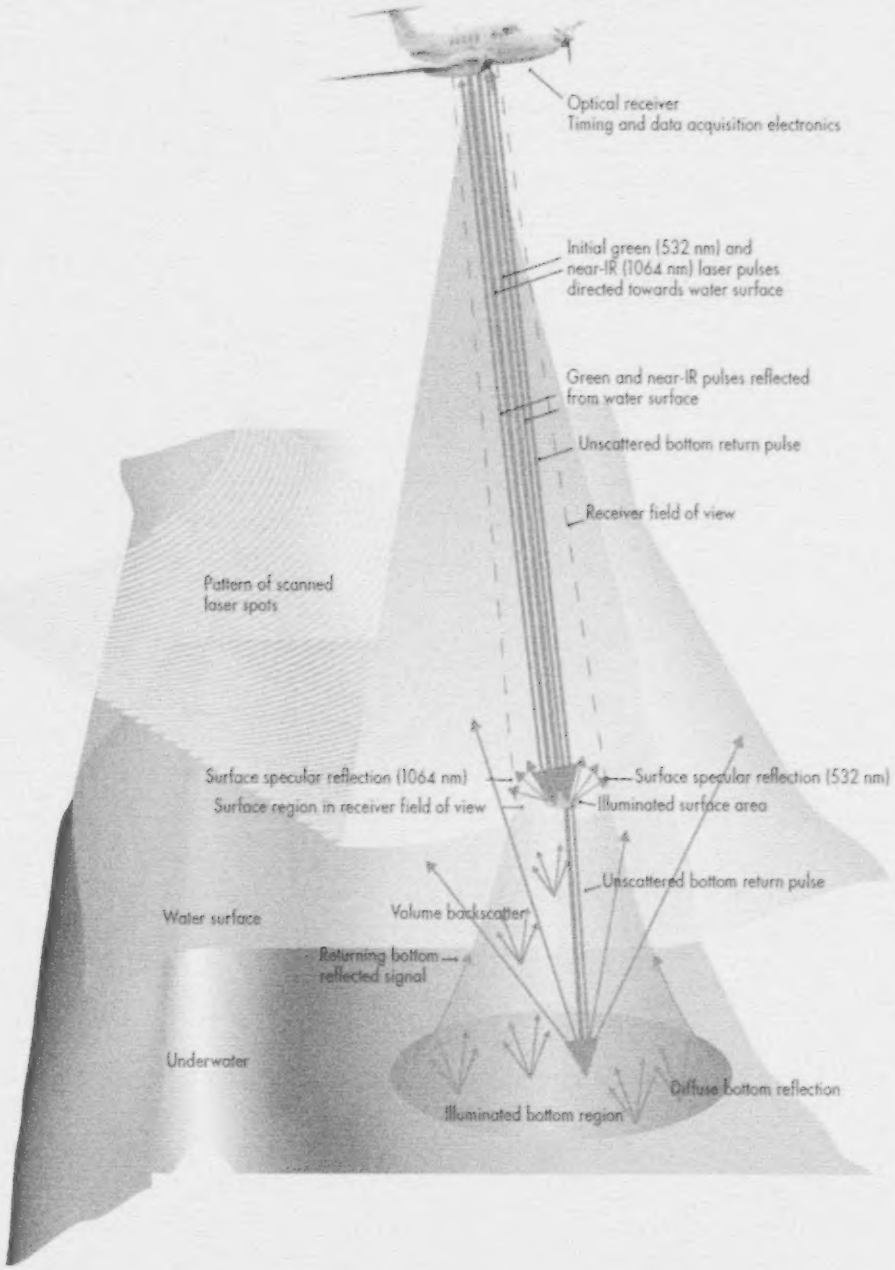

Figure 2: Airborne bathymetric lidar uses green and N1R laser. The green laser penetrates the water column to two Secchi depths and measures the timing and intensity of the returned laser pulse. Source: http://optech.ca/pdf/Brochures/SHOALS2007.pdf.

2.2.2 DEM Processing and Analysis

Digital Elevation Models (DEMs) and Colour Shaded Relief (CSR) maps were created for each surveyed bay using the lidar data. The digital elevation model (DEM) heights provided by FPI were referenced to the GRS-80 ellipsoidal model of the earth. To convert the elevations to orthometric heights a geoidal separation value derived from NRCan's Geodetic Survey HT2 was used and subtracted from the ellipsoidal heights to reference them to the Canadian Geodetic Vertical Datum 1928 (CGVD28). Details on GRS80- HT2 can be obtained here: http://www.nrcan.gc.ca/earth-sciences/products-services/land-geodetic-survey/geodetic-tools/5199.

The DEMs can be used to derive a variety of other map layers including slope, aspect (land facing orientation), as well as maps that can be used to improve interpretation of the bathymetry. Shaded relief maps have been constructed from the DEMs where the terrain was illuminated from the northwest at a 45 degree angle. In order to enhance the subtle relief present in the study areas, a five times vertical exaggeration has been applied to the terrain. The shaded relief maps are viewed and interpreted as greyscale maps which highlight the local relief, but do not depict the actual elevation (i.e. a slope in the valley will look the same as a slope at the top of a hill). Another series of map products that have been constructed consist of colour shade relief (CSR) maps. Colours have been assigned to the elevations based on the DEMs and merged with the shaded relief maps. The colourized elevation is then merged with the shaded relief that gives the terrain and bathymetry texture and enhances the information that can be interpreted from the map.

CSR maps have been built for all six DEM datasets and are presented in Section 3.1.3. Elevations less than 0 m CGVD28 (bathymetry) are coloured in shades of blue; elevations greater than 0 m CGVD28 (topography) are coloured green, yellow and red. Note that CGVD28 is approximately equal to mean sea level (MSL). These maps are qualitative and are designed for use as a backdrop to other information within the GIS. The CSR images have been converted into a compressed georeferenced format, JPEG 2000, which is compatible with most GIS systems.

The surface area of each 1 m depth interval was estimated from the DEM using ArcMAP in the following manner. First, depth values in the DEM were rounded up to the nearest integer. This converted every pixel of the raster into an integer, sorting the DEM into 1 m depth intervals, defined in Table 1. Then the number of pixels in each depth interval was multiplied by the size of each pixel (5 m x 5 m) to arrive at a value for surface area for each 1 m depth interval.

Table 1. Depth interval definitions.

1 m Depth (z) Interval Polygons	
Label	**Definition (depth range in m)**
1 m	0 < z < 1
0 m	-1 < z <= 0
-1 m	-2 < z <= -1
-2 m	-3 < z <= -2
-3 m	-4 < z <= -3
-4 m	-5 < z <= -4
-5 m	-6 < z <= -5
-6 m	-7 < z <= -6
-7 m	-8 < z <= -7
-8 m	-9 < z <= -8
-9 m	-10 < z <= -9

2.2.3 Supplementary Bathymetry

Several sources of depth data were available to compare with the lidar bathymetry (Table 2) such as echo soundings, depth measurements and digitized CHS bathymetric charts. Unfortunately there were problems importing the charts for all bays except Caraquet and Richibucto into ArcMap.

Table 2: Existing bathymetry data (X) for each bay and each data type. X* indicates there is a digitized chart but insurmountable issues prevented the charts from being imported into ArcGIS software.

Bay	Bathymetric Lidar (FPI)	Echo Soundings (DFO)	Field Samples (incl. depth) (DFO)	Digitized Chart (CHS)
Caraquet Bay, NB	X			X
Miscou Harbour, NB	X		X	X*
Tracadie Bay, NB	X		X	X*
Richibucto Harbour, NB	X	X		X
Bouctouche Bay, NB	X			X*
Cocagne Harbour, NB				X
Shippagan Bay, NB				X
St Mary's Bay, PEI	X	X		X*

2.2.4 DEM Depth Validation

The lidar-derived depths of the DEM were validated by comparing them to existing depths in a particular bay (depth data available per bay shown in Table 2). A common vertical datum was necessary for the comparison to be useful. Table 3 shows the values used to bring all depth data into CGVD28, the standard vertical datum.

Table 3: Vertical Datum corrections used to convert to CGVD28. Details on GRS80- HT2 can be obtained here: http://www.nrcan.gc.ca/earth-sciences/products-services/land-geodetic-survey/geodetic-tools/5199.

Data	Original Vertical Datum	Conversion to CGVD28
Lidar DEM	Heights relative to ellipsoid GRS80	GRS80 – HT2
Echo Soundings (DFO)	Assumed MSL	Richibucto and St Mary's: 0 m
Field Samples (incl. depth) (DFO)	Assumed MSL	Miscou and Tracadie: 0 m
Digitized Chart (CHS)	Chart Datum 2000	Caraquet: 0.9 m Richibucto: 0.5 m

The echo soundings and field samples did not have a complete meta-data record, so there was no indication of whether or not the elevations had been compensated for tidal elevations, and data were not time-stamped. Tidal range in the southern Gulf of St Lawrence is relatively small (2 to 2.5 m), so the assumption of MSL as the vertical datum for the echo soundings and field samples will not introduce extreme error if incorrect.

ArcMAP was used to extract points from the DEM at the location of a discrete depth value. Once all data were converted to CGVD28, a simple comparison of depths provided insight into the accuracy of the DEM.

2.2.5 Orthophoto Mosaics

Aerial photographs were captured by FPI coincident with the lidar collection. A DuncanTech DT4000 digital camera was mounted in a bracket at the rear of the lidar sensor and used to acquire one 24-bit, 4 megapixel color photo per second. The photos were post-processed by FPI into orthophoto mosaics. Table 2 shows the six bays that have orthophoto mosaics (all bays that have lidar coverage have orthophoto mosaics). The priority for FPI during the flights was lidar collection, and as a result, some of the aerial photos have quality issues including glint, cloud shadow, and surface roughness of the sea (Fig.3).

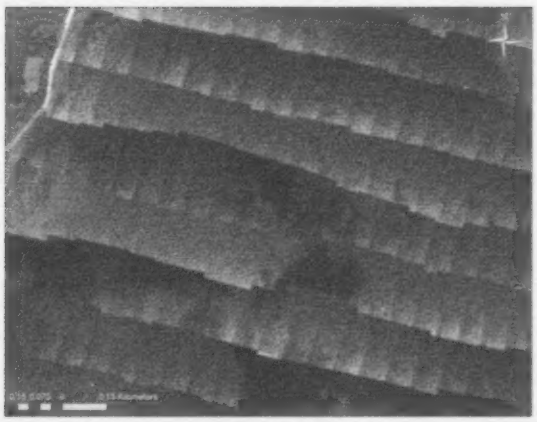

Figure 3: Orthophoto mosaic in St Mary's Bay, Prince Edward Island showing poor aerial photo quality. The southern edges of the individual orthophotos are affected by glint; dark patches near the center of the image are likely cloud shadow.

2.3 EELGRASS

2.3.1 FPI Eelgrass From Orthophoto Frames

Areas identified as having eelgrass coverage were delineated by FPI with enclosing polygons interpreting primarily the orthophoto frame imagery prior to mosaicking. Results relied on bottom visibility (due to water clarity and depth) and the FPI Data Analyst's interpretation. The individual aerial photo frames were used to identify eelgrass to overcome glint and shadow issues with the orthophoto mosaic imagery, an example of which can be seen in Fig.3. Groundtruthing for this 2001 data was conducted in St. Mary's Bay only.

2.3.2 Environment Canada and DFO

Environment Canada classified eelgrass in eight bays in New Brunswick using a combination of remote sensing images and field sampling (Table 4). Aerial photography and satellite imagery were used to classify eelgrass according to quality, or coverage; the classification schemes are defined in Appendix A. Five of the bays followed Environment Canada's field survey criteria that classify eelgrass as good, medium, or poor quality/absent eelgrass, while Shippagan Bay has used DFO's classification of dense, moderate, thin, or exposed eelgrass. Cocagne and Tabusintac Harbours included a polygon that represents eelgrass presence, but does not indicate quality. Aerial photography and satellite image classification were object-oriented, and conducted using eCognition Developer software (Mahoney, 2011).

DFO conducted visual field surveys of four of the bays (Table 4) during the same season in which the aerial photography had been captured. The field samples were used to assist in photo classification and to assess accuracy. For the remaining four bays, field data were collected along

transects in the bays using a differential GPS positioned towfish holding a video camera. More details on methodology can be found in Appendix A.

Table 4: Summary of Environment Canada (EC) and Department of Fisheries and Oceans (DFO) eelgrass data collection methods and years.

Region	Aerial photography EC	Quickbird satellite EC	Field survey DFO	Video camera DFO	Classification categories*
Miscou Hbr, NB	2009		2009		GQ, MQ, PQ
Tracadie Bay, NB	2009		2009		GQ, MQ, PQ
Richibucto Hbr, NB		2007		2007	GQ
Bouctouche Bay, NB	2009		2009		GQ, MQ, PQ
Shippagan Bay, NB		2007		2007	DE,ME,TE,EE
Neguac Bay, NB	2009		2009		GQ, MQ
Cocagne Hbr, NB	2008			2008	EP
Tabusintac Bay, NB	2008			2008	EP
St. Mary's Bay, PE			2011		EP

*Classification categories: GQ = Good Quality, MQ = Medium Quality, PQ = Eelgrass absent/Poor Quality; DE = Dense Eelgrass, ME = Moderate Eelgrass, TE = Thin Eelgrass, EE = Exposed Eelgrass; EP = Eelgrass Presence.

2.3.3 Eelgrass Coverage Per Bay

Eelgrass coverage per bay was calculated using ArcMAP for both FPI and EC eelgrass coverage by simply summing the area of each eelgrass polygon. A surface area field was computed for the FPI eelgrass polygons using the ArcMAP tool "Zonal Geometry as Table" because, unlike the EC eelgrass data, the FPI data did not include a surface area field. For EC eelgrass, the calculation was done separately for each class of eelgrass, Good Quality, Medium Quality, etc.

2.3.4 Eelgrass Coverage at 1 m Depth Intervals

To calculate the surface area of eelgrass beds in each depth interval, the DEM was rounded up to the nearest integer, as with the area per depth calculation above. Elevations greater than 1 m were rejected to avoid unnecessary computations on land while including the complete intertidal zone, and then the DEM raster was converted to polygons. Next the eelgrass polygons were converted into rasters. The ArcMAP tool, "Zonal Statistics as Table" was used to calculate the area of the eelgrass class within each "zone", or depth interval polygon. This procedure was followed for both the FPI and the EC eelgrass, for each lidar-surveyed bay.

2.4 AQUACULTURE

Data on oyster and mussel aquaculture was compiled from boat surveys conducted by the New Brunswick Department of Fisheries, Agriculture and Aquaculture (DFAA) for each bay in NB and by DFO for St. Mary's Bay in PEI, respectively. Data was collected for each year in which

an eelgrass survey was conducted (see Table 4) for a particular bay, 2007, 2008, 2009 or 2011. In 2011, aquaculture data was also acquired from the orthophoto mosaics obtained in September, 2011 for the bays covered during the lidar survey.

The aquaculture data consisted of lease area and the gear type (e.g. oyster strings, cages, and floating bags), dimensions (Table 5), area and amount present and the estimated biomass in each bay. Lease area was obtained from the appropriate leasing agency (NB leasing and DFO leasing). In this report it is defined as the area occupied by suspension bivalve aquaculture leases where sales have been reported in the last year. Lease area has been stable since 2007 except for Miscou which has not had any reported sales since 2011. The percent of the bay occupied by leases was calculated by dividing the total lease area in a bay by the whole area of the bay (Table 7) multiplied by 100.

For the 2011 aquaculture dataset, the two sources of data (boat surveys and orthophoto mosaics) were compared in terms of aquaculture gear distribution and biomass in each bay.

2.4.1 Aquaculture: Biomass Calculations – Boat Surveys

The biomass was estimated from boat surveys conducted by DFAA and DFO for each bay in NB and PEI, respectively. For NB oysters, all gear present in a bay was tallied and then each gear type was converted to a standard oyster bag equivalent (Table 5) to obtain the total number of bags for each bay. Biomass per bag was estimated to be 6.04 kg by Comeau et al. (2006) as described in their equation:

$$bm = \sum_{T=T1}^{T4} M_T \times D_T \times P_T = 6.04\ kg$$

where bm is the mass of one oyster bag, T is size category from 1 to 4 based on shell height. For each category, M is the average weight of one oyster, D is the average number of oysters contained in each bag and P is the percentage present in a typical lease. For PEI mussels, biomass was obtained by multiplying the number of socks by an average weight of 7.6 kg per sock (Drapeau et al. 2006). Aquaculture gear area for each bay is the sum of each gear type surface area multiplied by the total number of gear units of that type.

Table 5. Approximate dimension, surface area and oyster bag equivalence of each aquaculture gear type. For oyster gear, dimension is length × width × height. For mussel socks, dimension is length × radius.

Gear Type	Gear dimension (m)	Gear surface area (m^2)	Oyster bag equivalent
Floating Oyster Bag	0.8 × 0.4 × 0.1	0.32	1
Sub-Surface Oyster Cages	0.8 × 0.4 × 0.4	0.32	4
Oyster String Cages	1.8 × 0.9 × 0.6	1.62	16
OysterGro Cages	1.47 × 0.91 × 0.15	1.34	6
Dark Sea Cages	0.6 × 0.6 × 0.09	0.37	10
Oyster Table	0.8 × 1.2 × 0.2	0.96	6
Mussel Sock	1.83 × 0.07	0.015	n/a

2.4.2 Aquaculture: Biomass and Depth Calculations – Orthophoto Mosaics

For 2011, biomass was also calculated by interpreting and measuring line length and spacing on the orthophotos and using information on cage dimensions and distribution, and biomass per bag. Biomass per bag was estimated to be 6.04 kg as described in Comeau et al. (2006) and Comeau 2013.

In bays for which a DEM and digitized aquaculture data exist, the average depth at the aquaculture gear (longlines) was calculated in ArcMAP using the extraction spatial analyst tool.

2.4.2.1 Oyster Collector Lines

Collector lines are temporarily strung out between August and October outside aquaculture lease areas to collect oyster spat on various structures such as Chinese hats (Fig.4). The spat are used as seed to begin next season's aquaculture crop. Spat biomass was not calculated. Figure 5 shows collector lines in Bouctouche Bay as they appear in the orthophoto. Figure 6 shows the interpreted and digitized lines.

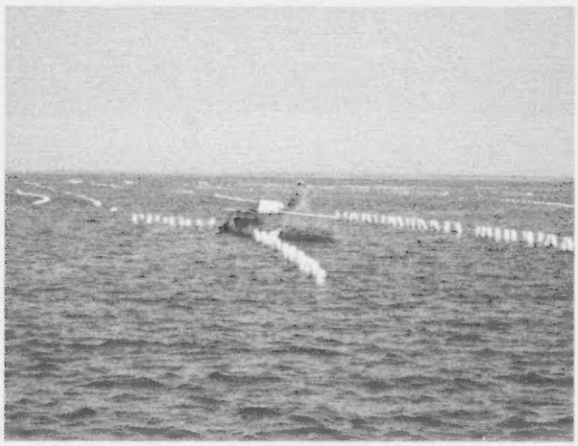

Figure 4: Collector lines in Bouctouche Bay, New Brunswick.

Figure 5: Collector lines in Bouctouche Bay, NB seen in the orthophoto mosaic from September, 2011.

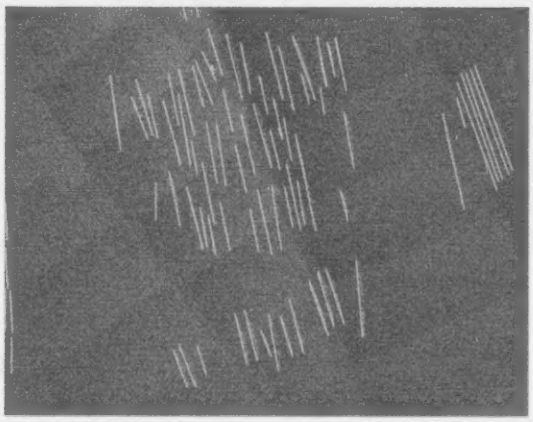

Figure 6: Orange lines are interpreted and digitized collector lines in Bouctouche Bay, NB.

2.4.2.2 Floating Oyster Bags (Single and Double)

Floating oyster bags were found in all bays except Bedec Bay (the eastern section of Richibucto Bay) in both single and double width lines. Each shallow vexar oyster bag is approximately 0.85 m × 0.40 m × 0.10 m (Doiron, 2006) and represents about 6.04 kg of oyster biomass (Comeau et al., 2006). Figure 7 shows a vexar bag in the foreground with white buoys and Figure 8 shows submerged floating bags with black buoys. Single lines are one bag wide and have 50 bags per line (Figure 9); double lines are two bags wide and have 100 bags per line (Figure 8 and Figure 10).

Figure 7: Floating oyster bags with white buoys; more are seen in the distance.

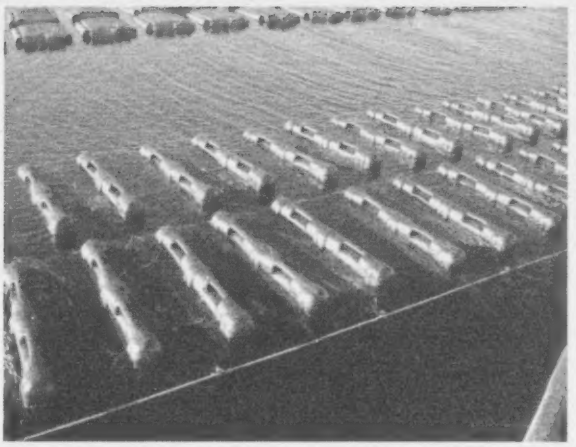

Figure 8: A double-wide line of floating oyster bags.

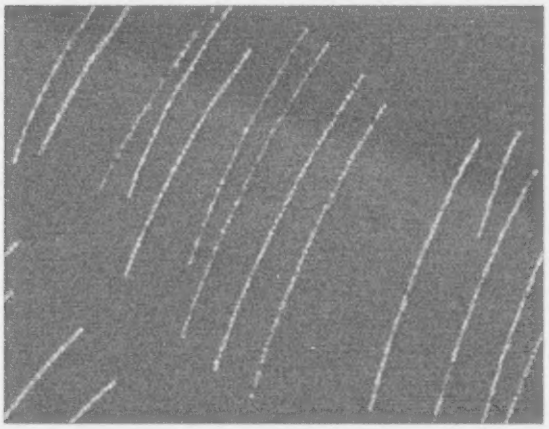

Figure 9: Single-wide floating bags in Tracadie Bay, NB in the FPI orthophoto mosaic from Sept., 2011.

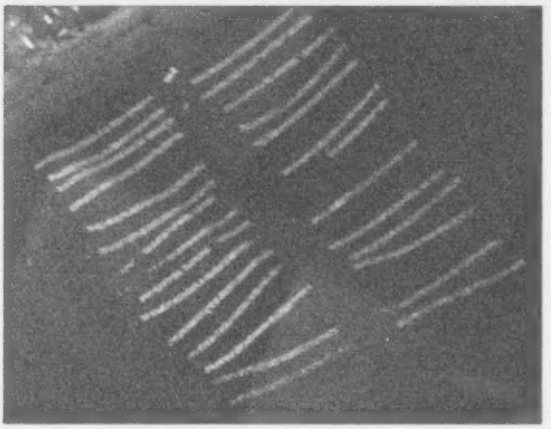

Figure 10: Double-wide floating bags in Richibucto Bay, NB in the FPI orthophoto mosaic from Sept., 2011.

Biomass is estimated based on line length and line width: single or double. Figure 8 shows that spacing of floating bags was very consistent at 1 bag/m for single-wide, and 2 bags/m for double-wide lines:

$$biomass = line\ length \times \frac{\#\ bags}{m} \times \frac{6.04\ kg}{bags}$$

Lines were interpreted and digitized from the orthophotos in a GIS, their lengths were calculated, and then used in the above equation as *line length*. Each line was classed as either single or

double wide, such that # *bags/m* was either 1 bag/m or 2 bags/m for single and double lines, respectively, for use in the above equation.

2.4.2.3 Sub-Surface Oyster Cages

Sub-surface oyster cages, present only in Tracadie Bay, NB, consist of four bags stacked vertically (6.04 kg/bag). Biomass was calculated based on line length and cage spacing as estimated from the orthophotos (Figure 11, Figure 12), as follows:

$$biomass = line\ length \times \frac{1\ cage}{4m} \times \frac{4\ bags}{cage} \times \frac{6.04\ kg}{bag}$$

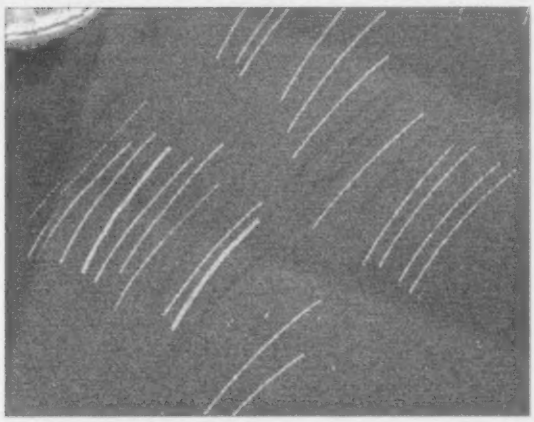

Figure 11: Dark lines are sub-surface oyster cages in the Tracadie Bay, NB orthophoto mosaic from Sept., 2011.

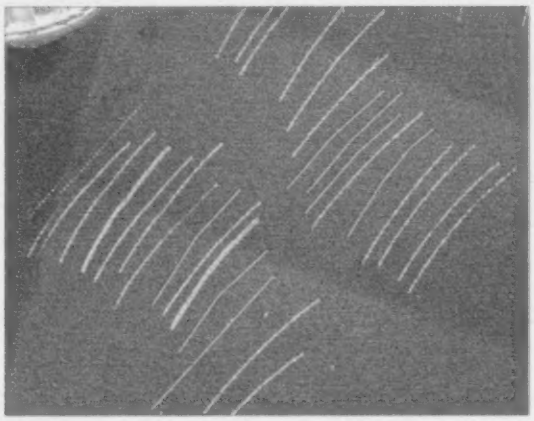

Figure 12: Orange lines are interpreted and digitized sub-surface oyster cages in the Tracadie Bay, NB orthophoto mosaic from Sept., 2011.

2.4.2.4 Oyster String Cages

Oyster string cages contain between ~3200 and ~4500 oysters (60 kg and 84 kg) cemented in clusters of three to strings (Fig. 13). There are 8-12 cages per line.

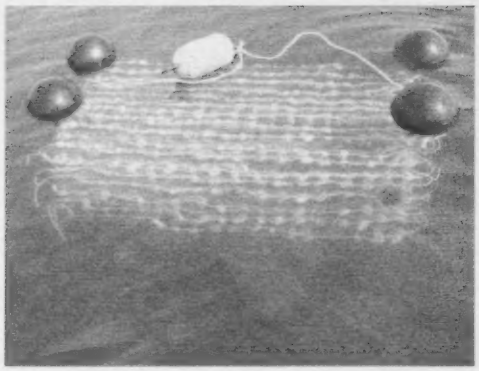

Figure 13: Oyster string cages.

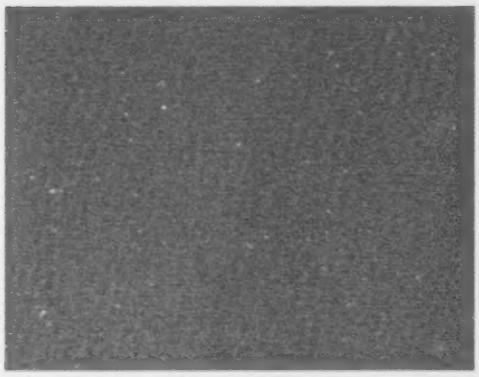

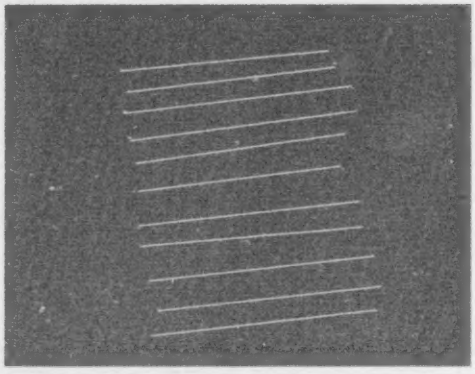

Figure 14: The white end buoys of the oyster string cages are barely visible in the left orthophoto; the lines digitized between the buoys in the image on the right represent the oyster string cages in the Caraquet Bay, NB orthophoto mosaic from Sept., 2011.

Biomass was estimated for each bay based on cage spacing and line length. Oyster string cages were easy to interpret in the orthophotos (Fig. 14), allowing an accurate measurement of spacing and length. The following equation was used to estimate biomass:

$$biomass = line\ lenght \times \frac{1\ cage}{4m} \times \frac{kg}{cage}$$

An estimate for cage spacing of 1 cage per 4 m was made for Tracadie and Caraquet Bays (the only bays that contained oyster string cages), and each line of oyster string cages was measured individually. In Tracadie Bay each cage contained 60 kg of oyster biomass (*kg/cage* = 60 kg); Caraquet cages contained 84 kg (*kg/cage* = 84 kg).

2.4.2.5 Oystergro Cages

Oystergro cages contain six bags of oysters per cage (three wide and two deep), with each bag the equivalent of approximately 6.04 kg of oysters. They are suspended by two long, dark and narrow floats (Figure 15 and Figure 16). In the bays surveyed, there were two typical setups: a longer line with shorter cage spacing and more cages per line (Figure 17), and a shorter line with fewer cages spaced farther apart (Figure 18). Oystergro cages were present in all six of the surveyed bays.

Figure 15: Oystergro cages in Bouctouche Bay, NB.

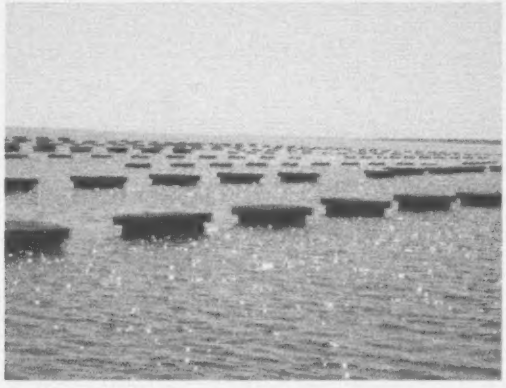

Figure 16: Upside-down Oystergro cages.

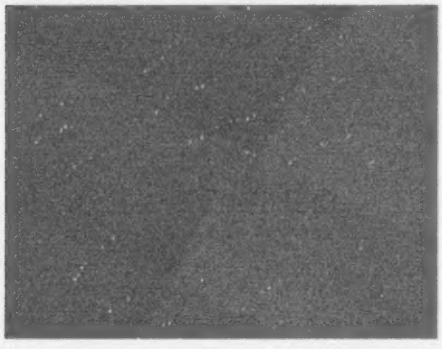

Figure 17: Oystergro cages in Tracadie Bay, NB with 10-12 cages per line spaced 3 m apart; average line length is 43 m. Image is FPI orthophoto mosaic from Sept., 2011.

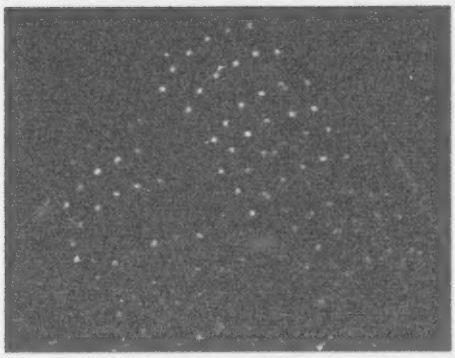

Figure 18: Oystergro cages in Caraquet Bay, NB with 6 cages visible per line spaced 6 m apart; average line length is 30 m.

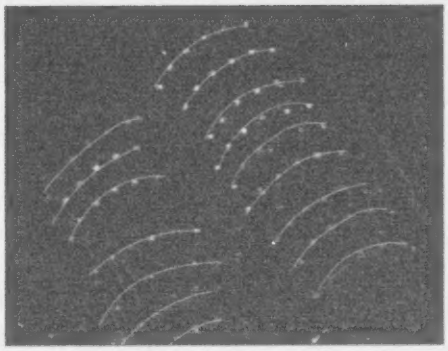

Figure 19: Digitized Oystergro cages seen in the Caraquet Bay, NB orthophoto mosaic from Sept., 2011.

Biomass was calculated based on cage spacing and line length as follows:

$$biomass = line\ lenght\ x\ cage\ spacing \times \frac{6\ bags}{cage} \times \frac{6.04\ kg}{bag}$$

An estimate for cage spacing was made for each bay, and each line of Oystergro cages was measured individually (Figure 19).

2.4.2.6 Dark Sea Oyster Cages

Dark sea cages (Figure 20) can have many levels (ten is a typical number) each containing the equivalent of one 6.04 kg bag. Lines tend to be 30 m long with 7 or 10 cages per line. Digitized lines were 30 m on average, so the lower estimate of cages per line was used in the following biomass calculation:

$$biomass = \frac{10\ cages}{line} \times \frac{10\ levels}{cage} \times \frac{6.04\ kg}{level}$$

Figure 20: Dark sea oyster cages.

2.4.2.7 Mussel Longlines

Mussel longlines, present only in St Mary's Bay, PEI, are a single line with several drop lines, socks, or sleeves, containing mussels and extending to 1.83 m deep (Figure 21). In St Mary's Bay the lines were on average 122 m long, with 0.45 m between socks, and 7.6 kg of mussels per sock (Drapeau et al., 2006), such that biomass was calculated based on measured line length as follows:

$$biomass = line\ length \times \frac{10\ socks}{0.45m} \times \frac{7.6\ kg}{sock}$$

Mussel longlines were interpreted from the orthophotos to be both floating on the surface as well as submerged below the surface, where each had white end marker buoys (Fig. 22). The floating longlines seen in Figure 23 show an example of longlines with and without digitized aquaculture; the left image, when compared to the previous figure, shows how the longline appearance can differ across the bay.

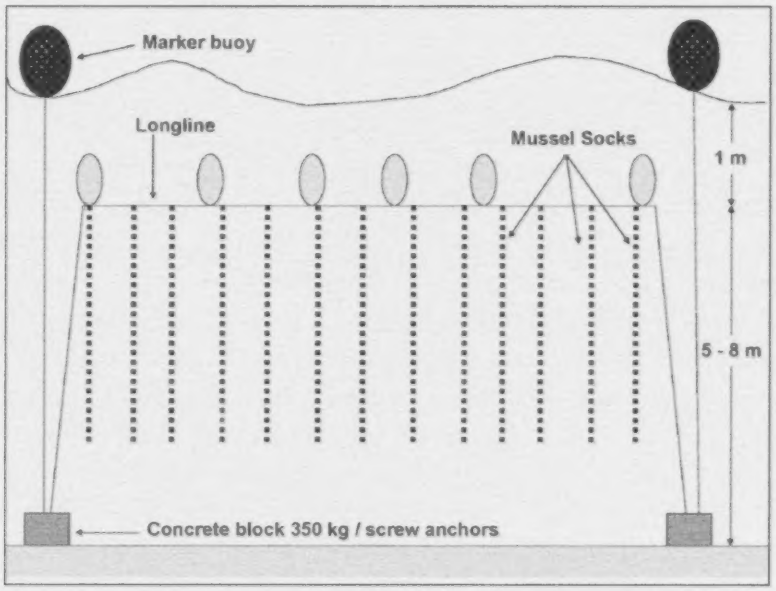

Figure 21: Typical design of a Prince Edward Island longline mussel farming setup from Drapeau et al. 2006.

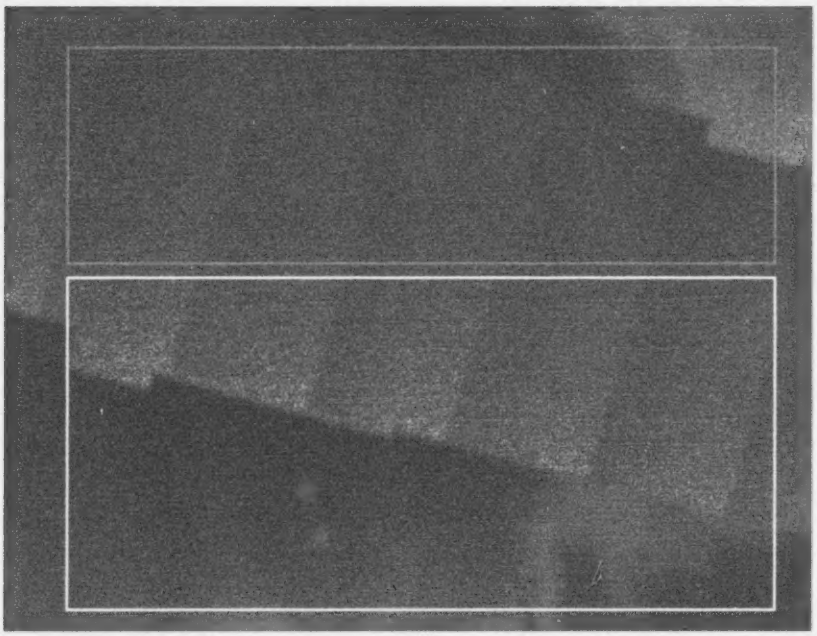

Figure 22: Mussel longlines in St Mary's Bay, PEI. The red box shows submerged lines with white end buoys visible; the yellow box shows floating longlines.

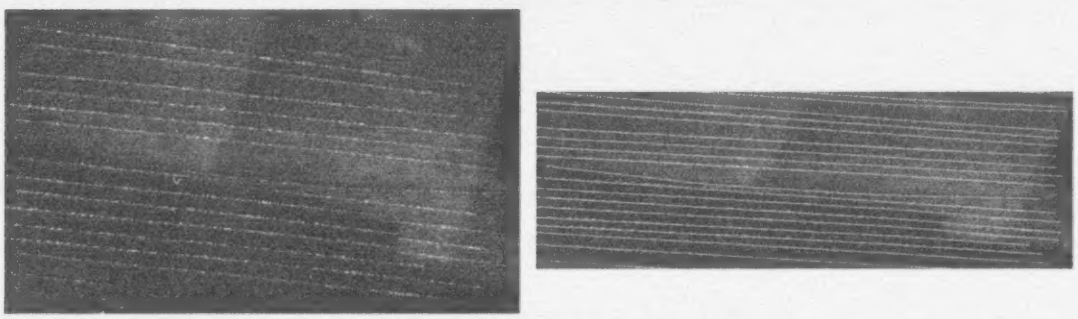

Figure 23: Left: Mussel longline buoys in St Mary's Bay, PEI, seen in orthophotos from FPI, Sept. 2011. Right: Digitized mussel longlines.

3. RESULTS

Section 3.1 contains results of the DEM surface area calculations, and figures of the DEM and CSR with 1 m depth intervals for each bay. In Section 3.2 tables present results of eelgrass area per depth for each bay, and total eelgrass area per bay. Figures of the DEMs with FPI eelgrass coverage and CSRs with EC/DFO eelgrass coverage are presented. Aquaculture results are presented in Section 3.3 in tables containing information on aquaculture spacing, line length, biomass of each aquaculture type, etc., for each bay. Figures show orthophotos with digitized aquaculture lines colour-coded by aquaculture type.

The results for Richibucto Bay are presented as three smaller regions: Aldouane, Bedec, and Richibucto (Figure 24). The DEM provided by FPI was for the entire region, which has been referred to as Richibucto to this point in the report, but to present and discuss the eelgrass and aquaculture results it has been subdivided.

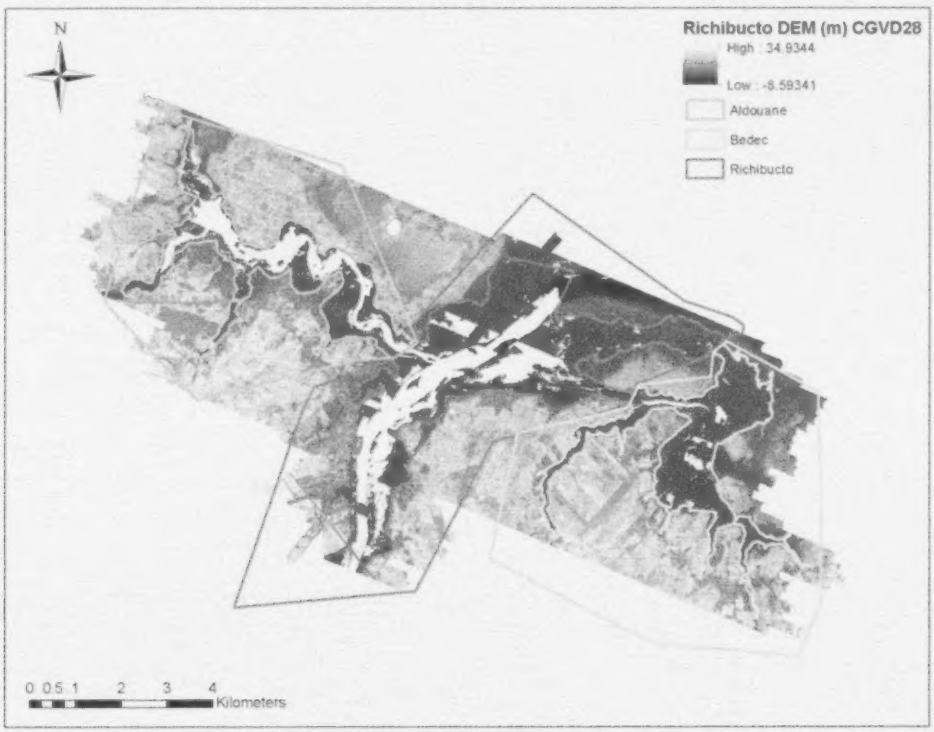

Figure 24: The extent of the Digital Elevation Model (DEM) shows the region, referred to as Richibucto that was collected by FPI. For biomass and eelgrass calculations, Richibucto has been divided into three smaller regions: Aldouane, Bedec, and Richibucto. The polygonal outlines were used to actually subdivide Richibucto, as the FPI coastline outlines are smaller than the DEM.

3.1 BATHYMETRY

3.1.1 Surface Area of DEM Depth Intervals

Table 6 shows the results of the DEM depth interval surface area calculations described in Section 0 (depth interval definitions are shown in Table 1). The total area, *Sum Depth Area*, is the sum of the surface area of the DEM depth intervals (0 to -10 m). Caraquet Bay has the greatest lidar-detected total surface area (3614 ha) while Aldouane has the smallest (410 ha). Aldouane also reported the shallowest depths (3 m), while Caraquet, Tracadie, and St Mary's reported the deepest depths (~9 m); lidar penetration did not exceed 10 m in any bay. In general, depth interval areas decreased with depth, such that the -1 – 0 m interval had the largest area, and the deepest interval had the smallest area. The exception to this trend was the shallowest interval (0 – 1 m), which had less area than the -1 – 0 m interval.

Table 6: Surface area of DEM depth intervals (ha). *Sum Depth Area* is the sum of the area in each depth interval, except 0-1 m interval.

Depth intervals	Surface area of DEM depth intervals (ha)											
	0 – 1 m	-1 – 0 m	-2 – -1 m	-3 – -2 m	-4 – -3 m	-5 – -4 m	-6 – -5 m	-7 – -6 m	-8 – -7 m	-9 – -8 m	-10 – -9 m	Sum Depth Area
Caraquet	274	1144	818	548	366	267	197	133	103	35	2.2	3614
Miscou	226	575	549	642	309	80	4.8	7.3	3.0	0.11		2170
Tracadie	883	2264	173	62	27	21	13	4.7	0.24	0. 13	0.0002	2565
Richibucto	172	675	302	78	30	28	26	26	5.4	0. 46		1170
Aldouane	70	282	128	0. 83								410
Bedec	155	341	229	35.6	0. 29							605
Bouctouche	196	1048	800	730	74	18	2.2	0. 54				2673
St Mary's	7400	34300	29400	32000	25300	24100	10900	3900	1800	1000	450	1632

3.1.2 Total Area Comparisons

The area of the polygons provided by FPI is summarized in Table 7, and is referred to as the *Whole Area* of each bay, in contrast to the area detected by the lidar. Table 8 shows some comparisons between *Sum Depth Area* (the sum of the surface area of DEM intervals from Table 6 and *Whole Area*.

Equation 1: Definitions of surface areas used to determine proportion of bay detected by Lidar.

Whole Area = areas in Table 7, area of polygons in Figure 1

Sum Depth Area = sum of DEM surface area contours in Table 5

Difference1 = Whole Area – Sum Depth Area

$$\%Difference1 = 100 \times \frac{Difference1}{Whole\ Area}$$

Table 7: Area of Bays shown in Figure 1, known as *Whole Area.* Although not all the bays in Figure 1 were surveyed, the area of the polygon provided by FPI was calculated to be used for various calculations in the Results section.

Bay Name	Area (ha)
Caraquet	6674
Miscou	3225
Tracadie	3123
Richibucto	1588
Aldouane	692
Bedec	649
Bouctouche	3015
Shippagan	8115
Tabusintac	3104
Cocagne	2009
Neguac	3813

Difference1 represents the area of the bay that was not detected by lidar, and ranged from ~3100 ha (Caraquet) to less than 100 ha (Bedec), with an average difference of ~800 ha. *%Difference1* highlights the difference relative to the total surface area of each bay. For example, *Difference1* = 282 ha and *%Difference1* = 41% for Aldouane. This means that the lidar did not penetrate all the way to the bottom in 41% of Aldouane; equivalently, the lidar *did* detect the bottom in 59% of Aldouane. *%Difference1* ranged from 7% in Bedec to 46% in Caraquet, with an average value of 26%. These calculations assume *Whole Area* is the best approximation of the correct area of each bay.

Table 8: *Difference1* represents the area of the bay that was not detected by the lidar. *%Difference1* shows the difference relative to *Whole Area*, the closest approximation available for the correct area of each bay.

	Difference1 (ha)	%Difference1 (%)
Caraquet	3059	46
Miscou	1055	33
Tracadie	559	18
Richibucto	418	26
Aldouane	282	41
Bedec	44	7
Bouctouche	343	11

3.1.3 Bathymetric Intervals, DEMs and CSRs

Figure 25- Figure 40 show 1 m bathymetric intervals on the DEM and CSR for each bay. The intervals, derived from the DEM, emphasize the slope of the bottom and the distribution of depth in each bay. The variation in the percentage of lidar coverage between bays evident in the figures can be explained by water clarity and the depth of the bay: the laser penetration is limited to 2-3 Secchi depths. Secchi depth is a measure of water transparency, and is typically shallow in muddy or phytoplankton-dense water, and deep in clear water in which the light encounters no obstacles. In clear water the lidar is able to reach the bottom of these shallow bays, but in bays that have low transparency or are clear but deep, gaps in the lidar are evident.

In Caraquet, 46% of the area of Caraquet was not detected by the lidar (Table 8, Figure 25) either because the water was muddy or cloudy, or too deep. In contrast, the absence of large holes in the DEM in Figure 29 suggests that water was clear in Tracadie Bay during the lidar survey and did not exceed 10 m, and Table 8 indicates that only 18% of the area of Tracadie was not detected by the lidar. Further discussion on lidar depth penetration in Caraquet is found in Section 4.1.

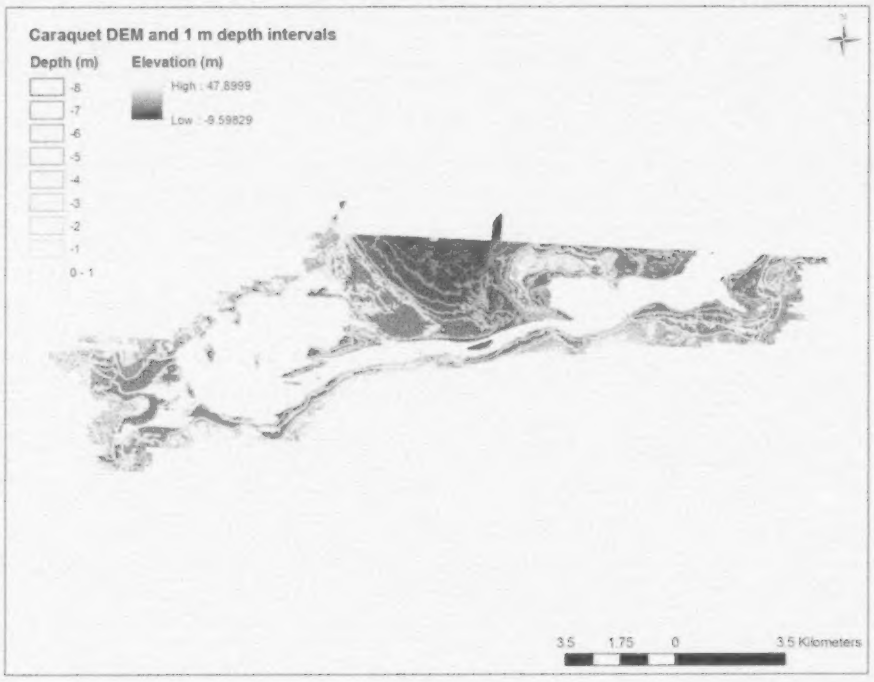

Figure 25: Caraquet DEM and lidar-derived 1 m depth intervals. All depths are CGVD28.

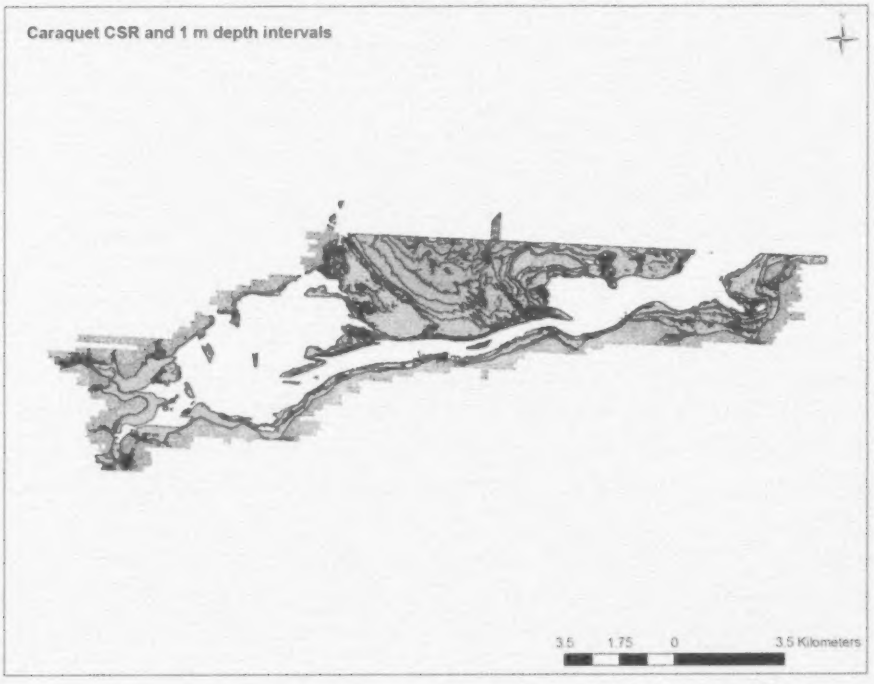

Figure 26: Caraquet 1 m depth intervals on elevation colour-shaded relief (CSR) image.

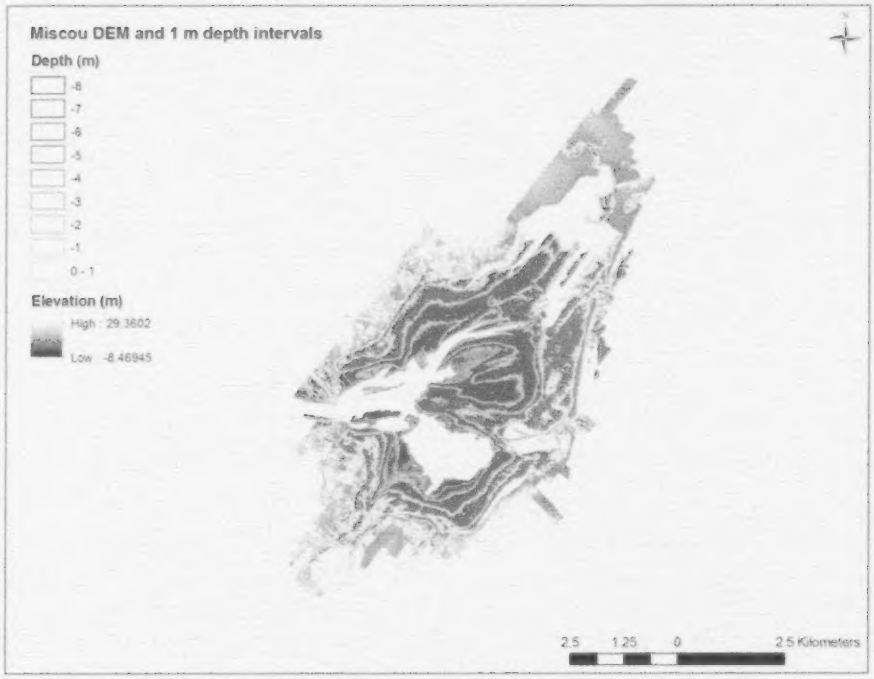

Figure 27: Miscou DEM and lidar-derived 1 m depth intervals. All depths are CGVD28.

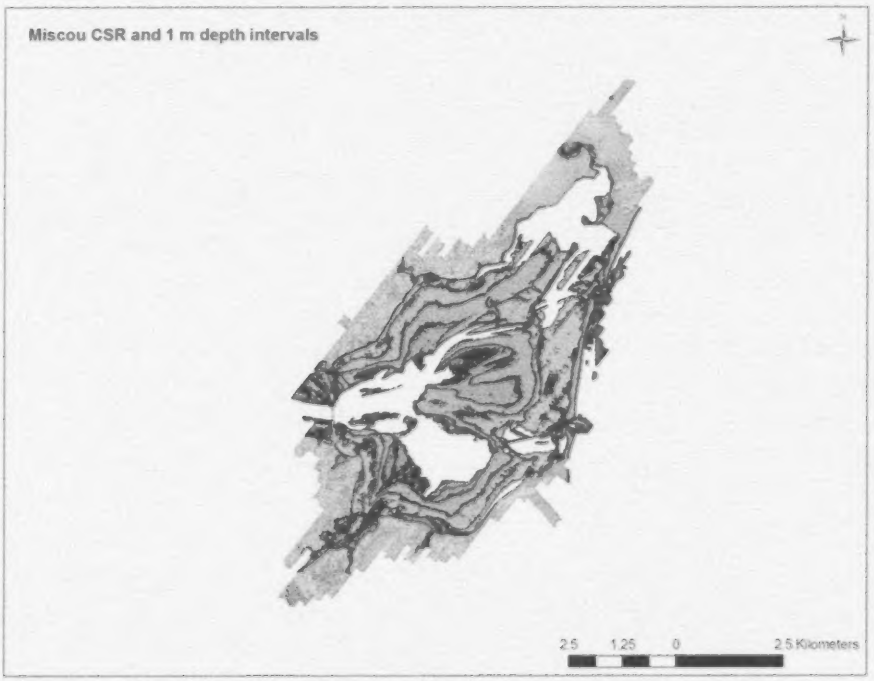

Figure 28: Miscou 1 m depth intervals on elevation colour-shaded relief (CSR) image.

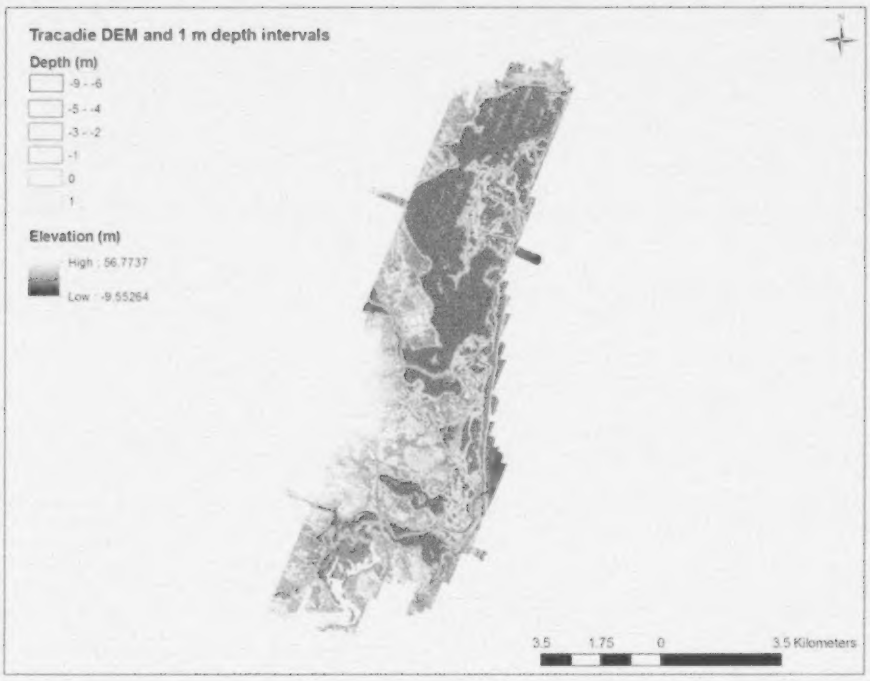

Figure 29: Tracadie DEM and lidar-derived 1 m depth intervals. All depths are CGVD28.

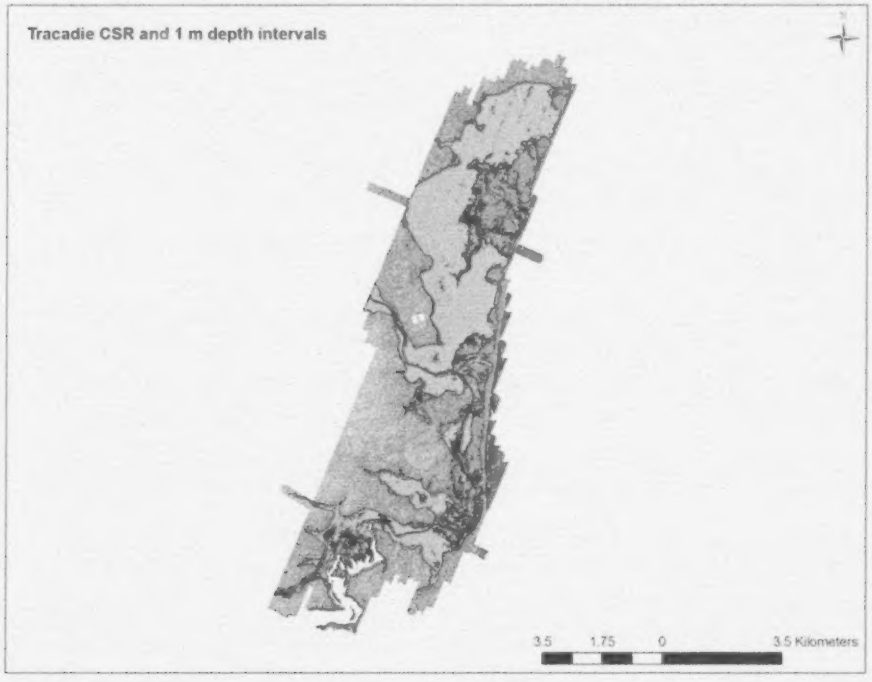

Figure 30: Tracadie 1 m depth intervals on elevation colour-shaded relief (CSR) image.

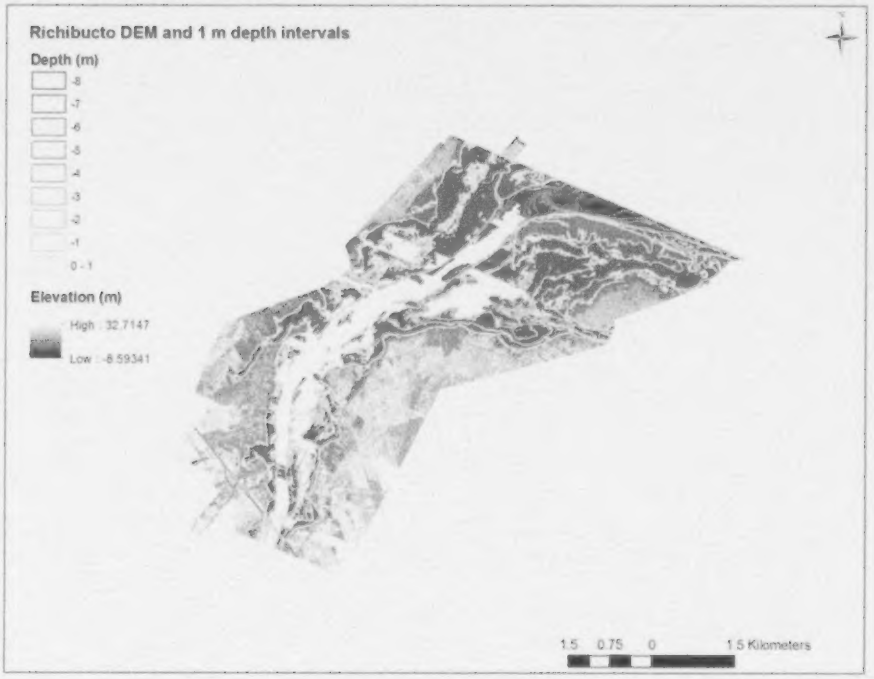

Figure 31: Richibucto DEM and lidar-derived 1 m depth intervals. All depths are CGVD28.

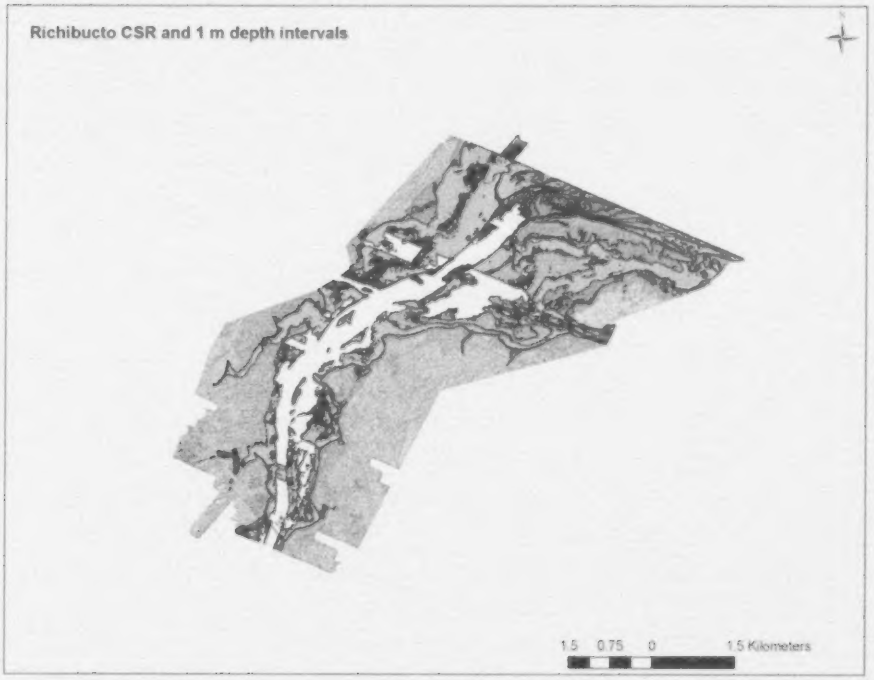

Figure 32: Richibucto 1 m depth intervals on elevation colour-shaded relief (CSR) image.

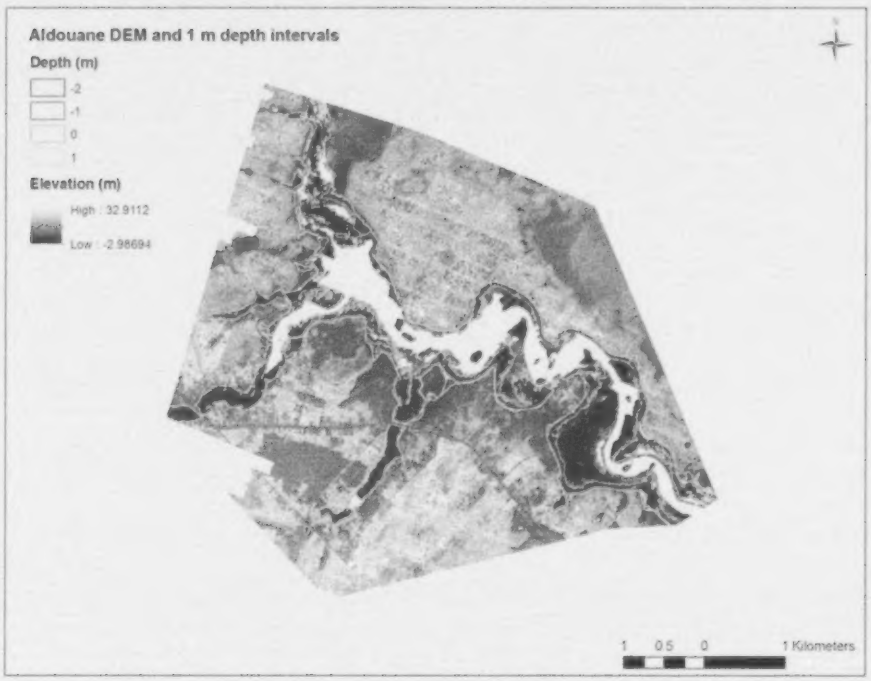

Figure 33: Aldouane DEM and lidar-derived 1 m depth intervals. All depths are CGVD28.

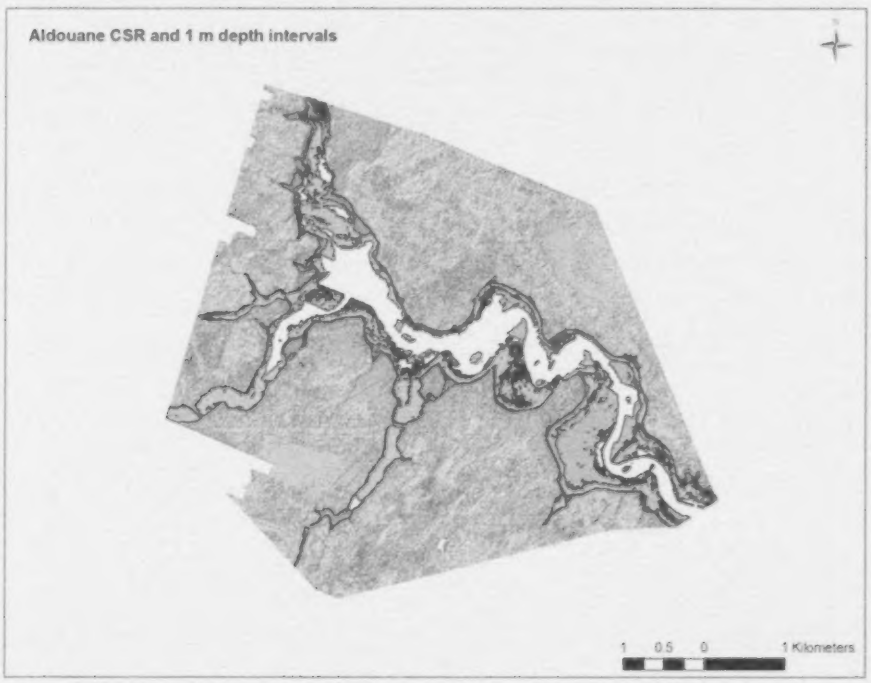

Figure 34: Aldouane 1 m depth intervals on elevation colour-shaded relief (CSR) image.

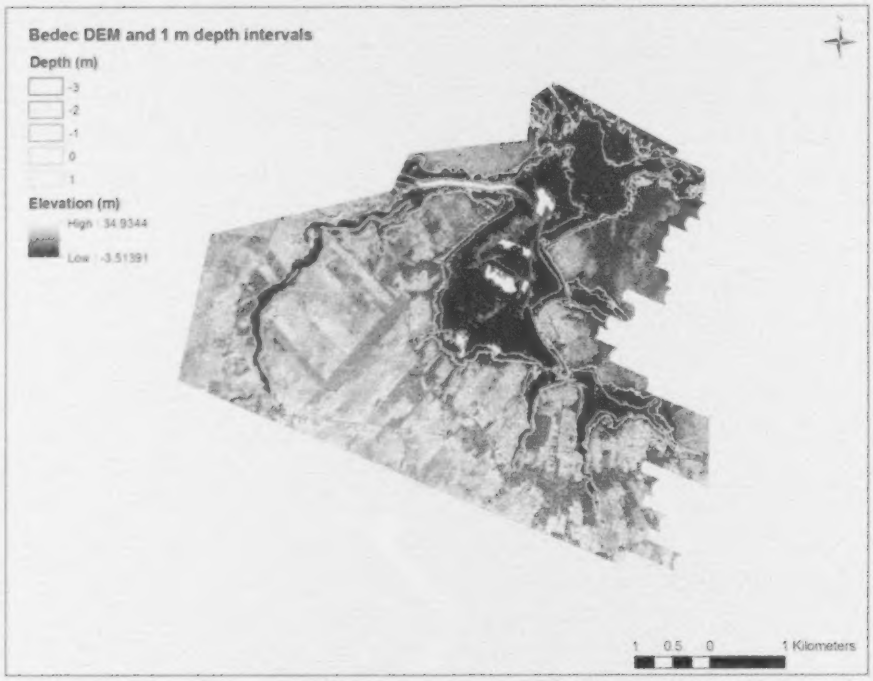

Figure 35: Bedec DEM and lidar-derived 1 m depth intervals. All depths are CGVD28.

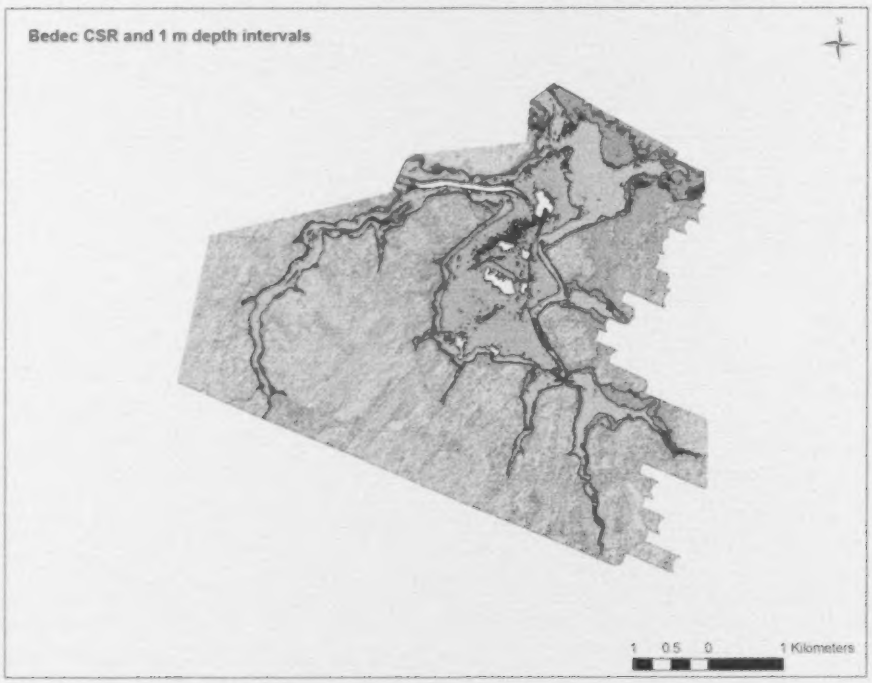

Figure 36: Bedec 1 m depth intervals on elevation colour-shaded relief (CSR) image.

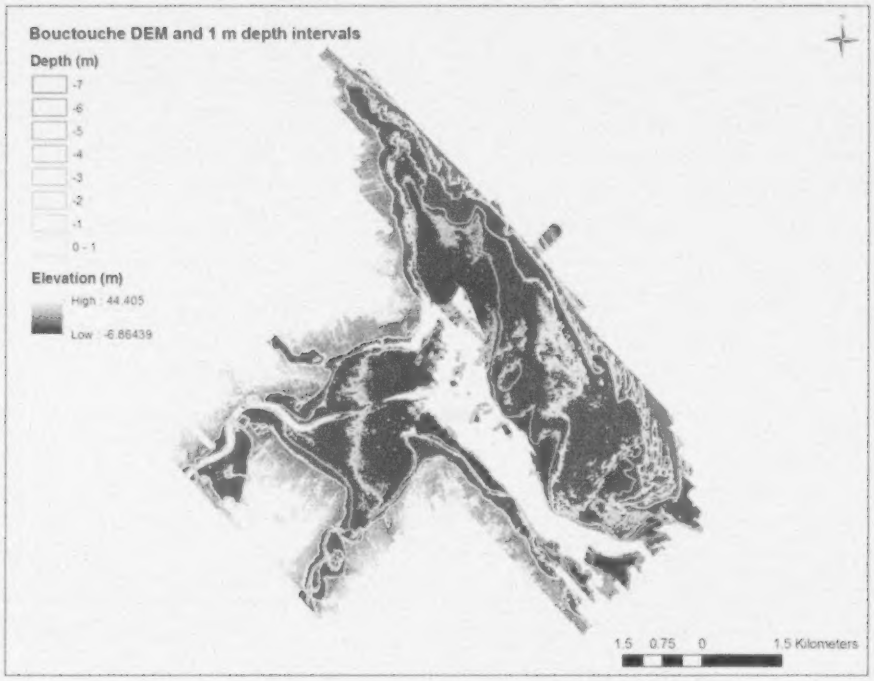

Figure 37: Bouctouche DEM and lidar-derived 1 m depth intervals. All depths are CGVD28.

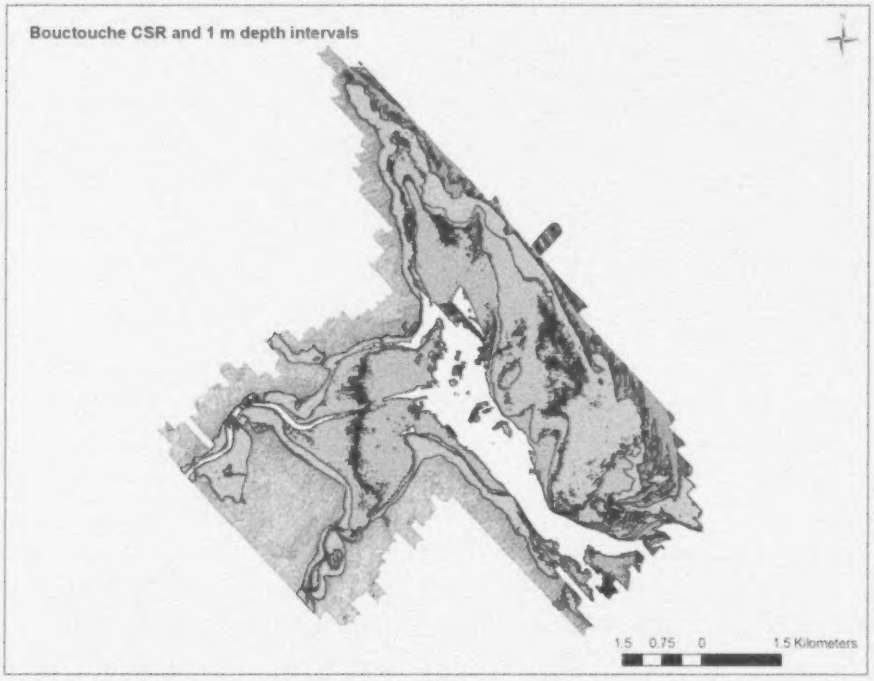

Figure 38: Bouctouche 1 m depth intervals on elevation colour-shaded relief (CSR) image.

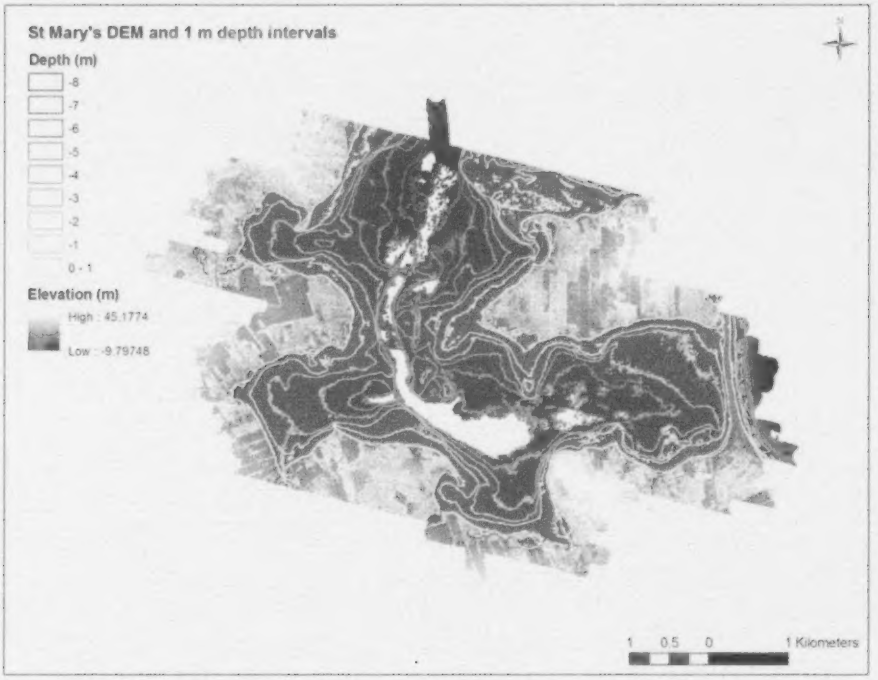

Figure 39: St Mary's DEM and lidar-derived 1 m depth intervals. All depths are CGVD28.

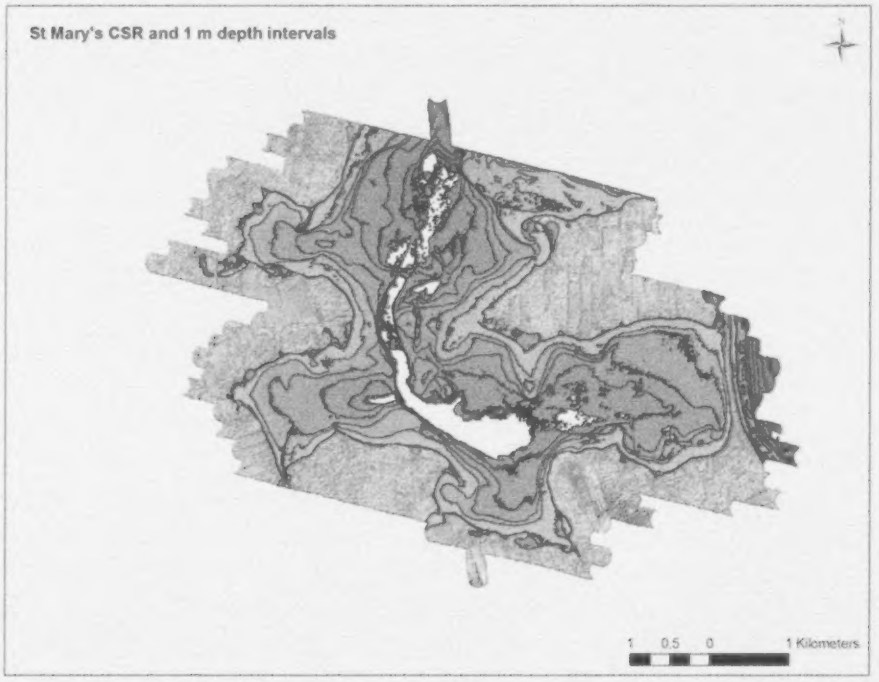

Figure 40: St Mary's Bay 1 m depth intervals on elevation colour-shaded relief (CSR) image.

3.1.4 DEM Comparison/Validation

The bathymetry values of the DEM were compared to various other sources of bathymetry data, from CHS charts to echo soundings. The data available for these comparisons are shown in Table 2 and results of the comparisons are shown in Table 9. Negative values in the table indicate that $z_{comparison}$ was deeper than z_{DEM}. The mean difference between the DEM and the other bathymetry data was less than 1 m, and standard deviations were less than -1.5 m. In the following equation, $z_{comparison}$ is depth from the comparison source, e.g. CHS Chart, echo sounding, etc.

$$\Delta z = z_{comparison} - z_{DEM}$$

The greatest Δz was -8.46 m in Richibouctou Bay, and the mean Δz between the echo sounder data and the DEM was 0.02 m. Vertical datum information for echo soundings and field samples were missing, and MSL was assumed. Conversions from CD to CGVD28 for CHS charts are shown in Table 3.

Table 9: Sources of data for DEM depth comparison. Negative values indicate that $z_{comparison}$ was deeper than z_{DEM}.

	Comparison source ($z_{comparison}$)	Number of points used	Minimum Δz (m)	Maximum Δz (m)	Mean Δz (m)	St. Dev. of Δz (m)
Caraquet	CHS Chart 402401	7	-1.49	3.72	0.79	1.49
Miscou	EC eelgrass pts	85	-4.79	1.91	-0.09	0.93
Tracadie	EC eelgrass pts	101	-2.04	0.06	-0.24	0.47
Richibucto*	DFO echo sounder	36438	-4.31	2.06	-0.61	0.47
Richibucto*	CHS Chart 490902	103	-8.46	6.30	0.02	1.22

***: referring to entire region of Richibucto rather than the sub-divided Richibucto, Aldouane, and Bedec.**

3.2 EELGRASS

The presence of eelgrass in each bay was determined by FPI using the orthophoto frames and used to define eelgrass polygons, as described in Section 2.3.1. EC/DFO eelgrass classification is based on a combination of field samples, satellite imagery, aerial photos, and in situ photos summarized in Table 4 and outlined in Section 2.3.2.

Figures 41 to 52 show FPI and EC/DFO eelgrass coverage for each bay. Comparisons between FPI and EC eelgrass surface area must be made with caution due to differences in data collection methods and temporal differences. Additionally, EC PQ classification is somewhat ambiguous, as it contains Poor Quality or Absent Eelgrass (see APPENDIX A:), making it difficult to compare to the FPI classification which indicates only a presence of eelgrass and no quality indicator.

Estimations of eelgrass surface area per depth interval for FPI and EC classifications are presented in Table 10. In general, eelgrass surface area decreased with depth after 0 m for all bays and all classifications. Eelgrass area per depth was proportional to area per depth (Table 6), such that in Miscou, where the -2 m interval had more surface area than the 0 m interval, there was more eelgrass at -2 m than at 0 m. Eelgrass extended to the deepest depth measured by the lidar in half of the bays (Caraquet, Richibucto, Aldouane, and Bedec). Nonetheless, 95% of eelgrass area was found at depths less than 4m. Table 11 presents secondary calculations for eelgrass coverage; parameters used are defined below:

Equation 2: Definitions of eelgrass surface area comparisons.

Total Polygon Area=sum of eelgrass area per depth interval defined in Table 1

Whole Area=areas in Table 7, Figure 1

Summed Total = Sum Eelgrass Area per Depth

Difference2 = difference between Total Polygon Area and Summed Total

No Data = % of eelgrass polygon that is No Data= Difference2/Total Polygon Area

%eelgrass = % of bay that has eelgrass = Total Polygon Area/Whole Area

Table 10: Eelgrass surface area (ha) per 1 m depth interval. See Appendix A for eelgrass quality definitions.

		Eelgrass surface area (ha)										
Bay name	**Depth intervals**	**1 m**	**0 m**	**-1 m**	**-2 m**	**-3 m**	**-4 m**	**-5 m**	**-6 m**	**-7 m**	**-8 m**	**-9 m**
Caraquet	**FPI**	59	733	499	339	275	246	195	132	103	26	0. 38
Miscou	**FPI**	74	351	224	90	24	8.9					
	EC GQ	14	312	398	503	235	36	0. 15				
	EC MQ	30	59	82	26	0.045						
	EC PQ	13	35	18	14	19	20	2.6	6.4	2.4		
Tracadie	**FPI**	265	1673	90	2.2	0.03						
Tracadie North	**EC GQ**	13	361	0.38								
	EC MQ	84	601	0. 36	0.07	0.005						
	EC PQ	244	656	10	13	1.9	0.022					
Richibucto	**FPI**	5.6	552	257	61	6.4	5	0.58	0. 14	0.017	0.017	
	EC GQ	2.9	292	113	13	2.0	0. 7	0. 55	0. 38	0.15	0.11	
Aldouane	**FPI**	7.7	249	123	0. 23							
	EC GQ	0. 90	143	43	0.055							
Bedec	**FPI**	11	289	226	35	0. 28						
	EC GQ	2.8	174	181	29	0. 10						
Bouctouche	**FPI**	6.0	733	392	35	1.15						
	EC GQ	0.3	376	199	5.2	0. 43						
	EC MQ	0. 9	134	284	516	3.5						
	EC PQ	3.3	149	27	183	2.6						
St Mary's	**FPI**	0. 5	101	121	109	35	3.6	0.048				

Table 11: Comparisons of different calculations of eelgrass polygons. Total Polygon Area=sum of eelgrass area per depth interval; Whole Area=areas in Table 7, Figure 1; Summed Total = Sum Eelgrass Area; Difference2 = difference between Total Polygon Area and Summed Total; No Data = % of eelgrass polygon that is No Data= Difference2/Total Polygon Area.

Bay name		Total Polygon Area (ha)	Summed Total (ha)	Difference2 (ha)	% No Data
Caraquet	FPI	4448	2607	1841	41
Miscou	FPI	909	771	138	15
	EC GQ	2001	1499	502	25
	EC MQ	233	197	36	15
	EC PQ	365	131	235	64
Tracadie	FPI	2177	2030	147	7
Tracadie North	EC GQ	376	375	1	0
	EC MQ	711	686	25	4
	EC PQ	955	932	22	2
Richibucto	FPI	1164	885	279	24
	EC GQ	1030	425	605	59
Aldouane	FPI	597	379	218	36
	EC GQ	440	187	252	57
Bedec	FPI	609	561	49	8
	EC GQ	467	387	80	17
Bouctouche	FPI	1180	1167	13	1
	EC GQ	595	580	14	2
	EC MQ	1124	938	186	17
	EC PQ	853	608	245	29
St Mary's	FPI	374	370	4	1
Shippagan	EC DE	1286			
	EC ME	1435			
	EC TE	543			
	EC EE	293			
Neguac	EC GQ	1295			
	EC MQ	580			
Cocagne	EC	935			
Tabusintac	EC	1326			

3.2.1 Total Eelgrass Area

The largest *Total Polygon Area* was FPI's estimate of eelgrass in Caraquet Bay (~4500 ha). The largest area classified as good quality by Environment Canada (EC QG) was in Miscou (~2000 ha). In Richibucto, Aldouane and Bedec, the FPI and EC GQ estimates for eelgrass agreed very well, to within ~150 ha. In Miscou and Bouctouche, the FPI eelgrass area was less than the sum of EC GQ and EC MQ. In Tracadie, the FPI estimate was conducted for the northern and southern sections of the bay while Environment Canada estimated eelgrass in the northern section only. This northern section had a greater proportion of poor quality/absent eelgrass than medium or good quality. In Bouctouche eelgrass classification was dominated by medium quality, followed by poor quality/absent and good quality.

Eelgrass surface areas for bays not surveyed by lidar are also included in Table 11. In Shippagan Bay, there was more dense and moderate eelgrass cover (EC DE and EC ME) than thin or exposed eelgrass (EC TE and EC EE). In Neguac, there was twice as much good quality eelgrass as there was medium quality.

3.2.2 Overlaps with No Data

The *Summed Total* defined in Equation 2 and shown in Table 11 is the sum of the eelgrass area at each depth interval. This value differs from *Total Polygon Area* because the eelgrass polygons overlap areas of No Data in the DEM, and the eelgrass per depth interval is not calculated for areas in the DEM of No Data. *Difference2* is the difference between *Total Polygon Area* and *Summed Total*, and *%No Data* represents what percentage of the eelgrass polygon overlaps sections of the DEM that are No Data. For Caraquet (Figure 41), *Difference2* was equal to ~1800 ha, meaning that there are 1800 ha of eelgrass polygon that overlaps No Data values in the DEM, representing 41% of the total area of Caraquet (Table 11). This is relevant because it means that the estimates of eelgrass area per depth are only as accurate as the DEM. For example, 500 ha of EC GQ eelgrass in Miscou overlaps with No Data values in the DEM, meaning that an area of 500 ha is potentially "missing" from the eelgrass surface area per depth calculations.

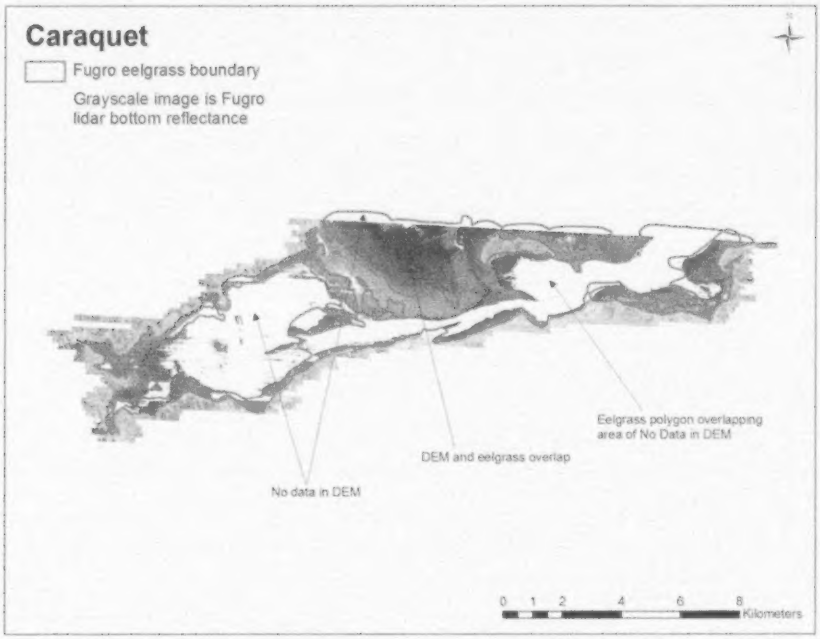
Caraquet
Fugro eelgrass boundary
Grayscale image is Fugro lidar bottom reflectance
Eelgrass polygon overlapping area of No Data in DEM
DEM and eelgrass overlap
No data in DEM
0 1 2 4 6 8
Kilometers

Figure 41. Caraquet FPI lidar bottom reflectance and eelgrass boundary. Arrows point to areas in the DEM with No Data, areas where the eelgrass polygon overlaps the DEM, and where the eelgrass polygon overlaps an area of No Data in the DEM.

3.3.3 Eelgrass Coverage per Bay

As was done in the case of Richibucto Harbour, the results for Shippagan Bay and Tracadie Bay are presented in smaller regions (Figure 39). The area of eelgrass presence is calculated from FPI and EC/DFO data for each bay. The percent of each bay that has eelgrass presence is estimated by *% eelgrass* in Table 12. This calculation is not based on the DEM, but is a simple calculation of *Total Polygon Area / Whole Area* of a bay (Equation 2). Bedec has the highest coverage, indicating that 94% of Bedec has some eelgrass presence, according to the FPI classification. St Mary's has the least amount of eelgrass presence, according to FPI, at 26%. According to EC classifications, 74% of St-Simon North is covered with either good or medium quality eelgrass, while only 27% of Shippagan South has good or medium quality EC eelgrass presence.

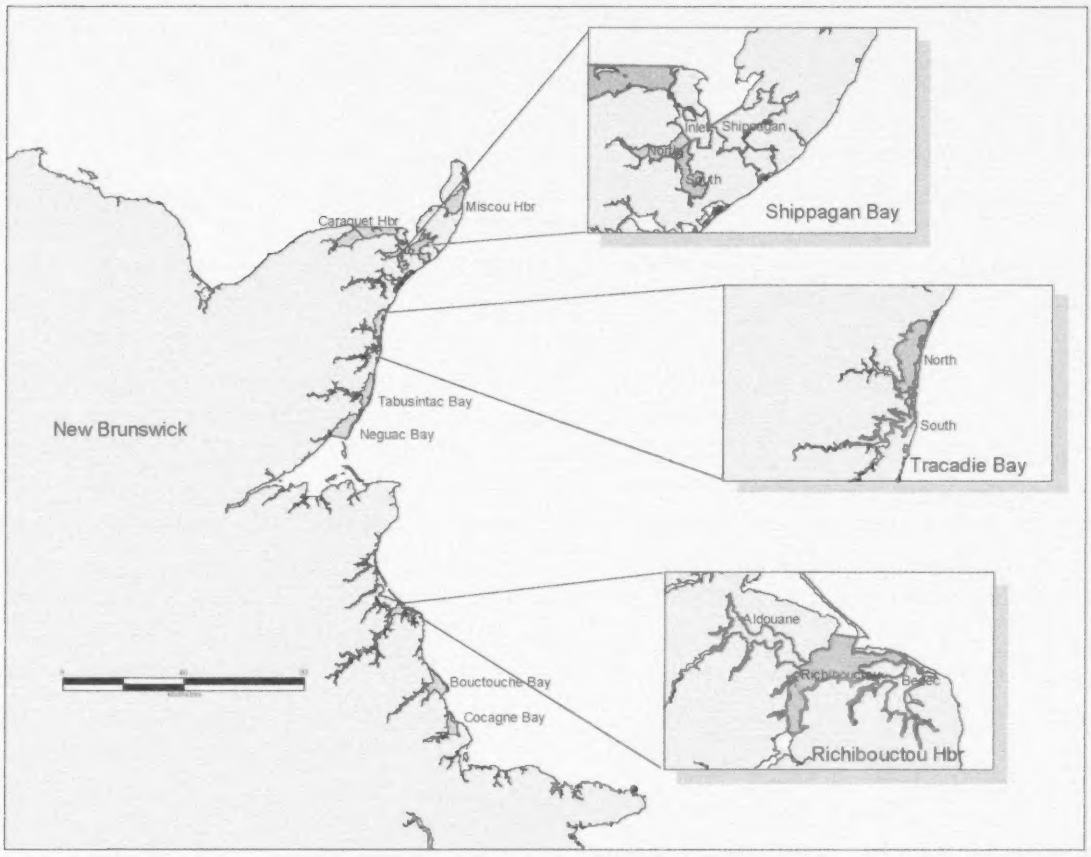

Figure 42: Map showing the division of Shippagan Bay and Tracadie Bay, New Brunswick into smaller regions (tributaries).

Table 12: Total eelgrass area in hectares and percent eelgrass coverage for each bay from FPI (%eelgrass = % of bay that has eelgrass = Total Polygon Area in Table 11/Whole Area in Table 6) and/or EC/DFO data.

Bay	EC/DFO eelgrass (ha) 2007	EC/DFO eelgrass (ha) 2008	EC/DFO eelgrass (ha) 2009	FPI eelgrass (ha) 2011	EC/DFO %eelgrass 2007-2009	FPI %eelgrass 2011
Caraquet, NB				4448		67
Miscou, NB			2234	929	69	29
St-Simon Inlet, NB	648				63	
St-Simon North, NB	613				74	
St-Simon South, NB	668				70	
Shippagan South, NB	761				27	
Tracadie North, NB			1087	1418	50	66
Tracadie South, NB				759		78
Tabusintac, NB		1326			43	
Néguac, NB			1875		49	
Aldouane, NB	440			597	64	86
Richibucto Hbr, NB	1030			1164	65	73
Bedec, NB	467			609	72	94
Bouctouche, NB			1719	1156	57	38
Cocagne, NB		935			47	
St Mary's, PEI				266		26

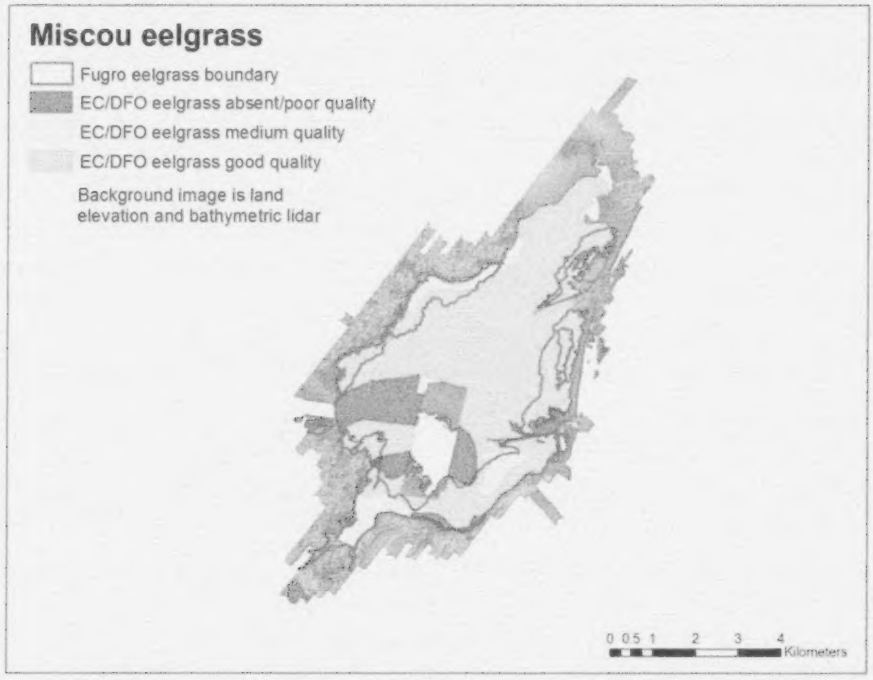
Miscou eelgrass
Fugro eelgrass boundary
EC/DFO eelgrass absent/poor quality
EC/DFO eelgrass medium quality
EC/DFO eelgrass good quality
Background image is land elevation and bathymetric lidar
0 0.5 1 2 3 4
Kilometers

Figure 43: Miscou FPI eelgrass boundary and EC/DFO eelgrass polygons. Background image is elevation colour-shaded relief (CSR).

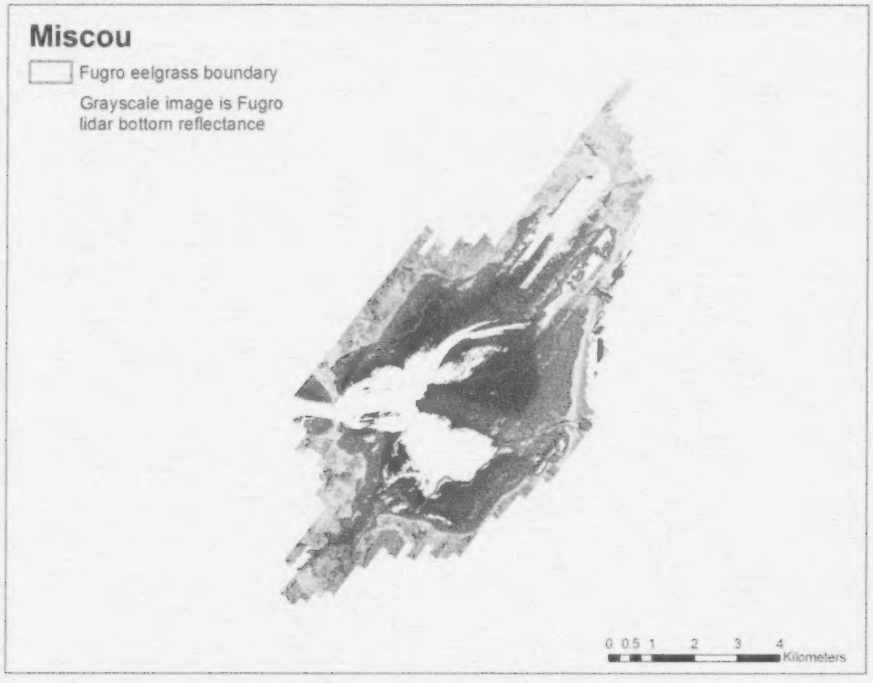

Figure 44: Miscou FPI lidar bottom reflectance and eelgrass boundary.

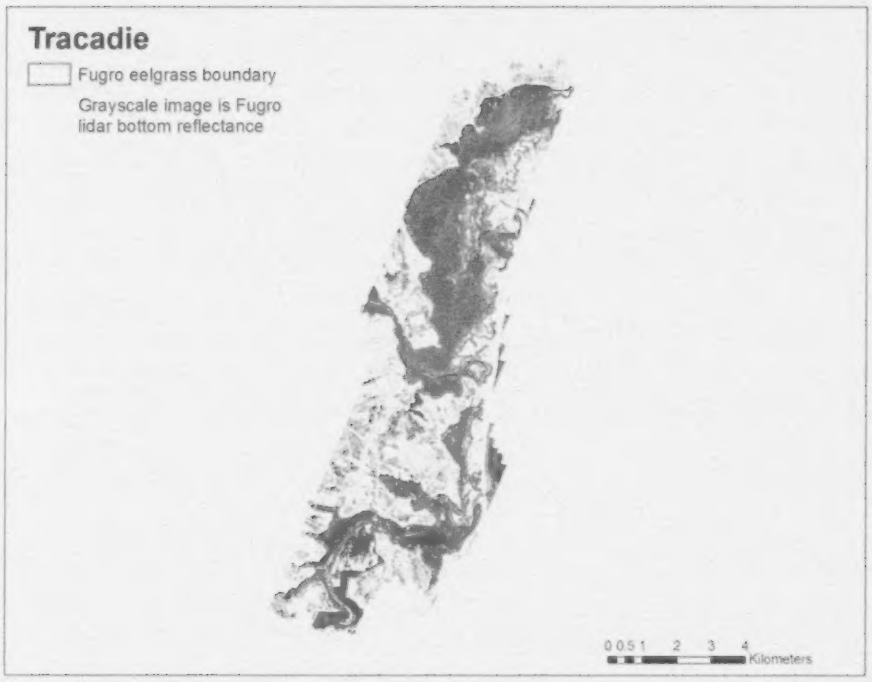

Figure 45: Tracadie FPI lidar bottom reflectance and eelgrass boundary.

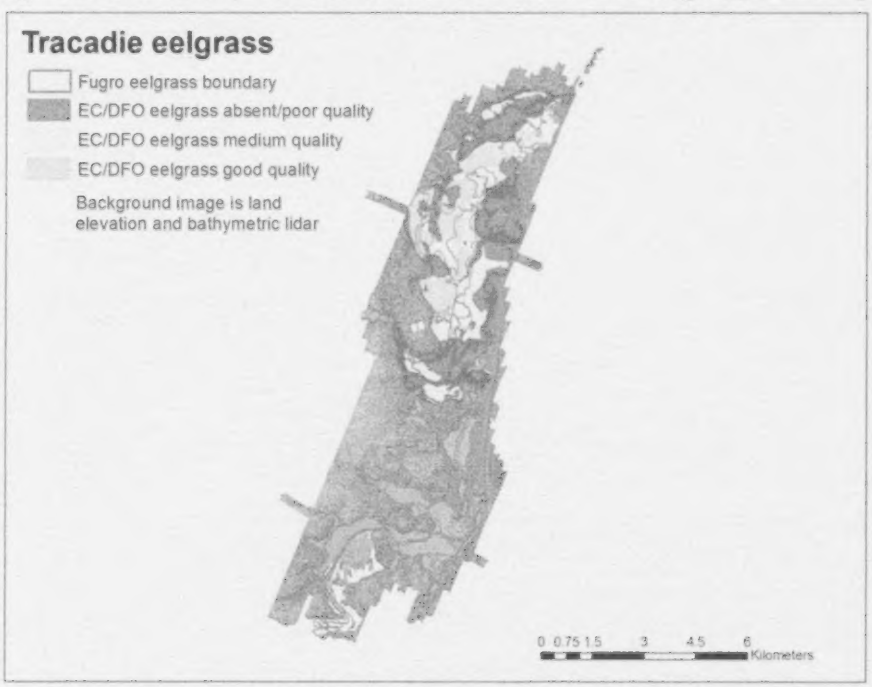
Tracadie eelgrass
Fugro eelgrass boundary
EC/DFO eelgrass absent/poor quality
EC/DFO eelgrass medium quality
EC/DFO eelgrass good quality
Background image is land elevation and bathymetric lidar
0 0.75 1.5 3 4.5 6
Kilometers

Figure 46: Tracadie FPI eelgrass boundary and EC/DFO eelgrass polygons. Background image is elevation colour-shaded relief (CSR).

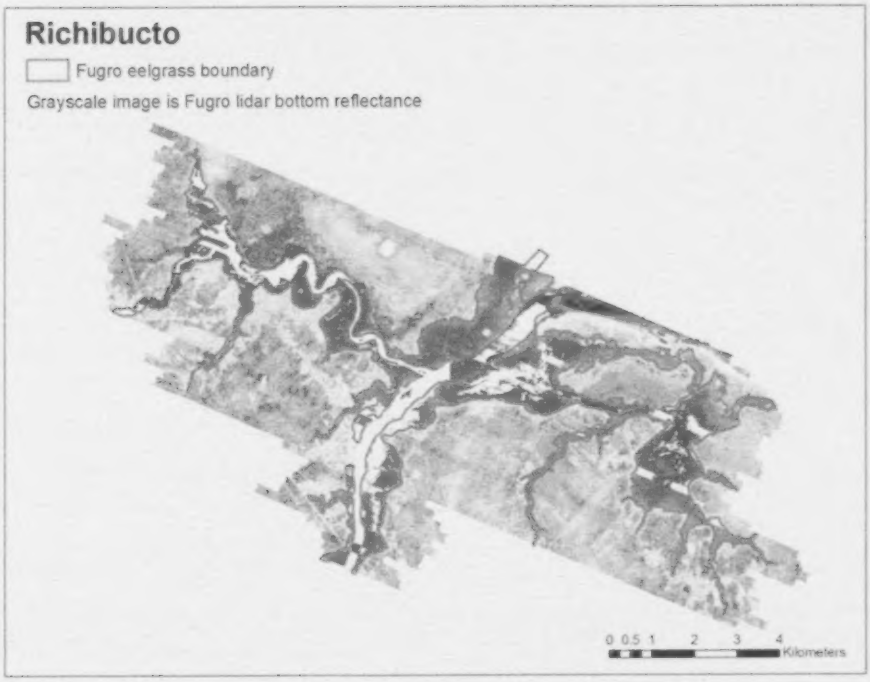

Figure 47: Richibucto FPI lidar bottom reflectance and eelgrass boundary.

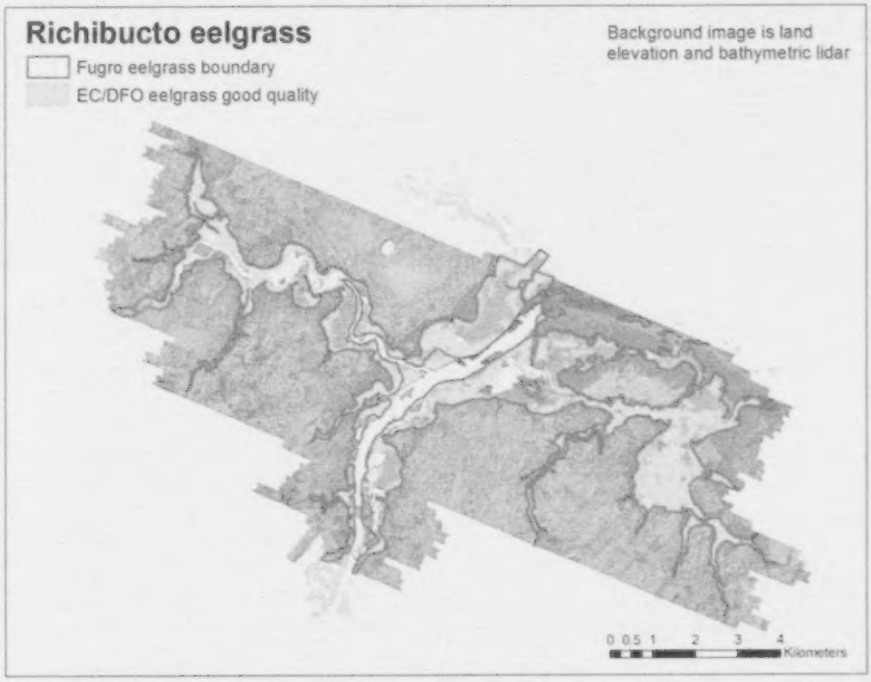
Richibucto eelgrass
Fugro eelgrass boundary
EC/DFO eelgrass good quality
Background image is land elevation and bathymetric lidar
0 0.5 1 2 3 4
Kilometers

Figure 48: Richibucto FPI eelgrass boundary and EC/DFO eelgrass polygons. Background image is elevation colour-shaded relief (CSR).

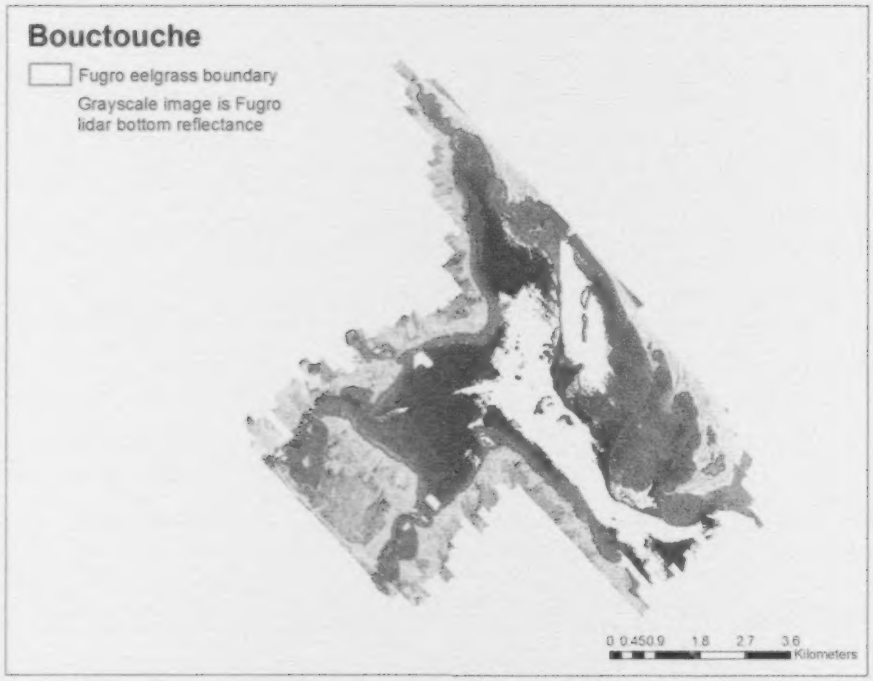

Figure 49: Bouctouche FPI lidar bottom reflectance and eelgrass boundary.

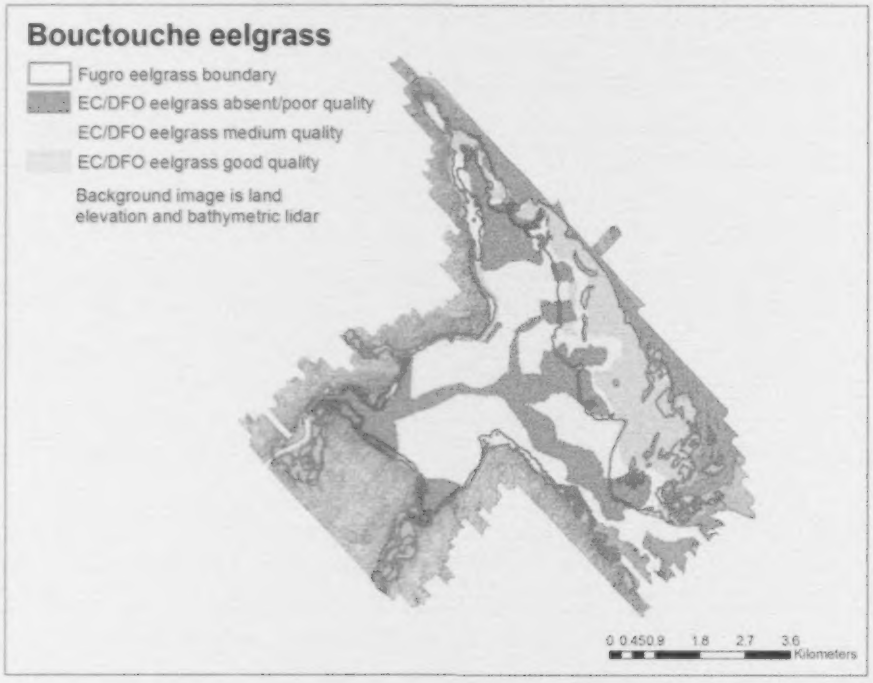
Bouctouche eelgrass
Fugro eelgrass boundary
EC/DFO eelgrass absent/poor quality
EC/DFO eelgrass medium quality
EC/DFO eelgrass good quality
Background image is land elevation and bathymetric lidar
0 0.45 0.9 1.8 2.7 3.6
Kilometers

Figure 50: Bouctouche FPI eelgrass boundary and EC/DFO eelgrass polygons. Background image is elevation colour-shaded relief (CSR).

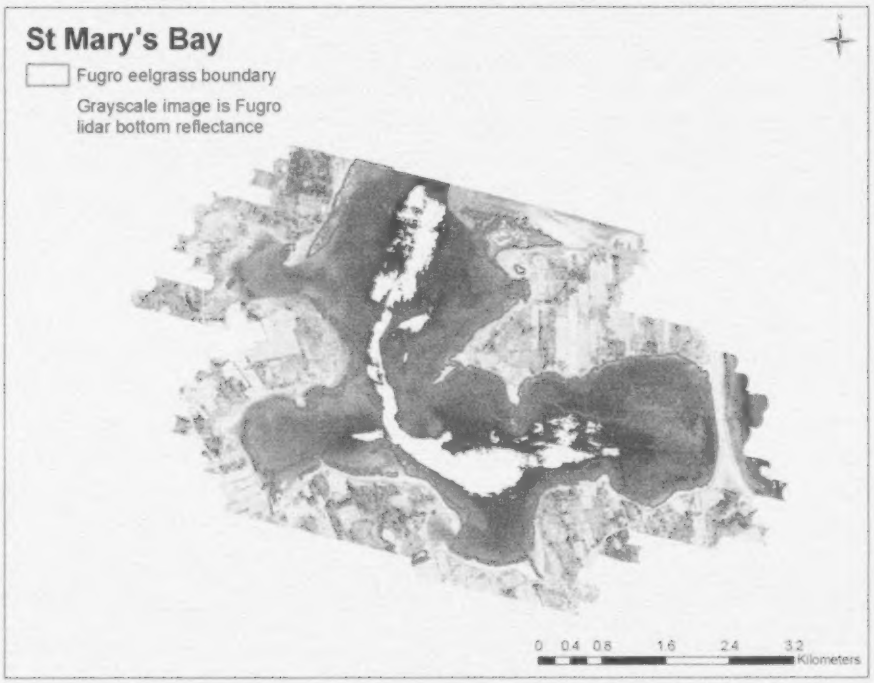

Figure 51: St Mary's Bay FPI lidar bottom reflectance and eelgrass boundary.

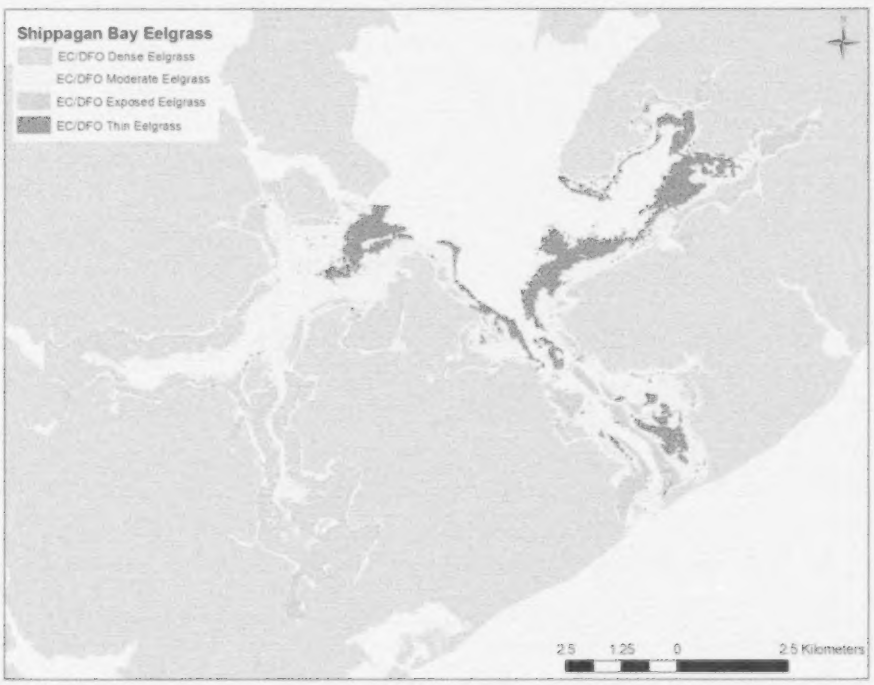

Figure 52: Shippagan Bay EC/DFO eelgrass polygons.

Neguac Bay Eelgrass
EC/DFO eelgrass absent/poor quality
EC/DFO eelgrass medium quality
EC/DFO eelgrass good quality
1 0.5 0 1 Kilometers

Figure 53: Neguac Bay EC/DFO eelgrass polygons.

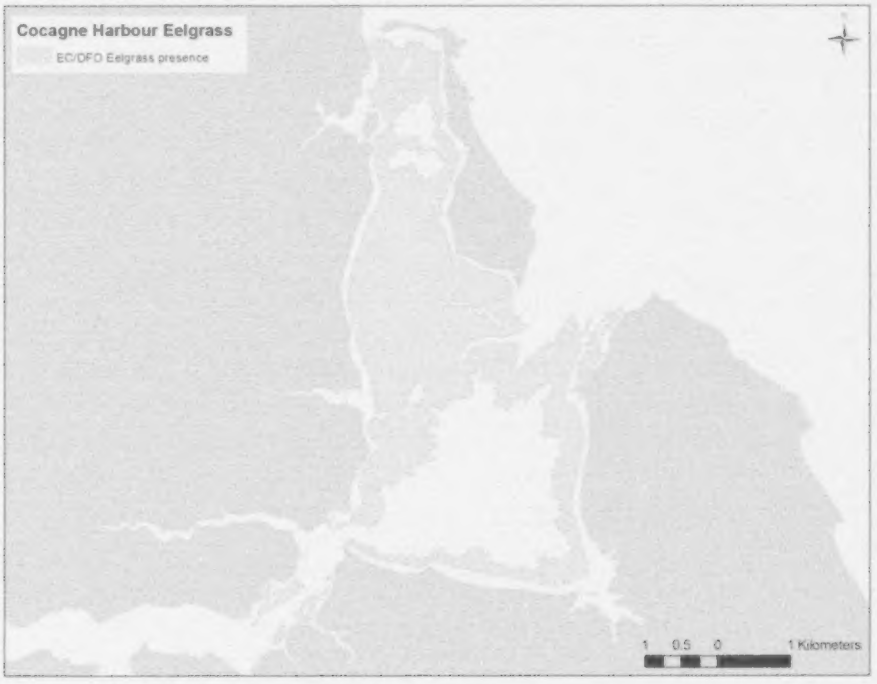

Figure 54: Cocagne Harbour EC/DFO eelgrass polygons.

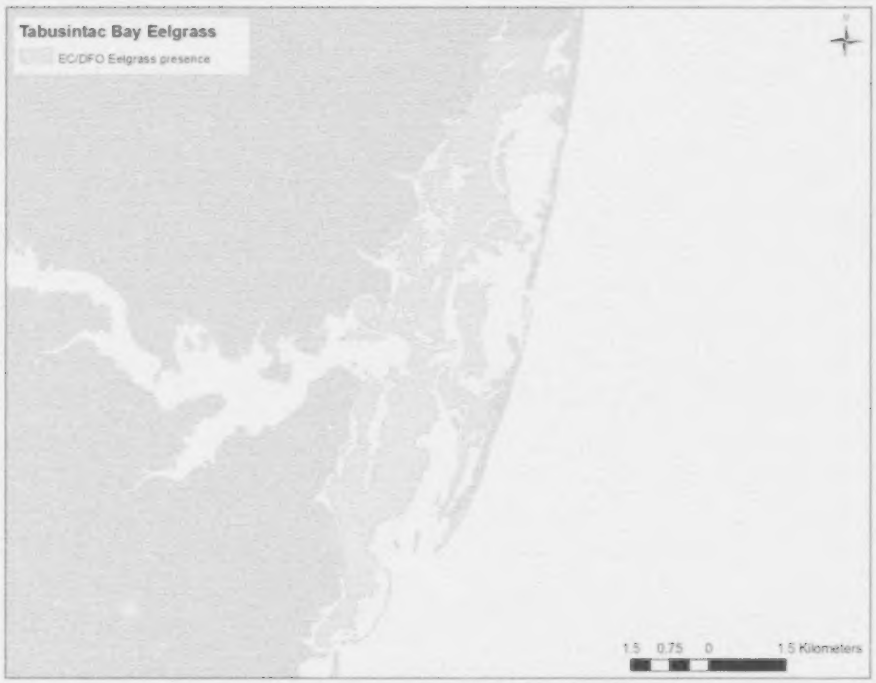

Figure 55: Tabusintac Bay EC/DFO eelgrass polygons.

3.3 AQUACULTURE GEAR AND BIOMASS – BOAT-BASED SURVEYS

Aquaculture data from the boat-based surveys is presented in Tables 13 and 14. Table 13 relates to the 2007 to 2009 period that corresponds to the years in which the EC/DFO eelgrass surveys were conducted while Table 14 provides data for 2011 only when the FPI eelgrass survey was conducted.

For the 2007 to 2009 period, biomass was highest for St Simon South (358t) and lowest for Shippagan South (8t) (Table 13). Biomass per area (total biomass per bay (t) / *Whole Area* (ha) (Table 11)), gives an indication of aquaculture density per bay. St Simon South, Bedec and Aldouane contained the most biomass per area with 0.37, 0.29 and 0.23 t/ha, respectively, while the other bays held less than 0.1 t/ha.

In 2011, mussel aquaculture in St Mary's Bay, PEI had an order of magnitude more biomass than oyster aquaculture in NB bays (Table 14). Of the oyster bays, Bedec had the greatest biomass and Miscou had none.

Considering only the 2011 dataset, mussel aquaculture in St Mary's Bay had an order of magnitude more biomass per bay than the oyster aquaculture bays with 2.85t/ha. Bedec and Aldouane continued to show high oyster biomass per area in 2011, relative to the other oyster bays studied, with 0.43 and 0.29 t/ha, respectively. In all years, the highest observed density of oyster bags per leased area was 1077 bags/ha in Miscou (Figure 57).

Table 13: Aquaculture lease area, lease area percentage of bay, aquaculture gear area (two dimensional), bivalve biomass (BM), bivalve biomass per bay area and bags per lease area for each bay for year corresponding to eelgrass surveys (2007-2009). All oyster aquaculture.

Bay	2011 (2009) lease area (ha)	% lease area	2007-2009 gear area (ha)	2007-2009 BM (t)	2007-2009 BM/ bay area (t/ha)	2007-2009 bags/ lease area (ha)
Miscou, NB	(8.33)	0.26	0.20	54	0.02	1077
St-Simon Inlet, NB	16.20	1.56	0.05	85	0.08	864
St-Simon North, NB	30.08	3.62	0.45	83	0.10	458
St-Simon South, NB	71.16	7.44	1.89	358	0.37	833
Shippagan South, NB	13.89	0.49	0.04	8	0.00	94
Tracadie North, NB	89.56	4.14	0.75	109	0.05	201
Tabusintac, NB	58.02	1.87	0.33	71	0.02	203
Néguac, NB	75.17	1.97	0.79	199	0.05	438
Aldouane, NB	50.99	7.37	0.36	160	0.23	520
Richibucto Hbr, NB	56.82	3.58	0.29	86	0.05	250
Bedec, NB	56.63	8.73	0.70	190	0.29	556
Bouctouche, NB	44.56	1.48	0.79	152	0.05	563
Cocagne, NB	67.03	3.34	0.18	79	0.04	194

Table 14: Aquaculture lease area, lease area percentage of bay, aquaculture gear area (two dimensional), bivalve biomass (BM), bivalve biomass per bay area and bags per lease area for each bay for year corresponding to FPI (lidar) eelgrass surveys (2011). All the New Brunswick calculations are based on oyster aquaculture and St. Mary's Bay PEI is based on mussel aquaculture.

Bay	2011 lease area (ha)	% lease area	2011 gear area (ha)	2011 BM (t)	2011 BM/bay area (t/ha)	2011 bags/ lease area (ha)
Caraquet, NB	35.68	0.68	0.17	50	0.01	232
Miscou, NB	0	0.26	0.00	0	0.00	0
Tracadie North, NB	89.56	4.14	0.41	94	0.04	174
Tracadie South, NB	2.42	0.25	0.01	3	0.00	207
Aldouane, NB	50.99	7.37	0.96	198	0.29	644
Richibucto Hbr, NB	56.82	3.58	0.53	124	0.08	361
Bedec, NB	56.63	8.73	1.03	278	0.43	813
Bouctouche, NB	44.56	1.48	0.77	209	0.07	777
St. Mary's , PEI	233.00	22.67	0.57	2833	2.85	1599

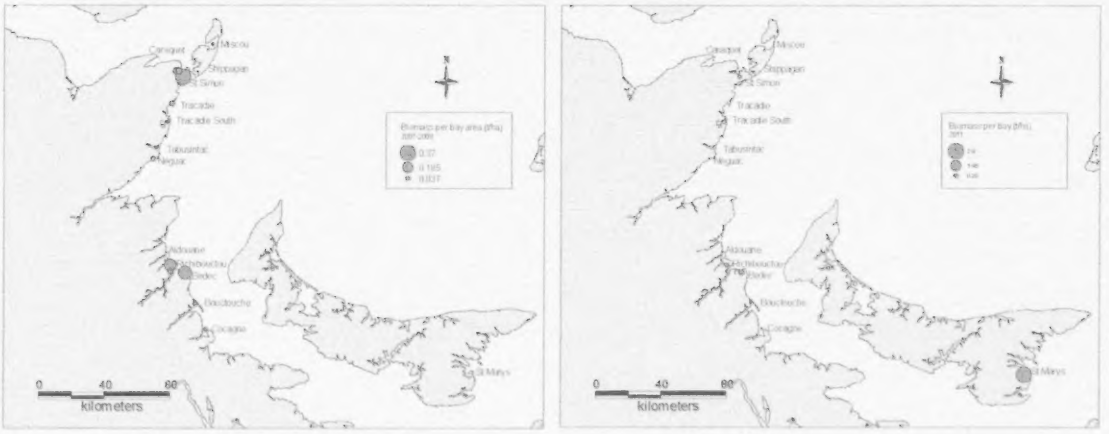

Figure 56: Biomass of oysters (or mussels for Prince Edward Island) per bay area (tons per hectare) for 2007-2009 (left) and 2011 (right).

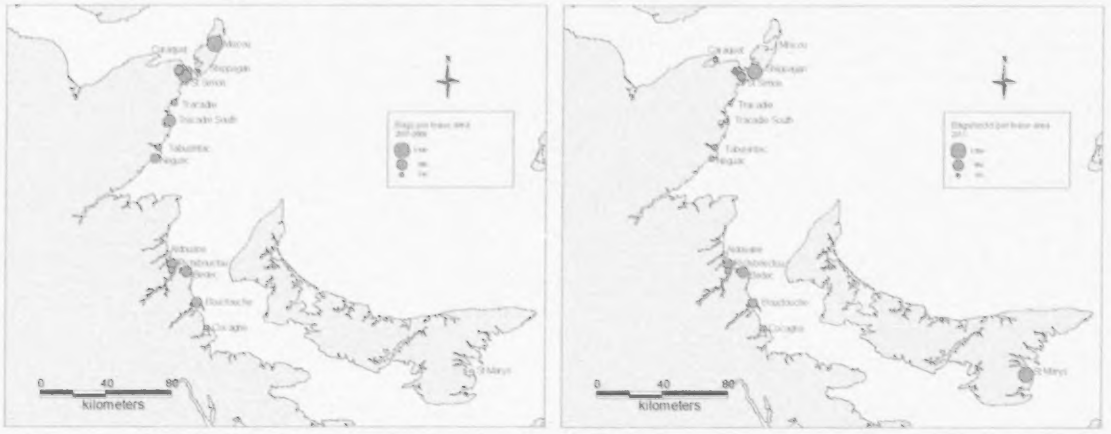

Figure 57: Number of oyster bags (or mussel socks for Prince Edward Island) per lease area (number per hectare) for 2007-2009 (left) and 2011 (right).

3.3.1 Aquaculture Gear and Biomass – Orthophoto Mosaics

Information derived from orthophoto mosaics on aquaculture gear types, line spacing and length for each bay is presented in Table 15. In the table, buoy/cage spacing means distance between buoys or cages within a line; line spacing indicates mean distance between lines; line length is mean line length (m). Orthophoto mosaics showing digitized aquaculture lines and lease areas are shown in Figure 58 through Figure 63. A total of 3618 aquaculture lines were digitized from the orthophoto mosaics in 2011. The majority of them held Oystergro cages in NB while they represented mussel longlines in St Mary's Bay, PEI. Lines ranged from 28 to 90 m in length depending on gear type and bay. Line spacing varied between 6 to 30 m but overall averaged 10 m. For mussel longlines in PEI, spacing varied between 4.5 and 10 m.

Oystergro cages tended to be evenly spaced and laid out in a grid-like manner, whereas oyster strings were more irregularly spaced. Floating bags were evenly spaced and did not appear in the large, grid-like groups characteristic of Oystergro, but appeared in smaller clusters throughout the bays.

In Caraquet Bay oyster aquaculture is composed of collector lines, single floating bags, oyster string and dark sea cages, but mostly Oystergro cages.

Single floating bags represent the greatest proportion of aquaculture type in Tracadie Bay (25%,) while Oystergro cages represent the least (7%). Most of the aquaculture in Tracadie is found in the northern section of the bay (Figure 59).

In Richibucto Oystergro cages made up 67% of the aquaculture. Seventy percent of the aquaculture in Aldouane was double floating bags. Oystergro cages are the only aquaculture gear present in Bedec. In Richibucto and Aldouane the aquaculture is located mostly in the nearshore, but in Bedec the cages appear to be more centered in the bay (Figure 60).

Bouctouche contains only collector lines and Oystergro cages, clustered in a cove in the north-west part of the Bay (Figure 61). Oystergro cages make up 86% of the aquaculture.

Longline mussel aquaculture in St Mary's Bay had evenly spaced lines in grid-like arrays. Average line length was 122m, but Figure 62 shows that lines ranged from ~ 90m to ~160m.

Table 15. Aquaculture gear spacing and line length and percentage of total for each gear type in each bay calculated from orthophoto mosaics.

	Collector Lines	Floating Bag Double	Floating Bag Single	String Cages	Oystergro Cages	Dark Sea Cages	Mussel socks
Caraquet Bay							
Buoy/cage spacing	N/A		1 bag/m	1 cage/4 m	1 cage/6 m	30 /line	
Line spacing (m)	15		15	30 - 50	8	10	
Line length (m)	33		83	28	30	90	
Percent of lines (%)	30		7	18	30	15	
Tracadie Bay							
Buoy/cage spacing	N/A	2 bags/m	1 bag/m	1 cage/4 m	1 cage/4 m		
Line spacing (m)	10-30	10	10	6 - 30	30		
Line length (m)	55	38	47	38	38		
Percent of lines (%)	10	25	33	25	7		
Richibucto							
Buoy/cage spacing		2 bags/m	1 bag/m		1 cage/5 m		
Line spacing (m)		10	8-10		8-12		
Line length (m)		42	38		65		
Percent of lines (%)		15	17		67		
Aldouane							
Buoy/cage spacing		2 bags/m	1 bag/m		1 cage/3 m		
Line spacing (m)		8-10	8		8-12		
Line length (m)		43	44		55		
Percent of lines (%)		70	4		26		
Bedec							
Buoy/cage spacing					1 cage/4 m		
Line spacing (m)					8-10		
Line length (m)					44		
Percent of lines (%)					100		
Bouctouche Bay							
Buoy/cage spacing	N/A		1 bag/m		1 cage/4 m		
Line spacing (m)	N/A		variable		10		
Line length (m)	58		38		39		
Percent of lines (%)	13		1		86		
St Mary's Bay							
Buoy/cage spacing							1 sock/0.45m
Line spacing (m)							4.5-10
Line length (m)							122
Percent of lines (%)							100

3.3.2 Biomass – Comparison Between Boat-based Surveys and Orthophoto Mosaics

Boat-based surveys provided estimates of total aquaculture biomass per bay (Tables 13 and 14). Totals are based on the number of lines per bay, with lines having a standard number of cages or bags at 6.04 kg/bag. The number of lines per bay was determined by visual counts in each bay. The boat-based survey estimates assume that each gear type (e.g. strings, floating bags) has a standard line length, in contrast to the orthophoto mosaics method, in which biomass depends on line length for most aquaculture gear types. Differences between boat-based survey *Total Biomass* and *orthophoto mosaics Total Biomass* in Table 16 reflect that difference in calculation, but also reflect the effectiveness of interpreting and identifying aquaculture gear from orthophoto mosaics.

Boat-based survey Total Biomass values agree well with the totals estimated from orthophoto mosaics. In every bay except Bedec and Bouctouche Total Biomass was less than boat-based survey Total Biomass. Assuming boat-based survey Total Biomass is the correct value of biomass per bay, a value for *%Difference2* is calculated as follows:

Difference2 = orthophoto mosaics Total Biomass - boat-based survey Total Biomass

%Difference2 = 100* (Difference2 / boat-based survey Total Biomass)

In Bedec and Bouctouche *%Difference2* was less than 1%, and was less than 10% for Tracadie, Richibucto and Aldouane. In Caraquet and St Mary's Bay, *%Difference2* was 29% and 28%, respectively. There was an average of 5t difference between orthophoto mosaics *Total Biomass* and *boat-based survey Total Biomass* for the oyster bays.

Table 16: Orthophoto mosaics total biomass per bay, boat-based survey total biomass. Difference2= orthophoto total biomass – boat-based survey total biomass, and Difference2=100*Difference2/boat-based survey total biomass.

Bay name	Orthophoto Total Biomass (t)	Boat-based Total Biomass (t)	Difference2 (t)	%Difference2 (%)
Caraquet	35.57	49.94	-14.37	29
Tracadie North	94.10	97.38	-3.28	3
Richibucto	114.54	123.77	-9.23	7
Aldouane	189.99	198.29	-8.30	4
Bedec	280.34	278.21	2.13	1
Bouctouche	211.13	209.02	2.11	1
St Mary's	2116.57	2833	-814	28

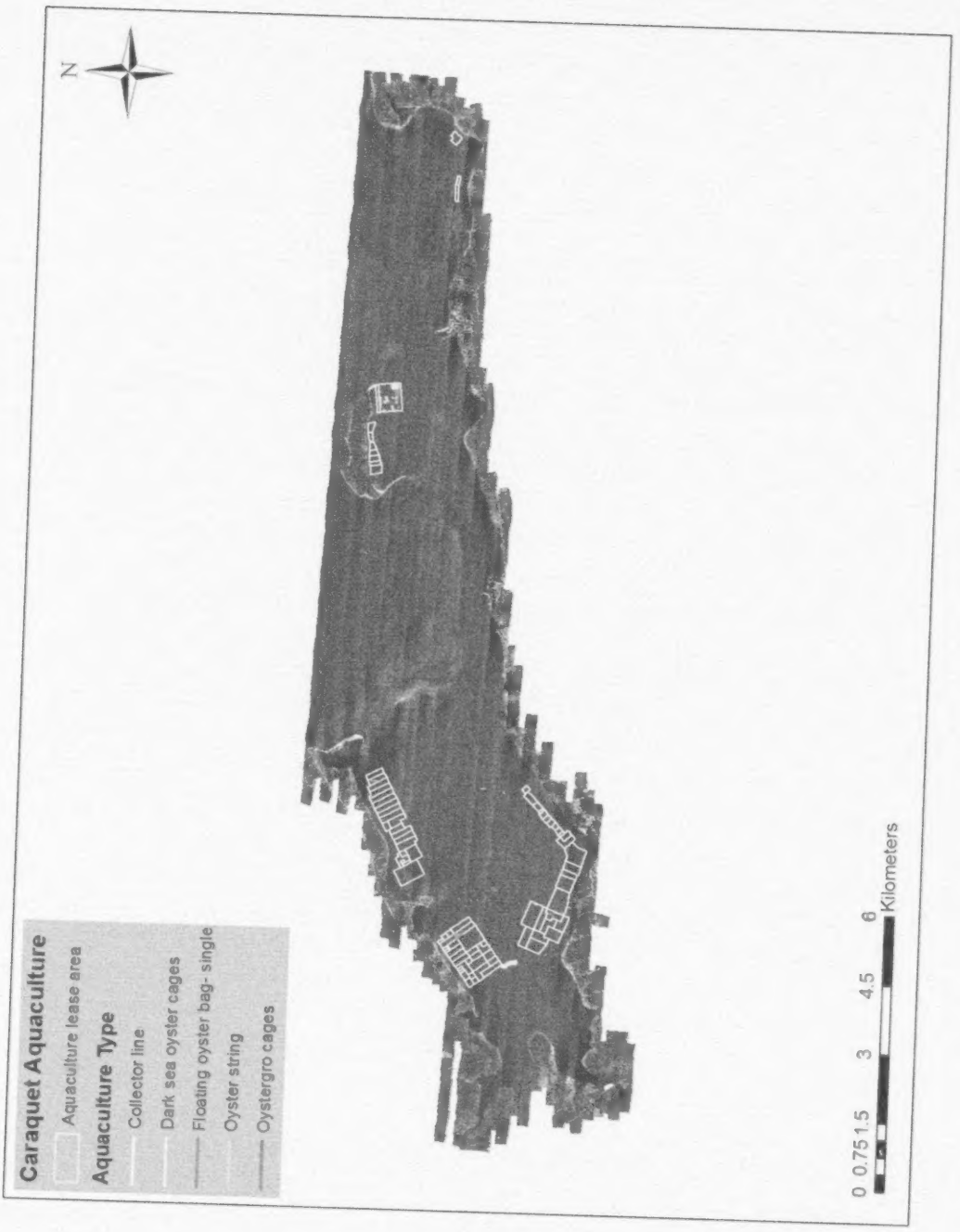

Figure 58: Caraquet orthophoto mosaic (FPI, Sept. 2011), aquaculture leases and interpreted aquaculture.

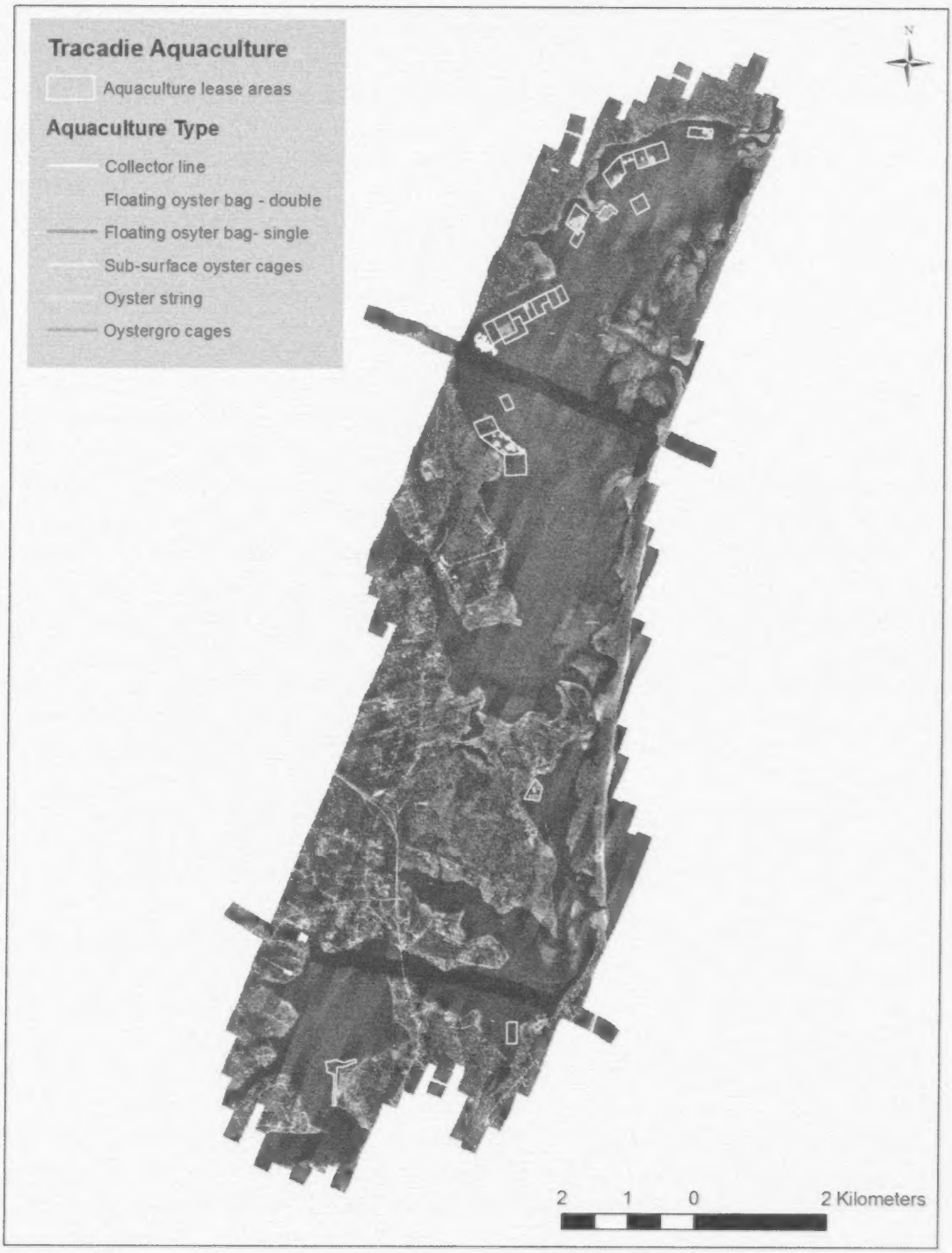

Figure 59: Tracadie orthophoto mosaic (FPI, Sept. 2011), aquaculture leases and interpreted aquaculture.

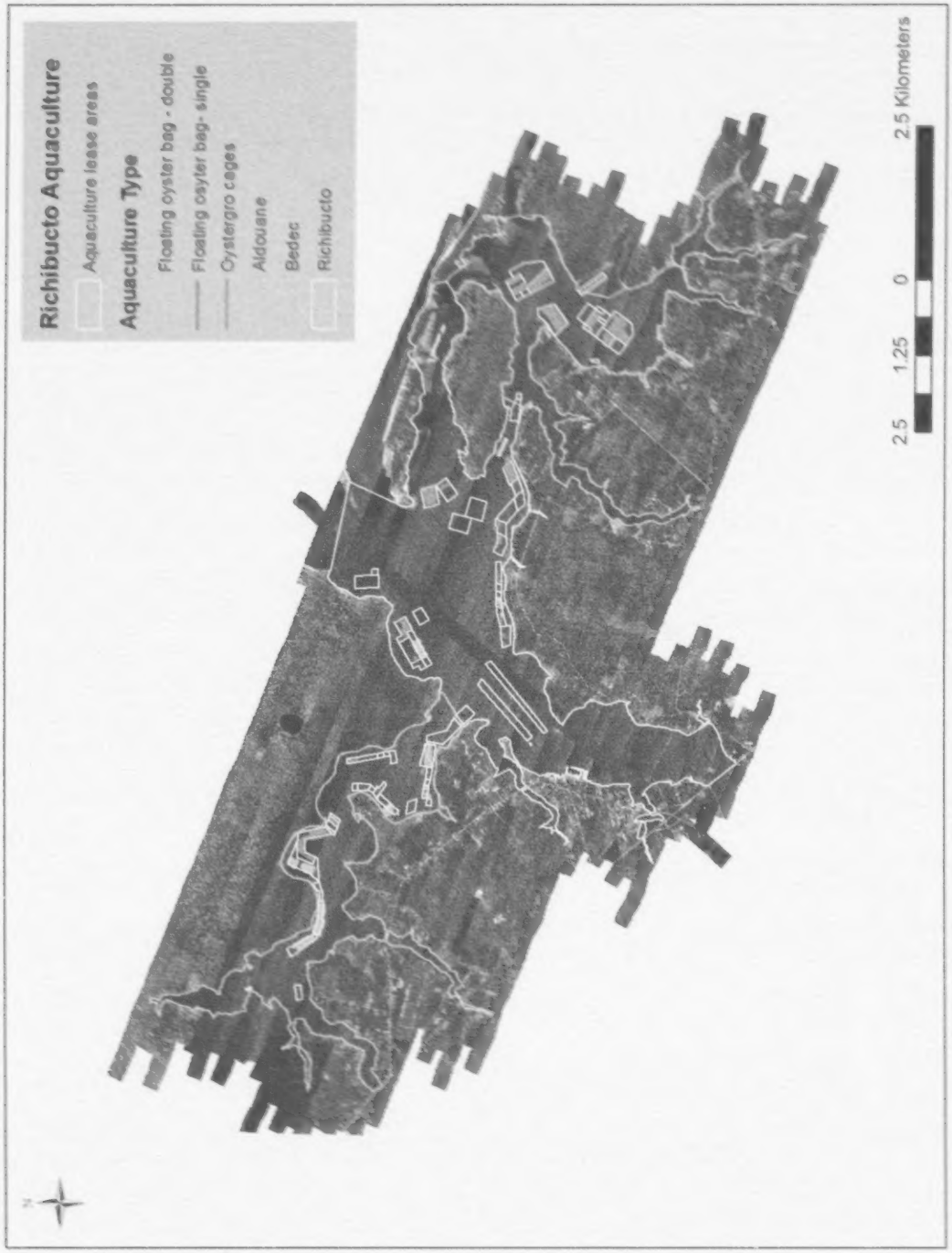

Figure 60: Richibucto, Aldouane, and Bedec orthophoto mosaic (FPI, Sept. 2011), aquaculture leases and interpreted aquaculture.

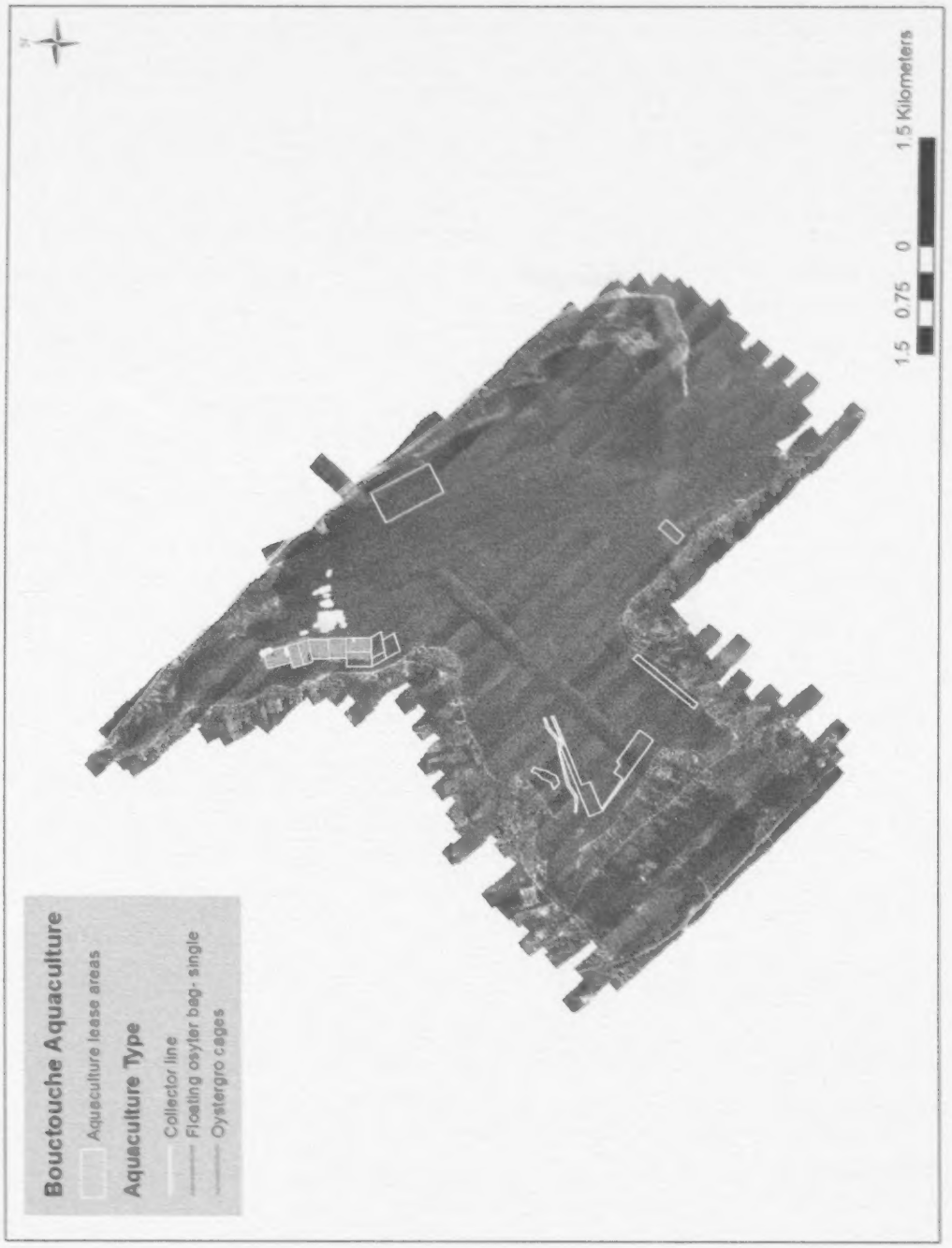

Figure 61: Bouctouche orthophoto mosaic (FPI, Sept. 2011), aquaculture leases and interpreted aquaculture.

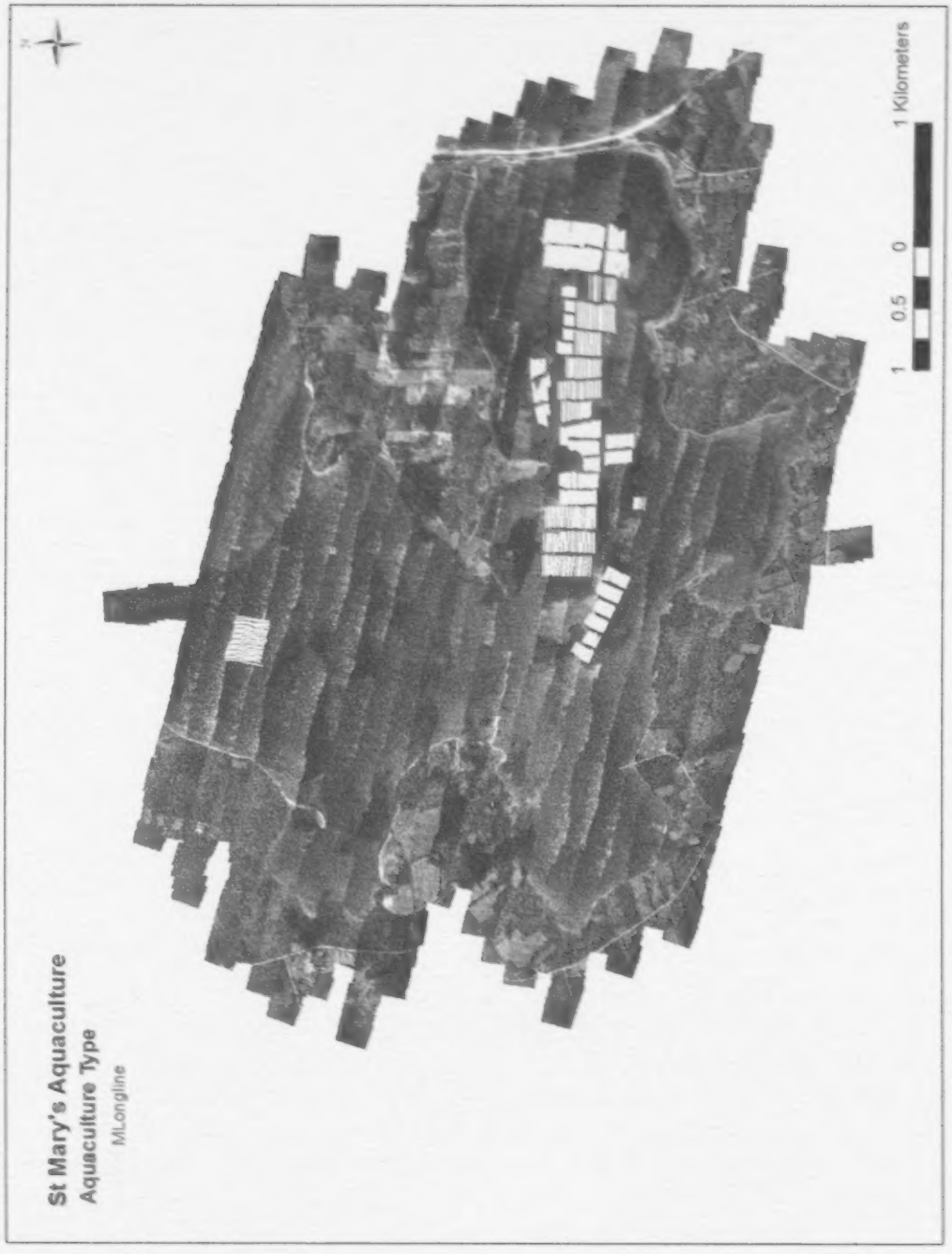

Figure 62: St Mary's Bay, PEI orthophoto mosaic (FPI, Sept. 2011) and interpreted aquaculture.

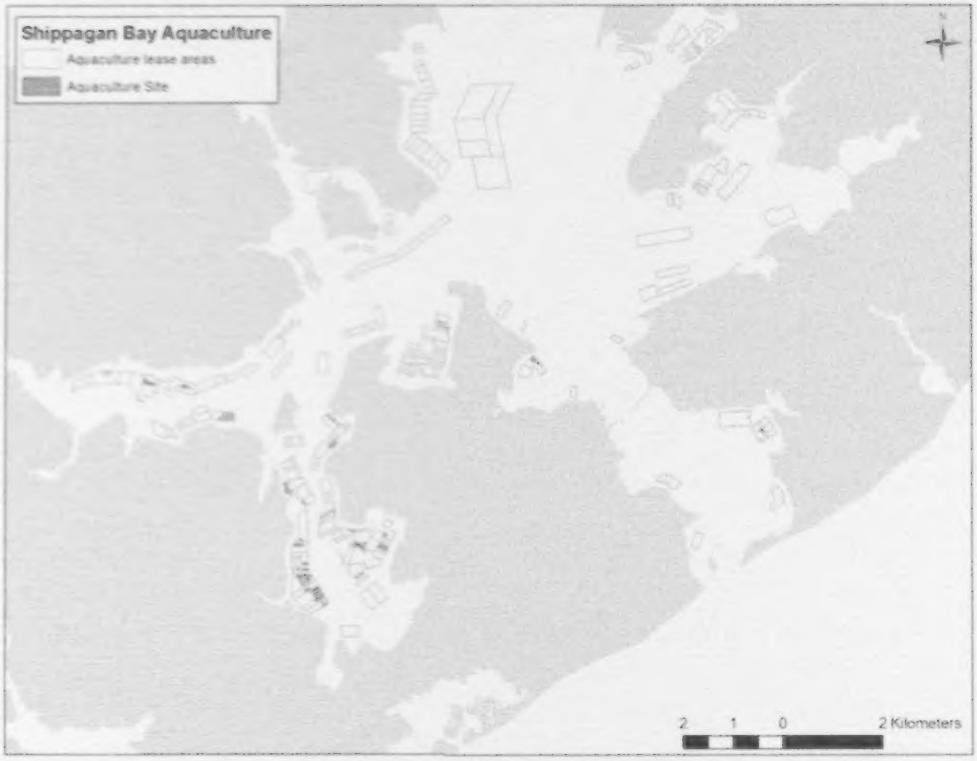

Figure 63: Shippagan Bay, NB aquaculture lease areas and EC-interpreted aquaculture polygons.

3.3.3 Eelgrass and Aquaculture and Depth

Figure 64 through Figure 70 show the bays for which a DEM, eelgrass polygons, and aquaculture data exist. This excludes Miscou since there was no aquaculture present in Miscou during September 2011. In Caraquet (Figure 64) and St Mary's Bay (Figure 70) all the aquaculture is outside of the eelgrass polygons. In Richibucto, Aldouane, and Bedec the majority of the aquaculture exists within eelgrass polygons (Figure 66-Figure 68). (Note that for these bays the only eelgrass classification was good quality.) In Tracadie and Bouctouche, aquaculture is present only in areas classified as poor quality eelgrass or eelgrass absent (Figure 65 and Figure 69). (See APPENDIX A: Eelgrass Field Survey Criteria).

The mean depth for oyster aquaculture gear in New Brunswick bays ranged from 0.48 to 2.1 m (Table 17). Mussel longlines in St. Mary's Bay PEI were found at an average depth of 4.16 m.

Table 17. Mean depth (m), depth ranges, and number of points used (n) of aquaculture leases (gear) for each bay.

Bay name	Mean Water Depth (m) at aquaculture leases*	Range	N
Tracadie Bay NB	0.48	0.04 - 0.90	1103
Aldouane Richibouctou NB	1.13	0.12 - 1.62	426
Bedec Richibouctou NB	1.75	1.05 - 2.14	1224
Richibouctou Hbr NB	1.15	0.48 - 2.51	745
Bouctouche Bay NB	2.1	0.13 - 2.50	1214
St Marys Bay PEI	4.16	1.12 - 8.6	1932

*According to lidar bathymetry 2011 and only where lidar penetrated to the bottom.

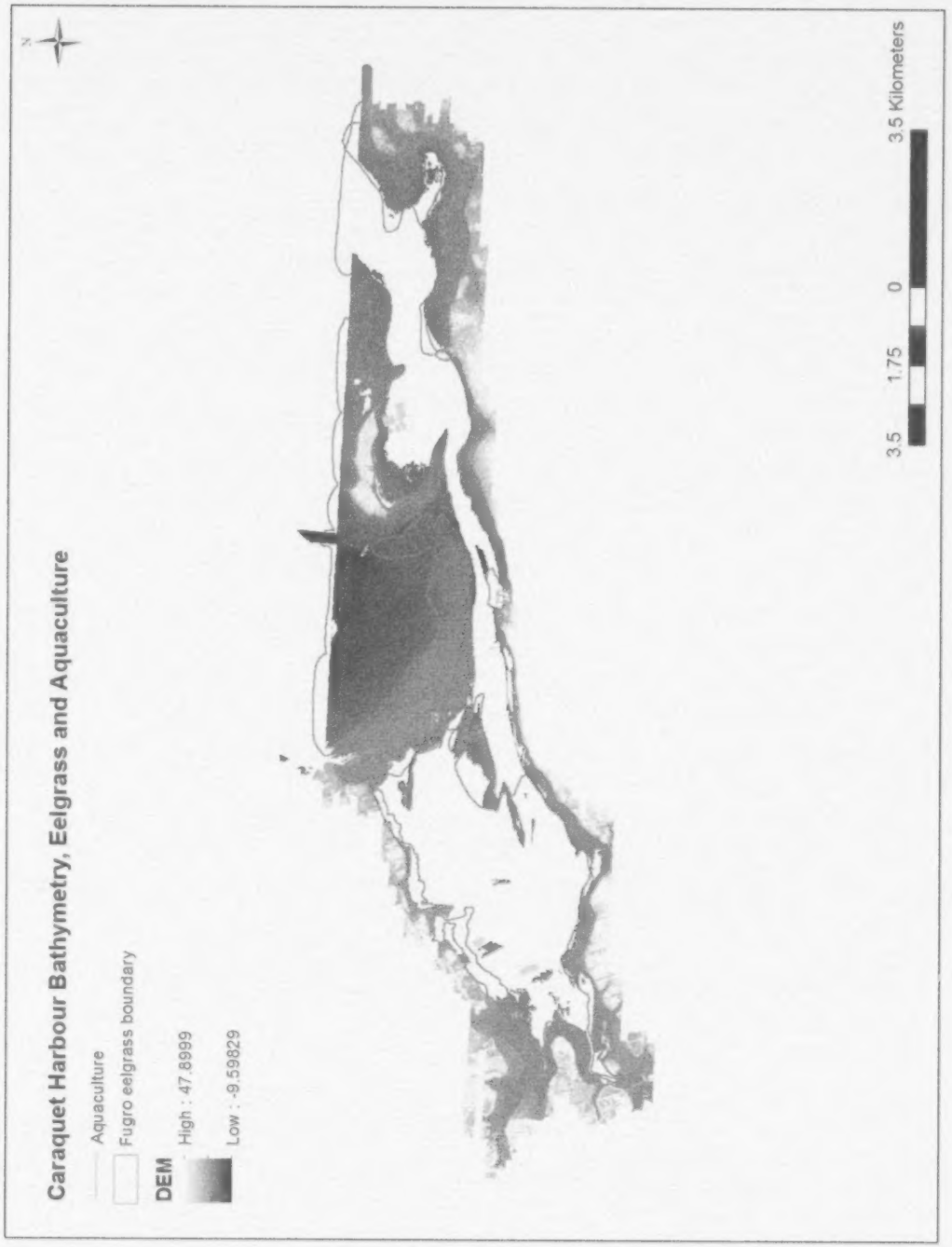

Figure 64: Caraquet Harbour DEM, FPI eelgrass and interpreted aquaculture.

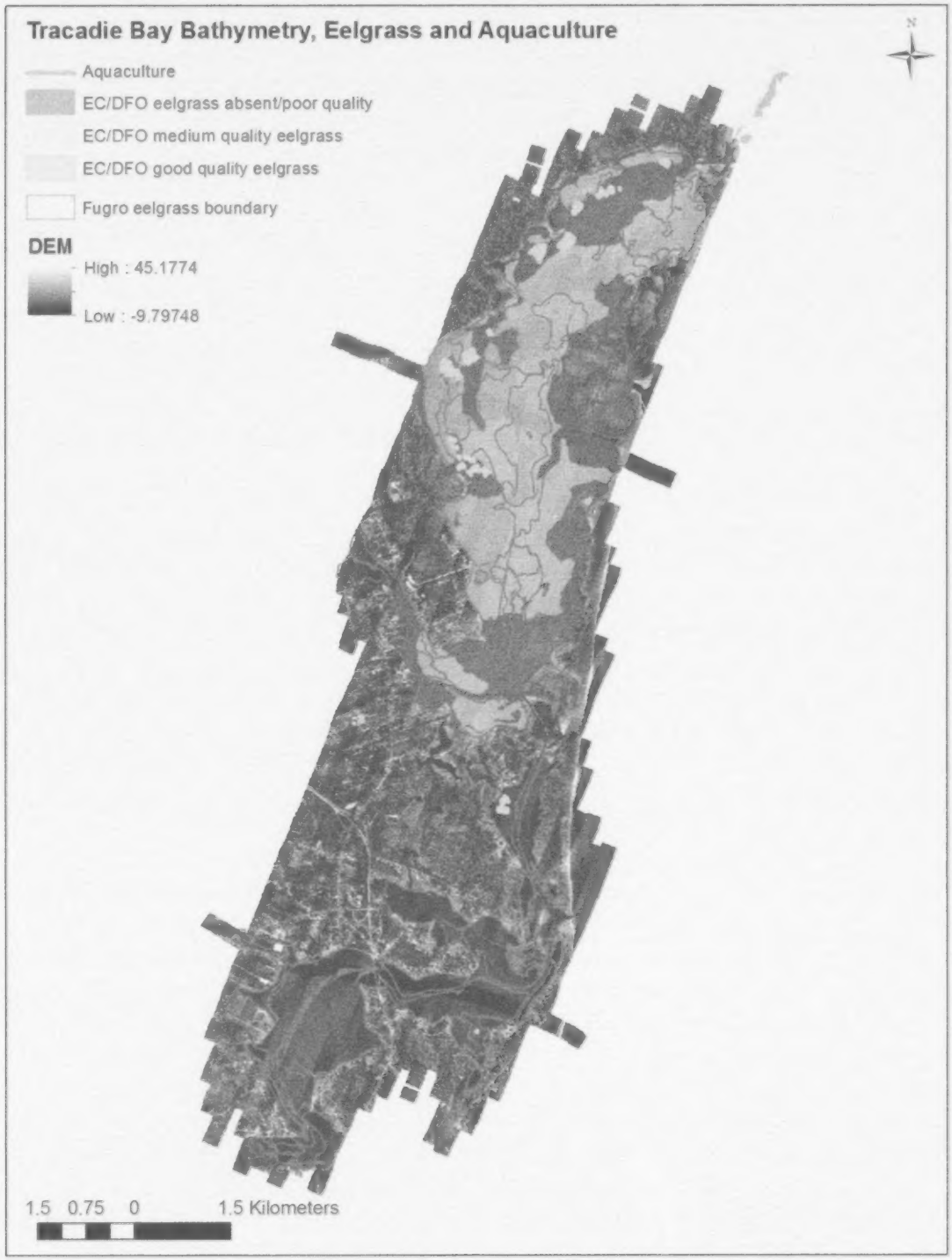

Figure 65: Tracadie Bay DEM, FPI and EC/DFO eelgrass, and interpreted aquaculture.

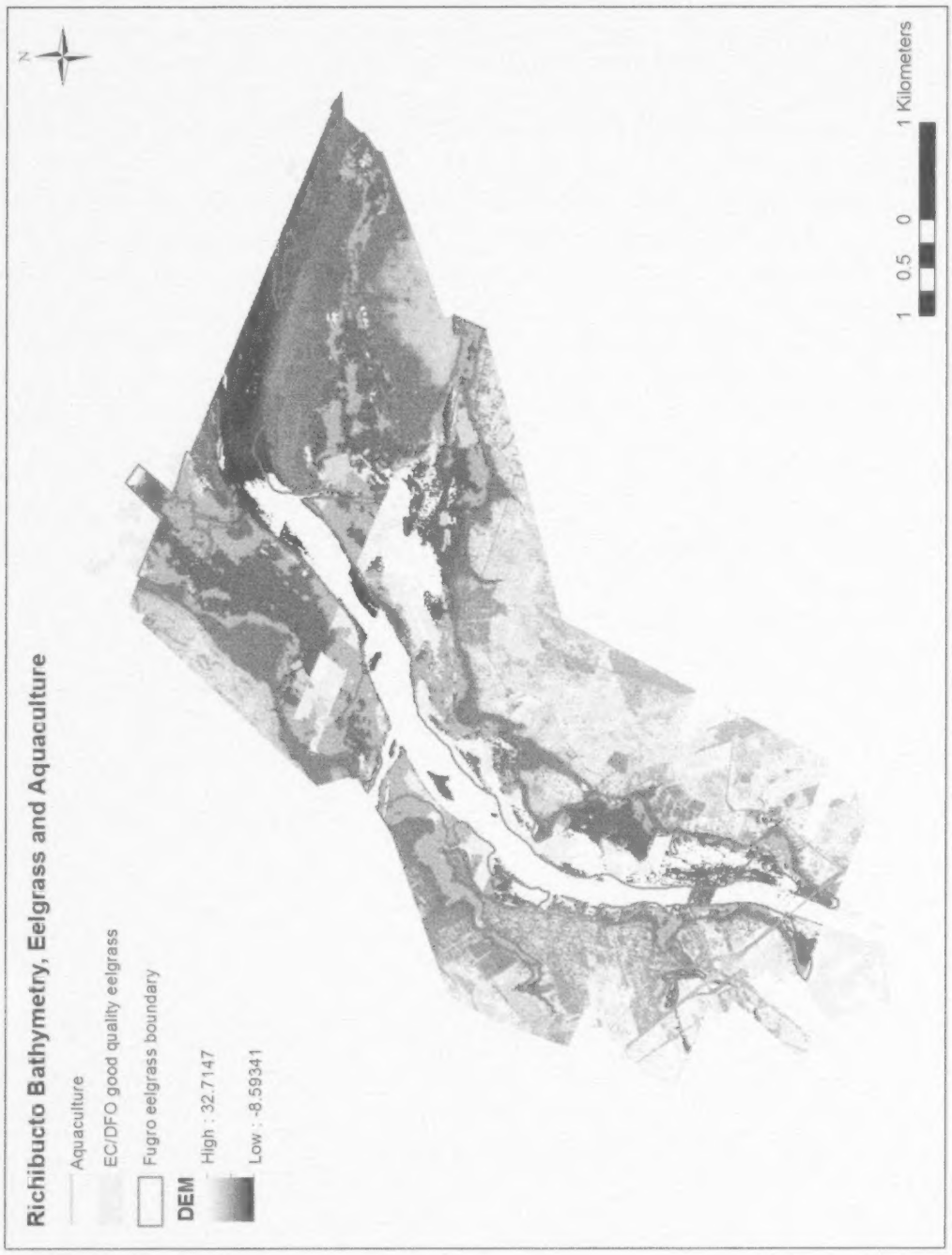

Figure 66: Richibucto DEM, FPI and EC/DFO eelgrass, and interpreted aquaculture.

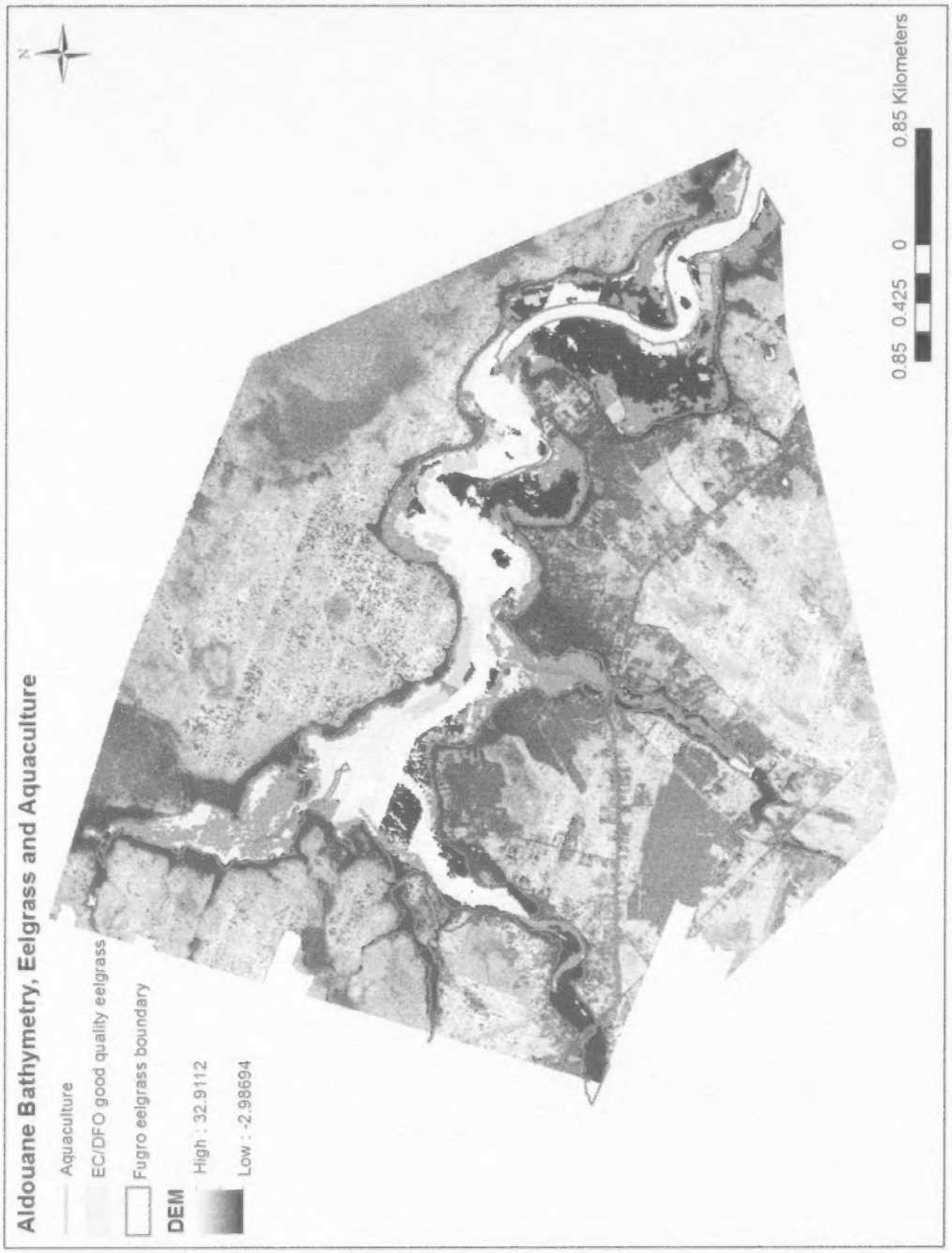

Figure 67: Aldouane DEM, FPI and EC/DFO eelgrass, and interpreted aquaculture.

Figure 68: Bedec DEM, FPI and EC/DFO eelgrass, and interpreted aquaculture.

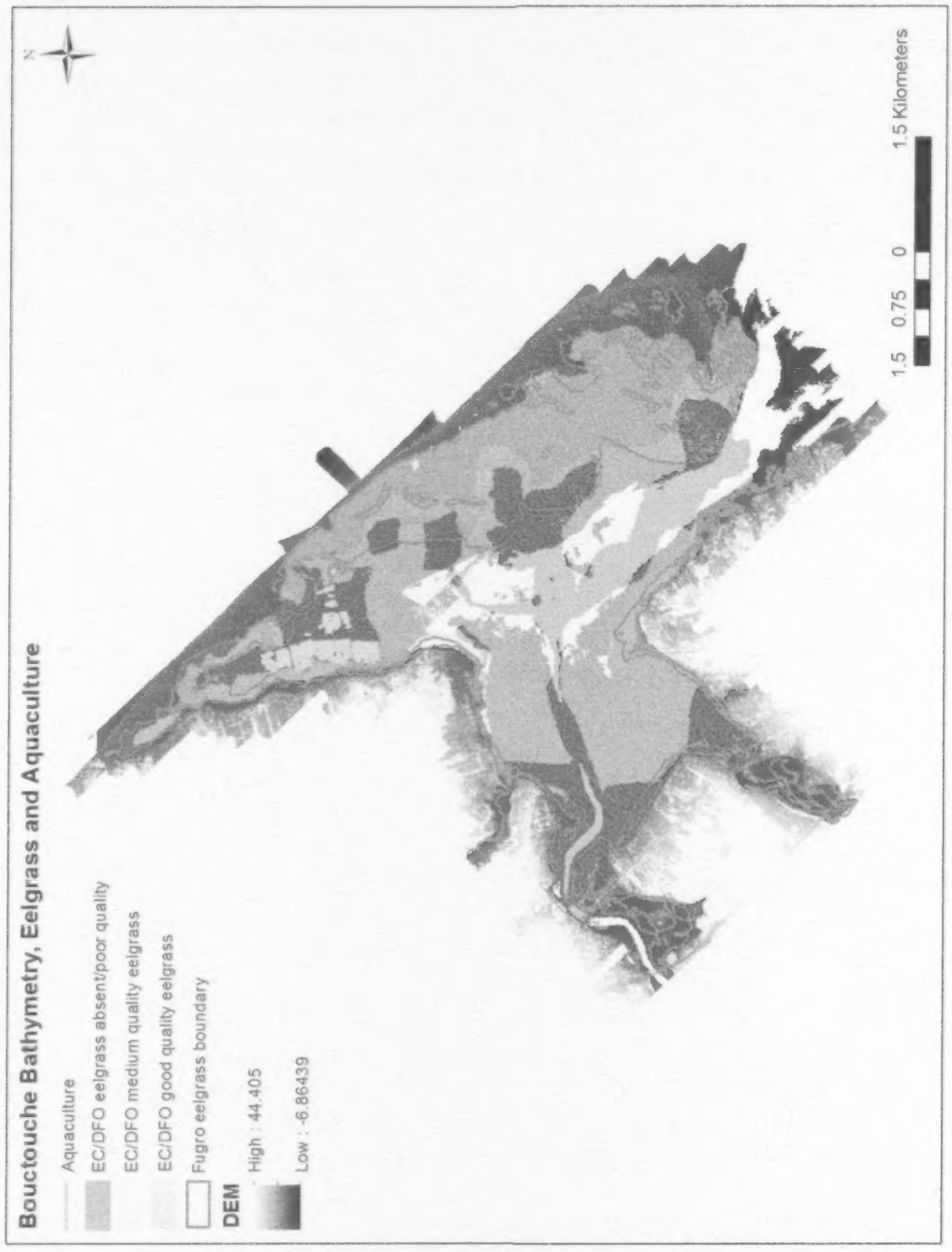

Figure 69: Bouctouche DEM, FPI and EC/DFO eelgrass, and interpreted aquaculture.

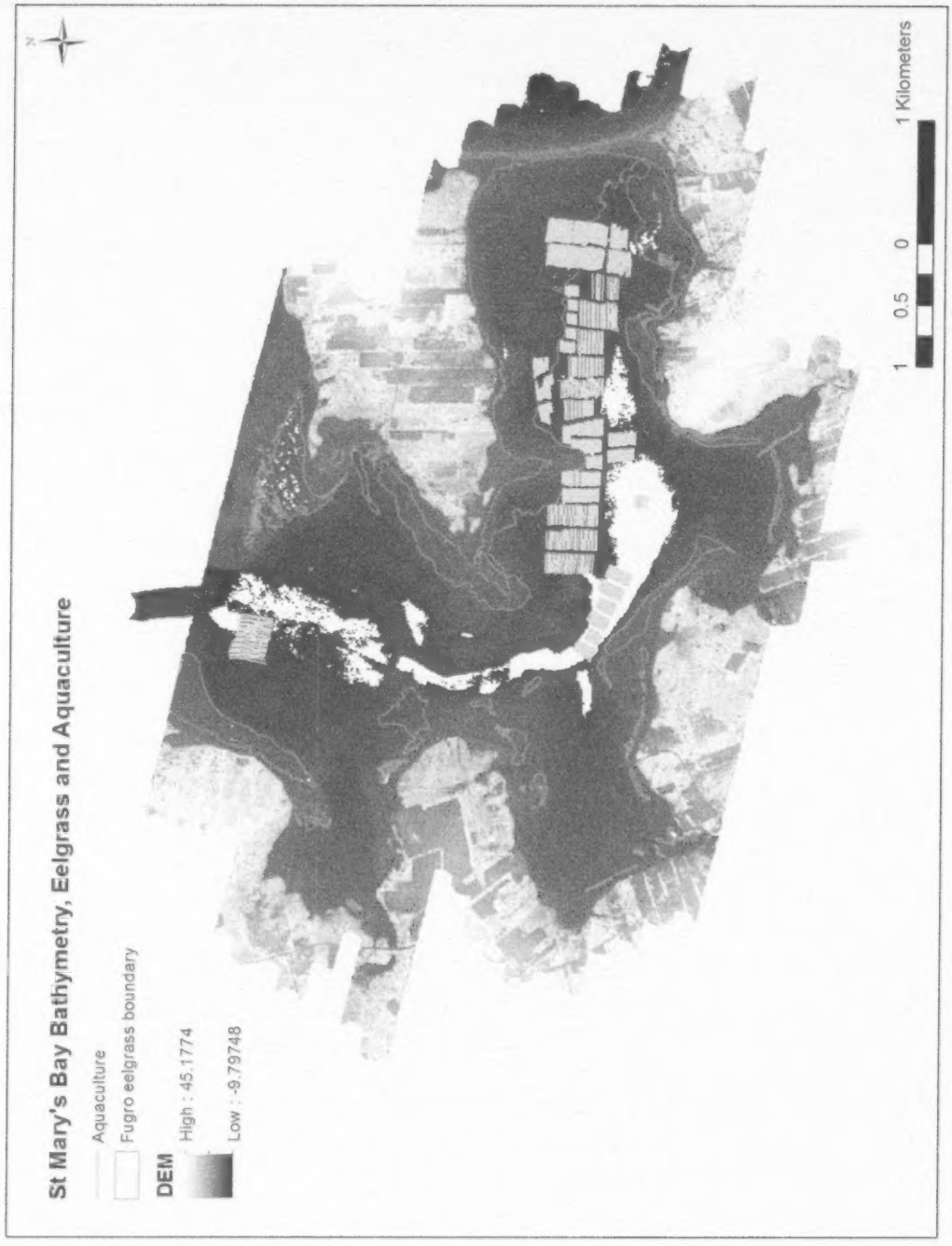

Figure 70: St Mary's Bay DEM, FPI eelgrass, and interpreted aquaculture.

4. DISCUSSION

4.1 BATHYMETRY

This bathymetric lidar survey was one of the first in Atlantic Canada. Bathymetric lidar was an effective method to collect a seamless dataset of land elevations and bathymetry. However, the technique is known to be limited by water clarity. Evidence of this is seen in Figure 71, where the lidar did not detect the bottom in 46% of Caraquet Bay (Table 8). The CHS chart values are relatively shallow (mean value -2.6 m, Figure 71) and suggest that water clarity limited the penetration of the lidar and not depth. A Secchi depth of between -0.4 m and -0.6 m would result in the lidar penetrating to -1.2 m, the shallowest CHS value in the DEM No Data region. Figure 71 also shows the orthophoto mosaics showing through the gaps in the DEM, and digitized aquaculture, which was minimal in Caraquet. It is difficult to conclude from the orthophotos if the water in the regions of No Data was particularly cloudy.

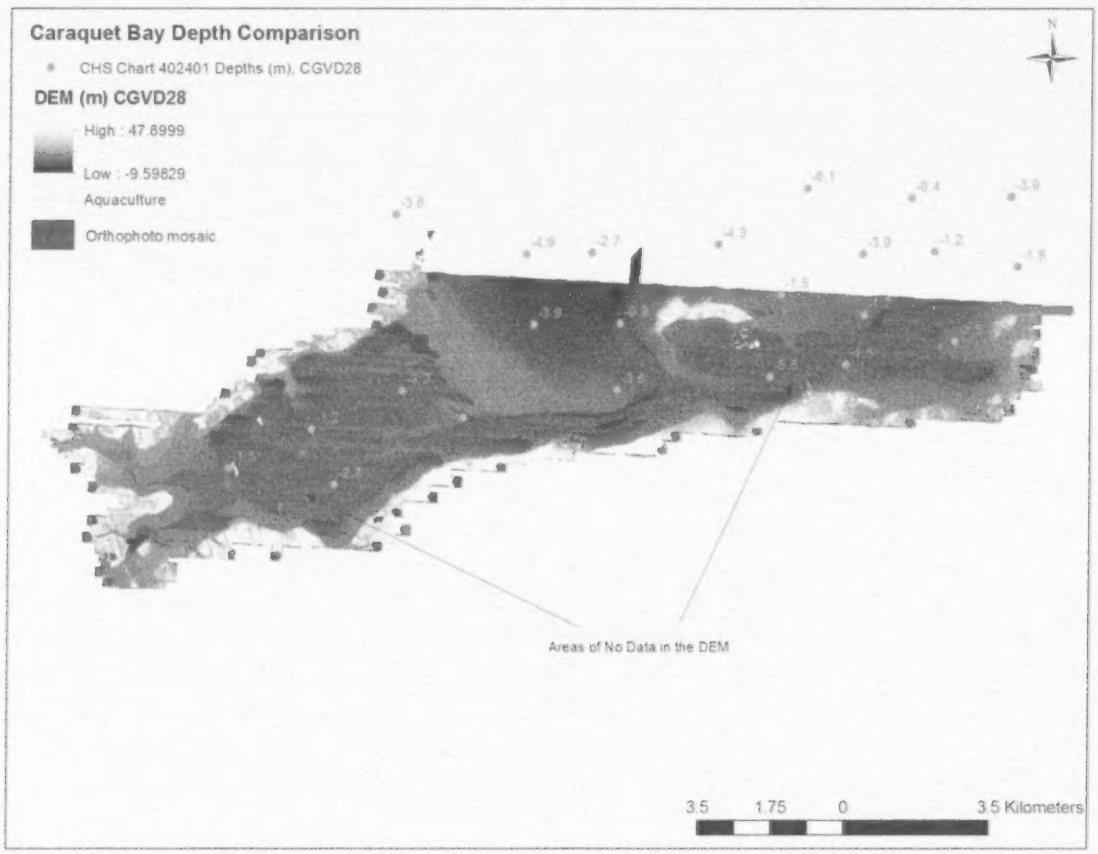

Figure 71: The turquoise image is the orthophoto mosaic; the greyscale image is the Digital Elevation Model (DEM) (m, CGVD28). Orange symbols are depth values from Canadian Hydrographic Service (CHS) chart 402401 adjusted from Chart Datum to CGVD28 as outlined in Table 3 and Section 2.2.4. Aquaculture is shown as yellow lines. Arrows indicate No Data values in the DEM.

Overall, the DEM depths agreed well with the other sources of bathymetry data. The mean Δz was -0.58 m and the standard deviation was 1.18 m. The negative mean value indicates that, on average, the DEM depths were shallower than the depths they were being compared to.

4.2 EELGRASS

Eelgrass coverage was estimated in two different ways in this study: FPI interpreted eelgrass using individual orthophoto frames, while EC/DFO used a combination of techniques (aerial and satellite photos, field samples, etc.). The EC/DFO eelgrass had the added value of giving quality indicators to the eelgrass polygons, in contrast to FPI's coverages which indicated only eelgrass presence. Some quantitative comparisons of FPI and EC/DFO eelgrass area found that for the six bays in which comparisons were possible, half had good agreement between FPI and EC/DFO eelgrass area, in two FPI estimated a smaller eelgrass area than EC/DFO, and in one bay FPI's eelgrass area was larger than EC/DFO's.

4.3 AQUACULTURE

The interpretation of aquaculture gear from aerial photographs was, overall, successful. The interpreted aquaculture lines agreed well with the information from boat-based field surveys on the quantity and type of aquaculture gear present in each lease.

In most cases the lines of buoys were easy to see in the orthophoto mosaics, and in some cases (Oystergro cages) it was possible to discern individual buoys from the photos. Sub-surface oyster aquaculture was more difficult to identify, and it was very challenging to identify dark sea cages. This is a probable explanation for the 30% difference between biomass estimates in Caraquet Bay, where a large proportion of the aquaculture was known to be dark sea cages. Oystergro was one of the simplest types of aquaculture to identify. In Bedec and Bouctouche, 100% and 86% of the total aquaculture was Oystergro, respectively, and estimates for total biomass agreed to within 1% of field survey estimates. This indicates that the interpretation of Oystergro from the orthophotos was successful.

Water surface roughness and photo glint introduced great variability into the orthophoto mosaics. The most severe case of this was in St Mary's Bay, where it was a simple task to identify aquaculture in some sections of the bay, but in other sections nearly impossible, even though all the aquaculture was mussel longlines. This difficulty in orthophoto interpretation is a likely cause for the 28% difference between the field survey estimate for total biomass in St Mary's Bay and the total estimate using the orthophotos. Since the lidar was given top priority for data collection during the survey flights and the aerial photos were a secondary priority, photos were taken whether or not ideal aerial photography conditions were present.

Biomass was estimated from the interpreted aquaculture lines based on information provided by field surveys on each gear type and the estimated biomass per bag (Comeau, 2013). In some cases the number of bags or cages per meter was standard for a particular aquaculture gear (e.g. floating bags), but in some cases an estimate of cage spacing was made using the orthophoto mosaics (e.g. oyster string cages).

5. CONCLUSIONS

Maps have been constructed for bathymetry, eelgrass coverage and bivalve aquaculture gear. These maps could be useful for marine spatial planning (ie. site selection for bivalve aquaculture leases) and decision making in the protection of fish habitat (eelgrass). To better understand the relationship between eelgrass coverage and bivalve aquaculture, the data resulting from this study will feed a concurrent study to assess the statistical relationship between the two at a bay-wide scale (Locke et al. 2014, In Prep.).

5.1 BATHYMETRY

Bathymetric lidar data was obtained for six bays in the southern Gulf of St Lawrence: five in New Brunswick and one in PEI. Seamless DEMs and CSR maps were constructed for each bay using the lidar data. Maximum lidar-detected depths ranged from ~-3 m in Aldouane to ~-9 m in several bays. Using a GIS, the surface area of 1 m depth intervals was calculated for each bay. The area of depth intervals generally decreased with depth. The percentage of area of each bay that was not detected by the lidar ranged from 7% in Bedec to 46% in Caraquet. Lidar detection was limited by water clarity and depth. The lidar-derived depths agreed to within ~1 m with other sources of bathymetry data such as CHS charts and echo sounder data.

5.2 EELGRASS

Aerial photographs were obtained during the lidar survey flights and used to map eelgrass coverage in the six surveyed bays. Additional eelgrass classifications, interpreted from a variety of sources ranging from aerial and satellite imagery to field samples, were produced by EC/DFO between 2007 and 2009. Eelgrass coverage per bay was calculated in a GIS for the FPI and EC/DFO eelgrass classifications. The greatest area of eelgrass coverage was the FPI estimate for Caraquet (~4500 ha); the smallest area of eelgrass was the FPI estimate for St Mary's Bay (266ha). The bay with the highest proportion of eelgrass was Bedec (94% coverage according to the FPI classification); the bay with the least amount of eelgrass was St Mary's Bay. FPI and EC/DFO estimates of eelgrass coverage tended to agree spatialy. The surface area of eelgrass in each depth interval was calculated and showed that eelgrass surface area decreased with depth.

A secondary product of the lidar survey was reflectance data, which provides information on seabed bottom type. The reflectance data did not prove to be effective t for mapping eelgrass

coverage on a bay-wide scale, but were found to be useful as a secondary eelgrass mapping tool, when uncertainties in eelgrass interpretation from aerial photographs were encountered.

5.3 AQUACULTURE

Aquaculture infrastructure was interpreted from FPI orthophoto mosaics generated using aerial photos captured during the lidar survey. Interpretation depended on photo quality and was limited by cloud shadow, light glint, and surface roughness. Overall, the interpretation of orthophoto mosaics was an effective way to digitize and identify aquaculture buoys and infrastructure. In five out of six bays with oyster aquaculture, the values for total biomass estimated in this study were within less than 10% of field survey estimates of total biomass per bay.

The digitized aquaculture lines were used to estimate biomass for each bay based on information on buoy spacing and biomass per buoy for each aquaculture gear type. Collector lines, double and single floating oyster bags, sub-surface oyster strings, oyster string cages, Oystergro cages, dark sea oyster cages, and mussel longlines were identified in the bays. St Mary's Bay was the only bay with mussel aquaculture, and it also contained an order of magnitude more bivalve biomass per hectare and lease area percentage than any of the bays with oyster aquaculture in New Brunswick.

5.4 RECOMMENDATIONS

Bathymetric lidar bottom reflectance ultimately was not investigated as a tool for mapping bottom type in this study. To improve upon the utility of intensity data one could develop and evaluate an algorithm to classify bottom type, specifically eelgrass, following Brennan and Webster (2006). This method would require the lidar point cloud, and is a method of classifying surfaces derived from lidar using a segmentation and rule-based object-oriented classification approach. Point cloud is a vector based structure where each point has its XYZ coordinates and some attributes.

The gaps in the DEMs caused by the depth penetration limitations of the lidar, particularly in the channels, could be supplemented with additional bathymetric datasets to produce a complete seamless terrain model for each bay. The acquisition of the individual orthophoto frames to construct an improved mosaic may help to resolve issues encountered with shadow and glint in the orthophotos.

A secondary product of the lidar survey was reflectance data, which provides information on seabed bottom type. The reflectance data was not used for mapping eelgrass coverage on a bay-wide scale as it was delivered after the aerial photos were interpreted; however it was found to be useful as a secondary eelgrass mapping tool, especially when uncertainties in the eelgrass interpretation from aerial photographs was encountered. To improve upon the utility of intensity data, it would be beneficial to develop and evaluate an algorithm to classify bottom type,

specifically eelgrass, similar to what Brennan and Webster (2006) have done for land cover mapping from lidar data. This method would require the lidar point cloud, and is a method of classifying surfaces derived from lidar (lidar plus elevation based surfaces) using a segmentation and rule-based object-oriented classification approach.

Another source of potentially useful remote sensing images for eelgrass distribution mapping is the Coastal Band (400 – 450 nm) of the Worldview 2.0 Satellite. This band supports vegetation identification and analysis, and supports bathymetric studies based upon its chlorophyll and water penetration characteristics (Satellite Imaging Corporation, 2012). At 0.5 m, resolution of the Worldview 2.0 satellite exceeds the 2.5 m resolution Quickbird satellite images used in this study.

Recommendations for any future bathymetric lidar projects include having a team in the field during the lidar surveys to measure Secchi depths and do echo soundings with appropriate tidal elevation adjustments to accurately validate the lidar elevation data. Having these data available to indicate the transparency and depth of the survey area would resolve ambiguity surrounding cases when lidar did not penetrate to the bottom.

6. ACKNOWLEDGEMENTS

This project was funded by the Program for Aquaculture Regulatory Research (PARR). The authors would like to thank Brad Firth and Dereck Mills at DFO for providing essential information on aquaculture lease occupations and spacing. A big thanks to Jean-Francois Mallet, John Davidson, André Nadeau, Jonathan Hill, Aaron Ramsay and Garth Arsenault for providing eelgrass field data and validation. Many thanks are also given to Jean-Francois Mallet, Venitia Joseph and Chantal Leger for their contribution in analyzing the numerous hours of underwater video. We also thank Erica Watson for data compilation and Luc Comeau for his help on oyster aquaculture biomass analysis.

7. REFERENCES

AMEC Earth and Environmental. 2007. Northumberland Strait Ecosystem Overview Report (File No. TE61035). Moncton, NB: Fisheries and Oceans Canada. http://www.glf.dfo-mpo.gc.ca/folios/00165/docs/rapport-amec-report-eng.pdf.

Brennen, R. and Webster, T.L. 2006. Object Oriented Land Cover Classification of lidar Derived Surfaces. Can. J. Remote Sens. 32: 167-172.

Canadian Aquaculture Industry Alliance. 2010. Aquaculture in Canada: Production and Markets. Retrieved on February 1, 2012: http://www.aquaculture.ca/files/production-markets.php

Canadian Hydrographic Service. 2012. Tides, Currents and Water Levels. Retrieved on February 1, 2012: http://www.tides.gc.ca/english/WaterLevelsAtYourFingerTips.shtml

Comeau, L.A., Arsenault, E.-J., Doiron S., et Maillet, M.-J. 2006. Évaluation des stocks et densités ostréicoles au Nouveau-Brunswick en 2005. Rapp. tech. can. sci. halieut. aquat. 2680.

Comeau, L.A. 2013. Suspended versus bottom oyster culture in eastern Canada: Comparing stocking densities and clearance rates. Aquaculture 410-411 :57-65.

Dealteris, J.T., Kilpatrick, B.D., and Rheault, R.B. 2004. A comparative evaluation of the habitat value of shellfish aquaculture gear, submerged aquatic vegetation and a non-vegetated seabed. J. Shellfish Res. 23: 867-874. http://www.crmc.ri.gov/aquaculture/riaquaworkinggroup/habitat_value_shellfish%20aquagear.pdf.

DFO. 2009. Does Eelgrass (*Zostera marina*) meet the criteria as an ecologically significant species? (Canadian Science Advisory Secretariat Science Advisory Report 2009/018). http://www.dfo-mpo.gc.ca/CSAS/Csas/Publications/SAR-AS/2009/2009_018_e.pdf

DFO. 2005. The Gulf of St. Lawrence - A Unique Ecosystem. (Cat. No. FS 104-2/2005). http://www.glf.dfo-mpo.gc.ca/e0006090

Doiron, S. 2006. Manuel de référence de l'ostréiculteur. Ministère de l'Agriculture, des Pêches et de l'Aquaculture, Nouveau-Brunswick.75p.

Drapeau, A., Comeau, L.A., Landry, T., Stryhn, H., and Davidson, J. 2006. Association between longline design and mussel productivity in Prince Edward Island, Canada. Aquaculture 261:879–889.

Flood, M., and Gutelius, B. 1997. Commercial Implications of Topographic Terrain Mapping Using Scanning Airborne Laser RaDAR. *Photogramm.* Eng. Remote Sens. 4: 327-366.

Fugro Pelagos, Inc. 2011. Canadian Hydrographic Service- Charting. Airborne Bathymetric lidar Survey. Report of Survey. (Reference No. – F5129-10-2001). San Diego, CA.

Guenther, G.C., Cunningham, A.G., LaRocque, P.E., and Reid, D.J. 2000. Meeting the Accuracy Challenge in Airborne lidar Bathymetry. *Proceedings of EARSeL-SIG-Workshop lidar, Dresden, Germany*, June 16-17, 2000. 27pp.

Hanson, A.R. 2004. Status and Conservation of Eelgrass (*Zostera marina*) in Eastern Canada. (Canadian Wildlife Service Technical Report Series #412). Atlantic Region. http://www.bofep.org/PDFfiles/Eelgrass_Technica_%20Report.pdf

Kennish, M.J. and Fertig, B. 2012. Application and assessment of a nutrient pollution indicator using eelgrass (*Zostera marina* L.) in Barnegat Bay-Little Egg Harbor estuary, New Jersey. Aquat. Bot. 96: 23-30.

Lee, K.-S., Short, F.T., and Burdick, D.M. 2004. Development of a nutrient pollution indicator using the seagrass, *Zostera marina*, along nutrient gradients in three New England estuaries. Aquat. Bot. 78: 197-216. http://www.sciencedirect.com/science/article/pii/S0304377003001530

Liu, X. 2008. Airborne lidar for DEM Generation: Some Critical Issues. Prog. Phys. Geog. 32: 31-49.

Locke, A. 2005. Changes In Eelgrass (Zostera marina) In Southern Gulf Of St. Lawrence Estuaries. Fisheries and Oceans Canada Retrieved on February 1, 2012: http://www.glf.dfo-mpo.gc.ca/e0006825

Mahoney, M. 2011.Environment Canada Eelgrass Classification Meta-Data Report. Pers. Comm.

McKenzie, L. 2008. Seagrass Educators Handbook. Retrieved on March 1, 2012: http://www.seagrasswatch.org/Info_centre/education/Seagrass_Educators_Handbook.pdf

Satellite Imaging Corporation. 2012. Worldview-2 Satellite Sensor. Retrieved on March 20, 2012: http://www.satimagingcorp.com/satellite-sensors/worldview-2.html

Schmidt, A.L., Wysmyk, J.K.C., Craig, S.E. and Lotze, H.K. 2012. Regional-scale effects of eutrophication on ecosystem structure and services of seagrass beds. Limnol. Oceanogr. 57:1389-1402.

Skinner, M., Courtnay, S.C. and McKindsey, C.W. 2013. Reductions in distribution, photosynthesis, and productivity of eelgrass *Zostera marina* associated with oyster *Crassostrea virginica* aquaculture. Mar. Ecol. Prog. Ser. 486:105-119.

Statistics Canada. 2010. Aquaculture Statistics_(Catalogue no. 23-222-X). http://www.aquaculture.ca/files/documents/StatsCanAquacultureData2010.pdf

Tallis, H.M., Ruesink, J.L., Dumbault, B., Hacker, S., and Wisehart, L.M. 2009. Oysters and aquaculture practices affect eelgrass density and productivity in a Pacific Northwest estuary. *J. Shellfish Res.*. 28: 251-261.

Vandermeulen, H. 2011. An echosounder system ground-truthed by towfish data: A method to map larger nearshore areas. Can. Tech. Report Fish. Aquat. Sci. 2958: v + 21p.

Washington State Department of Natural Resources. 2011. Eelgrass adopted as indicator of Puget Sound Health. Retrieved on February 1, 2011:

http://washingtondnr.wordpress.com/2011/02/18/eelgrass-adopted-as-indicator-species-of-puget-sound-health/

Wehr, A., and Lohr, U. 1999. Airborne Laser Scanning - An Introduction and Overview. *J. Photogramm. Remote Sens.* 54: 68-82.

APPENDIX A: EELGRASS METHODOLOGY

Field data provided by DFO was used along with aerial and satellite images to classify eelgrass polygons by EC (CWS) (summarized in Table 4).

1. DFO- EELGRASS FIELD SURVEY CRITERIA

Eelgrass boat surveys were conducted in Miscou (2009), Petite-Tracadie (2009), Nequac (2009) and St Mary's Bay (2011) using a predetermined random sampling grid covering the entire bays and estuaries. The sampling design consisted of one randomly located sample within a 300 by 300 meter grid. Samples which were located over land or over deep water were dropped. The number of available samples in a particular bay was usually larger than the available resources necessary for full coverage, so the sample locations were randomly sorted and then chosen sequentially until the maximum number of samples possible with the available resources was reached. The density, cover and quality of the eelgrass were noted at every station and various visual observations were also noted.

2. DFO - EELGRASS TOWFISH SURVEY METHODOLOGY (H. VANDERMEULEN)

Eelgrass boat surveys conducted in Saint-Simon (2007), Tabusintac (2008), Richibucto (2007), Bouctouche (2009) and Cocagne (2008) were made using predetermined bay-wide transects. Each transect was surveyed using an underwater video camera system ("*towfish*") towed on the side of a boat running at idle speed. Side scan sonar was also deployed but not used for eelgrass measurements. The video data was stamped with the running time and precise coordinates of the towfish. A snap shot of the video was then analyzed at approximately every two of minutes running time. The density, cover and quality of the eelgrass were noted at every station and various visual observations were also noted:

1. Transect partitioned (ex, 1a, 1b, 1c....) depending on the length of each transect.
2. Video is analysed with three main components: cover, density and quality.
3. Each of these components has a scale.
4. Video is stopped at 2 minute intervals.
5. The frame is then analysed for density and quality.
6. *Cover* is an overall data which is analysed throughout the 2 minute interval and not just at the stopped frame like the other 2 components (e.g.: full eelgrass cover, eelgrass cover w/ some bare patches, some eelgrass patches and bare sand).

The underwater video and photography analysis has been done by four individuals over a three year period. Thus, the authors would like to mention that there is a possibility of having interpretative variability in the data due to the subjectivity of analyzing qualitative data. Ideally, the analysis should have been done by the same individual to eliminate this possibility.

Table 18: DFO Habitat field survey criteria.

	Density	Cover	Quality
1	Dense (cannot see bottom)	Continuous bed	Green, luxurious eelgrass with very little or no epiphyte load (leaves visible, epigrazers common)
2	Average (variable density, bottom is visible)	Bed with bare patches	Green blades with medium-high density epiphyte cover (leaves barely visible) - blades not pulled down by this cover
3	Sparse to no eelgrass (may have algal cover)	No continuous bed, just clumps of eelgrass separated by bare sediment	Majority of leaf surface black or brown OR epiphyte cover so high no leaf surface visible (bent over stunted / fragmented blades covered in algal material) OR eelgrass remnants with presence of benthic Ulva or other algal mats
4	Bare bottom, no vegetation, clear sand / silt, etc.	No eelgrass	No eelgrass

3. ENVIRONMENT CANADA- CANADIAN WILDLIFE SERVICE (EC-CWS) (MATT MAHONEY) CLASSIFICATION

1. Good Quality Eelgrass: relatively dense, clean, green blades with minimal epiphytes or algal growth.

2. Medium Quality Eelgrass: predominantly green blades that may have some epiphyte or algal growth. These stands can be less than or equally dense as Good Quality Eelgrass, but the best grasses are certainly not as abundant.

3. Eelgrass Absent/Poor Quality: eelgrass is absent, or if it is present it is typically covered with epiphytes or other algae or dying or dead.

3.1 EC METADATA

Bouctouche

True colour aerial photography at 57 centimetre resolution was collected on September 2, 2009 by Nortek Resources of Thorburn, Nova Scotia (http://www.nortekresources.com/). Image

classification was conducted using eCognition Developer v. 8 Software, which first segments the image into spectrally similar units, which were then classified manually. Additionally, the Department of Fisheries and Oceans (Gulf Region, Moncton, NB) conducted a visual field survey in the same field season at 688 sites. Two-thirds of these sites were used to assist in image classification, while the remainder were used to assess accuracy. Eelgrass was classified correctly 83.7% of the time in a fuzzy accuracy assessment technique, whereby those classes that were 'off' by one class, e.g. Good Quality eelgrass classed as Medium Quality, were given half credit towards the overall accuracy. Of 187 sites that were within the classification area, 131 were correct, 51 were "one-off", and 5 were incorrect [(131 + (51/2))/ 187 = 0.837].

Cocagne

Visible ortho-rectified aerial photography was used to classify polygons containing eelgrass in Cocagne Harbour. Field data for image training and validation were collected along transects in summer 2008 using a dGPS positioned towfish holding a video camera that was later transcribed as XY geographic points to describe eelgrass presence and a qualitative description of density. The area was flown for photography on September 24, 2008. eCognition Developer 8 software was used to segment the imagery, essentially polygons. Polygons were then classified manually for the presence of eelgrass. Using field data revealed eelgrass presence to be mapped correctly 87.2% of the time.

Miscou

True colour aerial photography at 57 centimetre resolution was collected on August 20th and 24th, 2009 by Nortek Resources of Thorburn, Nova Scotia (http://www.nortekresources.com/). Image classification was conducted using eCognition Developer v. 8 Software, which first segments the image into spectrally similar units, which were then classified manually. Additionally, the Department of Fisheries and Oceans (Gulf Region, Moncton, NB) conducted a visual field survey in the same field season at 103 sites. From these sites 70% were used to assist in image classification, while the remainder were used to assess accuracy. Eelgrass was classified correctly 96.7% of the time (30/31 = 0.967).

Neguac

True colour aerial photography at 57 centimetres resolution was collected on September 2, 2009 by Nortek Resources of Thorburn, Nova Scotia (http://www.nortekresources.com/). Image classification was conducted using eCognition Developer v. 8 Software, which first segments the image into spectrally similar units, which were then classified manually. Additionally, the Department of Fisheries and Oceans (Gulf Region, Moncton, NB) conducted a visual field survey in the same field season at 126 sites. Two-thirds of these sites were used to assist in image classification, while the remainder were used to assess accuracy. Eelgrass was classified correctly 81% of the time in a fuzzy accuracy assessment technique, whereby those classes that were 'off' by one class, e.g. Good Quality eelgrass classed as Medium Quality, were given half

credit towards the overall accuracy. Of 39 sites that were within the classification area, 27 were correct, 9 were "one-off", and 3 were incorrect [(27 + (9/2))/ 39 = 0.81].

Richibouctou

Eelgrass classification in Richibucto Harbour, New Brunswick. Derived from a Quickbird satellite image collected on August 28th, 2007 at as close to low-tide as possible. Quickbird's ground resolution is 2.4 m. Classification was objected-oriented using Definiens software. Accuracy was 81.5%. Data used for accuracy and training was collected along transects using a differential GPS positioned towfish holding a video camera that was later transcribed as XY points to describe eelgrass presence.

St Simon

Eelgrass classification in Shippagan Harbour, New Brunswick. Derived from a Quickbird satellite image collected on July 27, 2007 at as close to low-tide as possible. Classification was object oriented using Definiens software. Data used for accuracy and training was collected along transects using a differential GPS positioned towfish holding sidescan sonar, and a video camera that was later transcribed as XY points to describe eelgrass presence.

Tabusintac

Visible orthorectified aerial photography was used to classify polygons containing eelgrass in Tabusintac Bay. Field data for image training and validation were collected along transects in summer 2008 using a dGPS positioned towfish holding a video camera that was later transcribed as XY geographic points to describe eel-grass presence and a qualitative description of density. The area was flown for photography on September 24, 2008. eCognition Developer 8 software was used to segment the imagery, essentially into polygons. Polygons were then classified manually for the presence of eelgrass. Using field data revealed eelgrass presence to be mapped correctly at a rate of 77.2%.

Tracadie

True colour aerial photography at 57 centimetre resolution was collected on September 2, 2009 by Nortek Resources of Thorburn, Nova Scotia (http://www.nortekresources.com/). Image classification was conducted using eCognition Developer v. 8 Software, which first segments the image into spectrally similar units, which were then classified manually. Additionally, the Department of Fisheries and Oceans (Gulf Region, Moncton, NB) conducted a visual field survey in the same field season at 101 sites. Approximately two-thirds of these sites were used to assist in image classification, while the remainder were used to assess accuracy. Eelgrass was classified correctly 79.3% of the time in a fuzzy accuracy assessment technique, whereby those classes that were 'off' by one class, e.g. Good Quality eelgrass classed as Medium Quality, were

given half credit towards the overall accuracy. Of 29 sites that were within the classification area, 18 were correct, 10 were "one-off", and 1 was incorrect [(18 + (10/2))/ 29 = 0.793].

APPENDIX B: ADDITIONAL INFORMATION ON LIDAR TECHNOLOGY

The products from a bathymetric Lidar survey can easily be used in collaboration to determine the boundaries of eelgrass in clear water. Each product is explained below:

- Orthoimagery: Georectified imagery has historically been the most used method of environmental mapping. Most eelgrass can be directly observed in airborne imagery; occasionally cloud cover can obscure the scene making interpretation difficult.

- Lidar Bottom Rugosity: Also known as 'bottom roughness', rugosity is a measure of the variability of the seabed. At the edge of eelgrass the roughness will increase, allowing for classification.

- Reflectance Imagery: The strength of the returned bathymetric laser pulse can be shown as an image where lighter objects reflect more energy and darker objects reflect less. Since eelgrass is often darker than the bottom, its boundaries can be clearly delineated from the lidar reflectance image, and aquaculture farms are also observable in the imagery. The reflectance image is one the most robust ways of classifying eelgrass using a Lidar bathymetric system.

- Fugro Pelagos attempted to evaluate water clarity of the area surrounding the aquaculture farms by examining the backscatter of the laser waveform as it passed through the water column. Unfortunately, due to the shallow depths where the aquaculture farms were located, volume backscatter values returned contained too much uncertainty to accurately determine water clarity. This was due to a physical limitation of the technology used by the survey concerning the pulse duration ('length') necessary to transmit the amount of energy required to penetrate the water column to the design depths and return enough of that energy for the receivers to detect. In the case of the SHOALS system and others like it, the pulse length is approximately 5ns in order to transmit the energies necessary to obtain depths in excess of 50 metres. The distance travelled by light in this 5ns timeframe is about 1.5 m; fortunately detection algorithms have been refined to allow the system to resolve the points at which the water surface and sea/lake bed are detected to within 0.2 m. However, the volume backscatter data which is essential to observe in the determination of water column information is masked between the surface and bottom returns in very shallow water, or is at best a very small portion of the returning signal from which measurements and assumptive reasoning is inconsistent. For future operations, Fugro Pelagos would suggest the utilization of hyperspectral imagery or new low-power, short-pulse, high density topo-bathymetry systems to increase the likelihood of water clarity classification in the shallower margins of the areas under study.

APPENDIX C: LIST OF ABBREVIATIONS

CD: Chart Datum

CGVD28: Canadian Geodetic Vertical Datum 1928

CHS: Canadian Hydrographic Service

CSR: Color-Shaded Relief

CWS: Canadian Wildlife Service (Environment Canada)

DEM: Digital Elevation Model

DFO: Department of Fisheries and Oceans Canada

EC: Environment Canada

FPI: Fugro Pelagos Inc.

GIS: Geographic Information System

GPS: Global Positioning System

GRS-80: Geodetic Reference System 1980

ha: hectare

IMU: International Measurement Unit

MSL: Mean Sea Level

NRCan: Natural Resources Canada

SWA: Shallow Water Algorithm

t: tons